Investigation of Tribological Performance of Silver Particle Based Additives Coated with Different Ligands

2021
MASTER THESIS
MECHANICAL ENGINEERING

Hamza Mohamed S ABUSHRENTA

Assoc. Prof. Dr. M. Huseyin CETIN

Investigation of Tribological Performance of Silver Particle Based Additives Coated with Different Ligands

Hamza Mohamed S ABUSHRENTA

T.C.

Karabuk University

Institute of Graduate Programs

Department of Mechanical Engineering

Prepared as

Master Thesis

Assoc. Prof. Dr. M. Huseyin CETIN

KARABUK

January 2021

I certify that in my opinion the thesis submitted by HAMZA MOHAMED S ABUSRENTA titled "INVESTIGATION OF TRIBOLOGICAL PERFORMANCE OF SILVER PARTICLE BASED ADDITIVES COATED WITH DIFFERENT LIGANDS" is fully adequate in scope and in quality as a thesis for the degree of Master of Science.

Assoc. Prof. Dr. M. Huseyin CETIN .....
Thesis Advisor, Department of Electrical and Electronic Engineering

This thesis is accepted by the examining committee with a unanimous vote in the Department of Mechanical Engineering as a Master of Science thesis. January 21, 2021

Examining Committee Members (Institutions)	Signature
Chairman : Assoc. Prof. Dr. Fuat KARTAL	.....
Member : Assist. Prof. Dr. Abdullah UGUR	.....
Member : Assoc. Prof. Dr. M. Huseyin CETIN	.....

The degree of Master of Science by the thesis submitted is approved by the Administrative Board of the Institute of Graduate Programs, Karabuk University.

Prof. Dr. Hasan SOLMAZ .....
Director of the Institute of Graduate Programs

"I declare that all the information within this thesis has been gathered and presented in accordance with academic regulations and ethical principles and I have according to the requirements of these regulations and principles cited all those which do not originate in this work as well."

HAMZA MOHAMED S ABUSHRENTA

ABSTRACT

M. Sc. Thesis

INVESTIGATION OF TRIBOLOGICAL PERFORMANCE OF SILVER PARTICLE BASED ADDITIVES COATED WITH DIFFERENT LIGANDS

Hamza Mohamed S Abushrenta

Karabük University
Institute of Graduate Programs
The Department of Mechanical Engineering

Thesis Advisor:
Assist. Prof. Dr. M. Huseyin ÇETIN
January 2021, 89 pages

Chemical stabilization of nanoparticles is of great importance in terms of cooling-lubrication performance and increasing their penetration into the wear zone of colloidal suspensions. Particles are covered with different ligands to ensure chemical stabilization. Due to the high stabilization performance of the ligand used in the synthesis of the nanoparticle, the amount of wear can be minimized by increasing the penetration ability of the particles. In this study, tribological performance of silver nanoparticle-based additives coated with different ligands was investigated by the parameters of friction coefficient, weight loss and surface roughness. Moreover, the agglomeration behavior of nanoparticles was analyzed by chemical characterization of the suspensions. The silver nanoparticles obtained were reinforced to the mixture of ethylene glycol and extreme pressure additives and the tribological performance of the prepared EG + EP + AgNP mixture was investigated.

The study was carried out in two stages. Firstly, in order to determine the optimum EP ratio, the lubricants obtained by adding EP to EG fluid in different proportions were subjected to wear tests at the parameters of 20 N load and 40 rpm speed. In order to

determine the optimum EP additive ratio, wear tests were carried out under dry, pure EG, EG + 5% EP, EG + 10% EP and EG + 15% EP conditions. The tribological performance of EG + EP fluids was analyzed by examining the friction coefficient, weight loss and surface roughness parameters. According to the results obtained from the wear tests, it was determined that EG + 5% EP reduced the friction coefficient and weight loss by ~ 28.7% and ~ 71.7%, respectively compared to ethylene glycol, and it was observed that it provided a good surface quality. It has been determined that EG + 10% EP and EG + 15% EP fluids are less effective on the friction coefficient, weight loss and surface roughness compared to EG + 5% EP. According to the analysis results, it was concluded that optimum results were obtained at 5% concentration.

In the second stage, 6 different liquids were prepared by mixing the AgNP additive in different proportions and coated with different ligands at the optimum ratio determined for the EP additive. Colloidal suspensions prepared by adding 2%, 5% and 8% rate nanosilver particles were used in the experiments and the optimum nanosilver concentration was determined. Wear tests were applied separately for gelatin and PVA coated nanosilver particles, thus the effect of different coating materials was also examined. The tribological performance of EG + EP + AgNP fluids was analyzed by examining the friction coefficient, weight loss and surface roughness parameters. According to the results obtained, the optimum concentration ratio for both coating materials was determined as 2%. Comparing the coating materials for the EG + 5% EP + 2% AgNP suspension, it was determined that the gelatin coated particles reduced the friction coefficient and wear volume by ~ 12.06% and ~ 53.36%, respectively, compared to the PVA coated particles. When SEM and 3D topography images were examined, it was seen that better surface morphology was obtained with gelatin coated particles. According to the analysis results, it was concluded that optimum results were obtained with the suspension prepared with gelatin coated nanosilver particles at a concentration of 2%.

Keywords **:** Nano-silver, Extreme pressure, 3d topography
Science Code : 91419

ÖZET

Yüksek Lisans Tezi

FARKLI LIGANDLAR ILE KAPLANMIS GUMUS PARTIKUL TEMELLI KATISKILARIN TRIBOLOJIK PERFORMANSLARININ ARASTIRILMASI

Hamza Mohamed S Abushrenta

Karabük Üniversitesi
Fen Bilimleri Enstitüsü
Makina Mühendisliği Anabilim Dalı

Tez Danışmanı:
Doç. Dr. M. Huseyin ÇETIN
Ocak 2021, 89 sayfa

Nanopartiküllerin kimyasal stabilizasyonu, kolloidal süspansiyonların soğutma-yağlama performansı ve aşınma bölgesine penetrasyonunun arttırılması açısından büyük önem taşımaktadır. Kimyasal stabilizasyonun sağlanması amacıyla partiküller farklı ligandlarla kaplanmaktadır. Nanopartikülün sentezlenmesinde kullanılan ligandın stabilizasyon performansının yüksek olması sayesinde, partiküllerin penetrasyonu kabiliyeti arttırılarak aşınma miktarı minimize edilebilmektedir. Bu çalışmada, farklı ligandlarla kaplanmış gümüş nanopartikül esaslı katkı maddelerinin tribolojik performansı, sürtünme katsayısı, ağırlık kaybı ve yüzey pürüzlülüğü parametreleri ile incelenmiştir. Ayrıca, süspansiyonların kimyasal karakterizasyonu ile nanopartiküllerin topaklanma davranışı analiz edilmiştir. Elde edilen gümüş nanopartikülleri, etilen glikol ve aşırı basınç katışkısı karışımına takviye edilmiş ve hazırlanan EG + EP + AgNP karışımının tribolojik performansı araştırılmıştır.

Çalışma iki aşamada gerçekleştirilmiştir. Öncelikle optimum EP oranını belirlemek için EG sıvısına farklı oranlarda EP ilave edilerek elde edilen yağlayıcılar 20 N yük ve 40 rpm hız parametrelerinde aşınma testlerine tabi tutulmuştur. Optimum EP katkı

oranını belirlemek için aşınma testleri kuru, saf EG, EG +% 5 EP, EG +% 10 EP ve EG +% 15 EP koşullarında gerçekleştirilmiştir. EG + EP sıvılarının tribolojik performansı sürtünme katsayısı, ağırlık kaybı ve yüzey pürüzlülüğü parametreleri incelenerek analiz edilmiştir. Aşınma testlerinden elde edilen sonuçlara göre EG + 5% EP'nin EG'ye kıyasla sürtünme katsayısı ve ağırlık kaybını sırasıyla ~%28,7 ve ~%71,7 oranında azalttığı belirlenmiş ve iyi bir yüzey kalitesi sağladığı görülmüştür. EG +%10 EP ve EG + %15 EP sıvılarının sürtünme katsayısı, ağırlık kaybı ve yüzey pürüzlülüğü üzerinde EG + %5 EP'ye kıyasla daha az etkili olduğu belirlenmiştir. Analiz sonuçlarına göre optimum sonuçların %5 konsantrasyonda elde edildiği sonucuna varılmıştır.

İkinci aşamada, farklı oranlarda ve farklı ligandlarla kaplanmış AgNP katkısı, EP katkısı için belirlenen optimum oranda karıştırılarak 6 farklı sıvı hazırlanmıştır. Deneylerde %2, %5 ve %8 oranlarında nanogümüş partikülleri eklenerek hazırlanan kolloidal süspansiyonlar kullanılmış ve optimum nano gümüş konsantrasyonu belirlenmiştir. Aşınma testleri, jelatin ve PVA kaplı nano gümüş parçacıklar için ayrı ayrı uygulanmış, böylece farklı kaplama malzemelerinin etkisi de incelenmiştir. EG + EP + AgNP sıvılarının tribolojik performansı sürtünme katsayısı, ağırlık kaybı ve yüzey pürüzlülüğü parametreleri incelenerek analiz edilmiştir. Elde edilen sonuçlara göre her iki kaplama malzemesi için optimum konsantrasyon oranı 2% olarak belirlenmiştir. EG + %5 EP + %2 AgNP süspansiyonu için kaplama malzemeleri karşılaştırıldığında, jelatin kaplı partiküllerin PVA kaplı partiküllere kıyasla sürtünme katsayısı ve aşınma hacmini sırasıyla ~ %12,06 ve~ %53,36 oranında azalttığı belirlenmiştir. SEM ve 3D topoğrafya görüntüleri incelendiğinde jelatin kaplı partiküller ile daha iyi yüzey morfolojisi elde edildiği görülmüştür. Analiz sonuçlarına göre optimum sonuçların %2 konsantrasyonda jelatin kaplı nanogümüş partikülleri ile hazırlanan süspansiyon ile elde edildiği sonucuna varılmıştır..

Anahtar Kelimeler **:** Nano-gümüş, Yüksek basınç katkısı, 3d topografya
Bilim Kodu **:** 91419

ACKNOWLEDGMENT

First thanks, God Almighty, and later my father and mother for all their struggles from the day of my birth until this time. You are everything I love you in God, the most love, and I also extend my sincere thanks to my family who has always been a support and support to me in all circumstances. Thanks, and gratitude to my country my brothers to me my sisters to my friends.

I am satisfied to thank all those who encouraged, directed and contributed with me through my preparation of this thesis by denoting to the needed references and resources in any phase of its phases, and I thank in particular my honorable Dr. M. Huseyin ÇETIN the discusser for the research or the message for my support and guiding me with advice and correction and for selecting the title and subject, and my thanks go to the administration of the Faculty of Engineering at the University of Karabuk in the Department of Mechanical Engineering at the university for providing the best environment for teaching engineering sciences in the best conditions for science students.

CONTENTS

Page

Page

Page

Page

LIST OF FIGURES

Page

Page

LIST OF TABLES

Page

SYMBOLS AND ABBREVIATIONS INDEX

SYMBOLS

A	:	Radius of circular region	M
A	:	Nominal contact area	m2
A'	:	Cross sectional area of ploughing track	m2
Ar	:	Real contact area	m2
d	:	Track width of wear scar	M
E'	:	Effective elastic modulus	Pa
F	:	Friction force	N
Fs	:	Shearing force	N
Fp	:	Ploughing force	N
G	:	Dimensionless material parameter	M
hmin	:	Minimum film thickness	M
H	:	Indentation hardness	N/m2
Hmin	:	Dimensionless minimum film thickness	
k	:	Thermal conductivity	W/mK
k	:	Elipticity parameter	
K	:	Thermal diffusity	m2/s
K	:	Wear coefficient	
L	:	Wear scar length	M
lb	:	Effective diffusion length	M
N	:	Normal load	N
p,P	:	Contact pressure	N/m2
Pe	:	Peclet number	
Q	:	volume removed per unit sliding distance	m3/m
q	:	Heat generated per unit area	W/m2

r	:	*Radius of curvature*	*M*
r	:	*Ball radius*	*M*
Ra	:	*Average surface roughness*	*M*
Rq	:	*R.m.s of surface roughness*	*M*
Rx,	:	*Effective radius in x and y direction*	*M*
S	:	Shearing strength	N/m2
Tb	:	Total contact temperature	℃
Tc	:	Bulk material temperature	℃
ΔTnom	:	Nominal contact temperature	℃
ΔTf	:	Flash temperature rise	℃
U	:	Dimensionless speed	
V	:	Velocity	m/s
Vw	:	Total wear volume	m3
w	:	Wear scar width	M
w	:	Applied load	*N*
W	:	Dimensionless load	
μ	:	Coefficient of friction	
v	:	Poisson ratio	

ABBREVIATION

ANOVA	:	Analysis of Variance
ASTM	:	American Society for Testing and Materials
COF	:	Coefficient of Friction
ZDDP	:	Zinc Dialkyl Dithiophosphate
PEG	:	Polyethylene Glycol
PVP	:	Polyvinylpyrrolidone
PVA	:	Polyvinyl Alcohol
PSA	:	Prostate-Specific Antigen
TEM	:	Transmission Electron Microscopy
MWFS	:	Metalworking Fluids

HOSO	:	High Oleic Sunflower Oil
PFAD	:	Production and Utilization of Palm Fatty Acid Distillate
EG	:	Ethylene Glycol
ST	:	Surface Tension
WD	:	Wettability Angle

PART 1

INTRODUCTION AND LITERATURE

The mechanical properties of the used alloys determine the material strength of plain bearings used in the industrial systems. However, the temperature, resistance of corrosion and wear can be enhanced by the lubrication impact. The control of these elements contributes to enhance the fatigue strength of the bearings and increase the working life. Currently, copper-based tin bronzes are commonly used as bearing material. These alloys characterize by self-lubricating properties, high thermal conductivity and wear resistance [1]. Moreover, load-carrying capacity is a very significant standard to select materials because bearings are exposed to heavy load and high speed [2]. Tin bronze alloys in plain bearing applications were studied and investigated in the literature [3]. Zhu et al. (2020) studied the tribological performance of CuNiSn bronze alloy on different loads (1 and 4 N) and different ambient temperature (18 ◦C and 110 ◦C) circumstances. The result of the study mentioned that the behavior of both wear and friction depend on temperature and load and that the resistance of wear reduced when temperature increases [4]. Unlu et al (2007) investigated the capacity of load carrying, wear and friction properties of the plain bearings made of CuSn10 bronze. SAE 1050 steel was used as abrasive. Researches and experiments were implemented under different pressure-velocity (0.0125, 0.025 and 0.05 N / mm s) and lubrication conditions. The experimental results showed that the values of weight loss and friction factor which were obtained under dry conditions are higher than those obtained under lubrication conditions [2].

Unlu and Durmus investigated the wear loss and friction coefficient in CuSn10 alloyed radial bearings by the use of artificial neural networks approach. Their experiments were implemented in oily and dry conditions with different velocity and loads. They realized a lower coefficient of wear and friction ratio in lubrication condition than the dry test conditions. As well as, the researchers reported that friction coefficient is a

function of friction force and normal force and that the friction force decrease when the velocity and load decrease [5]. The shaft and bearing of plain bearings include metal-to-metal contact. Currently, most of shaft used in manufacturing systems are made of steel [6]. The friction coefficient of tin bronze-steel contact has been conveyed as about 0.6 - 0.8 in the literature [7]. The function of lubrication may not be offered with adequate effectiveness under heavy operating circumstances. Consequently, the friction coefficient between metals will be increased and deformations including plastering, cracking and abrasion arise on the surfaces [5]. Moreover, the ratio of oxidation increase because of increasing of temperature and material loss due to tribe-corrosion are more than forecasted [7]. It is detected that lubricant applied to plain bearings such as self-lubricating bearings considerably decrease the friction coefficient [5]. Also, the additive added to oil my furtherly increase the tribological performance. These additives may be added to lubricants in order to increase heat transfer capability, prevent corrosion, increase wettability and oil film strength [8]. For instance, due to the extreme pressure added to lubricants, the metal surface and lubricant react tribo chemically and a high-strength oil film is shaped [9]. Thanks to this way, metal-metal contact is prevented and wear, friction and temperature are decreased. Recently, nanoparticles use as additive became so common. Particularly, nanoparticles that increase, the heat transfer capability, increase the strength of oil film, liquid penetration and wettability.

In this method, it shows high tribological performance on abraded and cut surfaces [10,8]. The chemical properties, dimensions and morphology are factors of tribological performance [11]. For instance, particles with spherical form unlike the fibrous nanoparticles where they are more easily dispersed in liquids and show lower coefficient of friction [12]. Moreover, spherical particles may increase the quality of surface with the impact of mechanical behaviors including filling, mending and rolling [13]. The fields of using nanoparticles from different composites by numerous approaches are very extensive. Nevertheless, in order to use a lubricant under high-temperature conditions, heat transfer of nanoparticles additive must be the main factor. As well as, the colloidal stability and agglomeration tendency of nanoparticles are very significant factors in terms of sustainable use. The high surface energy of nanoparticles allow them to clump freely [14]. Nanoparticles synthesized without the ligand merge

application with each other and their size increase. Consequently, they may act abrasive in the wear area [11]. Ligand must be applied to the particles during the production process in order to guarantee the colloidal stability. Organic agents including glucose, polyethylene glycol (PEG), polyvinyl pyrrolidone (PVP), gelatin and polyvinyl alcohol (PVA) may be used as the ligand. These ligands connected to the nanoparticles surface work on keeping the particles far from each other and inactivate the active atom surfaces [15].

Cetin et al. (2020) studied the impact of different concentrations of gelatin-coated nanosilver particles on tribological performance and behavior of clumping. By testing the temperature change, weight loss, friction coefficient and results of surface roughness they gotten from the wear experiments, they mentioned that the pilling particles behavior negatively impact the resistance of wear. Studies performed currently are focused on producing, characterizing and adding silver nanoparticles as additives to liquids [12,16,17]. Silver metal is commonly used in modern industrial fields due to its superior properties. It is widely used in electronic and electrical industry because of its oxidative stability and conductivity [18]. The fungicidal and anti-bacterial properties of silver generate a broad field of use particularly in biomedical applications [19]. Despite that, biological and chemical seniors characterize by broad range of use such as soap, textile products, paste, wound dressings, photovoltaics and food [19,20]. Adding silver nanoparticles as additives to cutting fluids offers a high movement in thermal properties if compared with other metal oxide nanoparticles [12]. The reason of this is that silver enjoys by very high thermal conductivity factors (~ 429 W / mK) if compared with other types of metals [21]. Sarafraz et al. (2016) practically studied the heat transfer coefficient, viscosity and thermal conductivity of biologically produced nanosilver particles with spherical morphology. The result of their study detected that nanosilver particles present high thermal performance and this nanofluids can be used as lubricant or coolant in engines with high heat flux conditions [22]. The impact of silver nanoparticles on lubricant is not only on the heat transferability. Consequently, many studies have proven that it has an impact on decreasing wear and friction on surfaces [23]. The results of those studies showed that silver nanoparticles separate the roughness on the metal-metal contact surface, decrease the grooves on the worn surface and cause high tribe film

formation by collecting on the surface of lubricating. So, smoother surfaces are gotten [10, 16].

Another study conducted by Prabu et al (2018) showed that silver present low modulus of solidity and elasticity, thus particles are deformed because of high pressure and friction force in the metal interface. It is noticed that the particles deformed because of sliding movement on surface fill the eroded surfaces [16]. Yu et al (2018) mentioned that recently, researches and studies were performed to prepare thin films with superior tribological properties in a broad range of temperature. It has been mentioned that the most efficient method for this is to manufacture films which show self-lubricant properties with different temperatures. Researches detected that WCN-Ag films with some silver added may show self-lubricating properties in the temperature range of 25–600 ° C [24].

It is clearly seen from the literature that nanoparticles additives offer high tribological performance on metal surface. Nevertheless, it is discovered that the properties of nanoparticles used in these researches was not efficiently defined before the study. Determination the stability of nanoparticles to be used on surface subject to abrasion is very significant in order to avoid the loss of material because of abrasion. Even though, the least amount of abrasion and unevenness on the surface may have high effect on fatigue strength of metal materials. Also, efficient heat transfer on metal surfaces is very efficient to protect the mechanical features of materials. The tribological performance study of tin bronzes in the synthesized and characterized nano-silver-added lubricant medium is considered a unique study in the literature. 100Cr6 alloy has been used as abrasive and CuSn10Zn alloy has been used as tin bronze. High powerful ethylene glycol were determined as a base lubricant. Nanoparticle (2%, 5%, 8%) and EP (5%, 10%, 15%) additives have been added to the ethylene glycol base with various concentrations.

In nanoparticle application, particles of nanosilver are coated with two different ligands (PVA and gelatin). The colloidal stability, agglomeration behavior, morphology and size of the nanoparticles have been performed. Classification processes were delivered by zeta potential, particle size analysis (PSA), transmission

electron microscope (TEM), ultraviolet and visible light (UV - Vis) absorption spectroscopy graphics. Moreover, the surface tension and wettability of the added oils set with various concentrations have been tested and their tribological behaviors have been examined. In tests, 40 rpm sliding speed were determined to wear factors and 20 N for loads. The empirical results have been evaluated according to scanning friction coefficient data, 2D volume loss, 3D topography analysis and electron microscopy (SEM).

PART 2

THEORIC BACKGROUND

At this part of our study, we will present the literature associate the topic of this study. It starts by giving a general background about tribology (lubrication, friction and wear) and primary chemistry phases of the oxidation process and plant oils. This will be accompanied by a literature review associated with the goals of our study. As well as, this part will review Silver Nanoparticles, Synthesis of Silver Nanoparticles and its tribological performance.

2.1. FRICTION

Friction is a strength of resistance to a tangible movement among two contacted surfaces. Guillaume Amontons (1663-1705) is firstly researcher who published the friction laws where those laws asserted that the force of friction is relative to the natural load applied also independent of the obvious zone of contact [42]. The primary equation of the friction force F is shown below (Eq. 2.1):

$$F = \mu N \tag{2.1}$$

Where N represents the normal load and μ represents the coefficient of friction. Thus, Bowden and Tabor (1950) were explained the more specifics model of metallic friction. They stated that the force of friction represents a summation of two elements, the ploughing force (Fp) and the adhesive force (Fs) and its equations is shown below (2.2) [43]:

$$F = Fs + Fp \tag{2.2}$$

Through the comparative movement of two contact bodies, the force of adhesion is needed in order to snip the contact junctions where cohesion occurs, while the ploughing force is required to plough the solder surface asperities over the softer surface. Bowden and Tabor (1950) proposed that contact arose only in the sharpness of the surface [43]. The mentioned contact zone is called the real contact zone, and from the apparent contact zone, it is very limited and autonomous. The real contact zone is correlated with the load applied where the asperities can be deformed. The following formula is formulated from these assumptions equations is shown below (Eq. 2.3).

$$F = Ar.s + A'p \tag{2.3}$$

Where Ar represents the real contact zone, s represents the shearing strength of the metallic junctions, A' represents the cross sectional zone of the reinvesting track and p represents the pressure to cause plastic for the softer metal (near to the depression value of solidness) [44].

When those load will be applied, the softer material asperities distort in the contact zone till the real zone of contact is adequate to support the load. at this case, N=pAr. So, equation 2.4 is written as heeds:

$$F = \frac{NS}{P} + A'p \tag{2.4}$$

At the end, the friction coefficient can be written as follows (Eq 2.5):

$$\frac{F}{N} = \frac{S}{P} + \frac{A\,'p}{N} \tag{2.5}$$

Bowden and Tabor (1950) presented that the ploughing force of ball-on-flat contact is similarly reliant on the ploughing track width, d and curvature radius, r of the contact and can be written as follows (Eq. 2.6).:

$$Fp = \frac{d\ 3\ p}{12r} \tag{2.6}$$

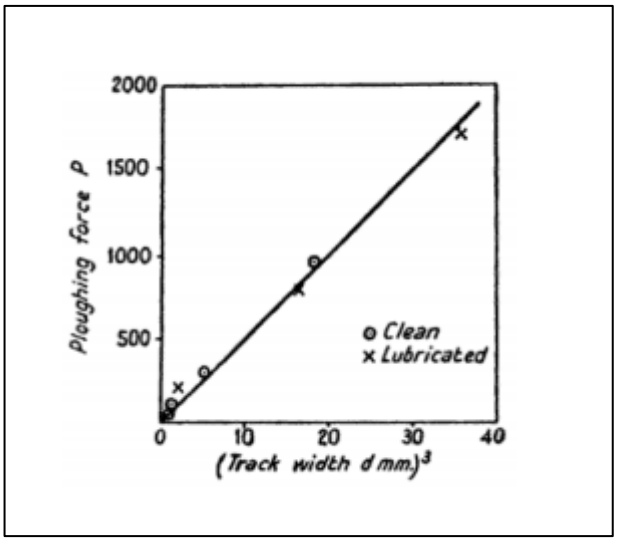

Figure 2.1. The track width impact in the ploughing force for indium with flat steels of dry and lubricated surfaces [28].

The above theoretical results consistent with the test data that shown in Figure 2.1. The line in Figure 2.1 represents the expected value.

2.1.1. Tribometer and Friction Force Measurement

It is very significant to academics and researchers to understand the test rig system or tribometer before conducting tribological study. Most of the tribometers which used in experimental studies are conventionally designed and existed for small scale to repeat the application in the real systems. They consist a linear reciprocating friction samples, pin-on-disk-tribometers and four-ball-tribometers. The application may be somewhat close to a quad-ball, a quad-ball is a ball-bearing system while a pin-to-disc may imitate a disc brake system. The sliding movement in a linear replying friction tester may repeat the movement of the piston ring in the internal combustion engine. Figure 2.2 shows the characteristic configuration of commercial thermometers with normally applied load orientation.

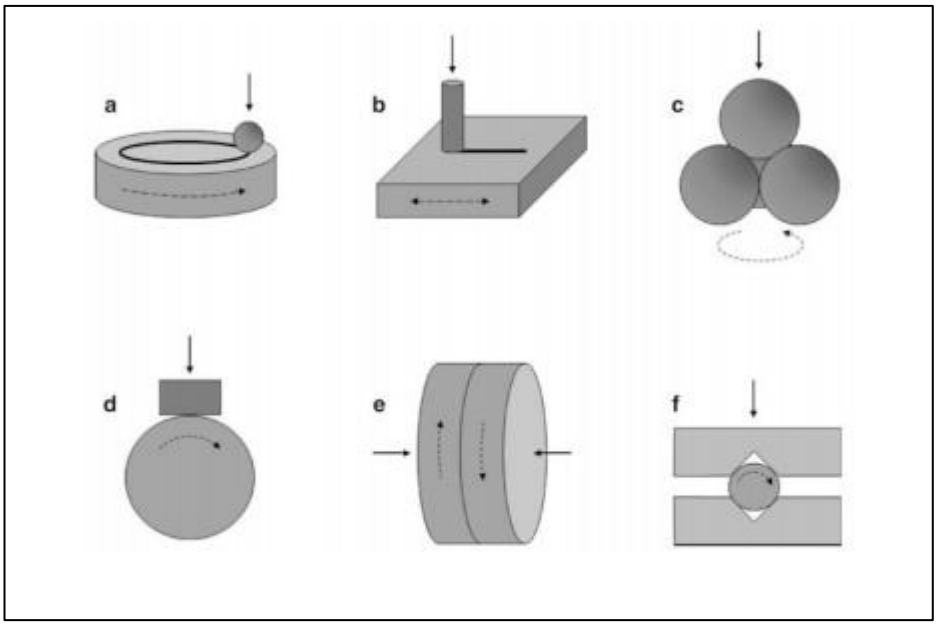

Figure 2.2. (a) ball-on-disc, (b) reciprocating pin-on-flat, (c) four-ball, (d) block-on-wheel, (f) flat-on-flat, and (f) pin and vee-block; Typical formation of the commercial tribometer where normal load is specified by the arrows [29].

The primary is prepared to measure the frictional force of the thermometer by relating the normal load among double connected objects which are marked by the comparative movement (one body is stationary whereas the other partner's body is moving). Hence, the normal force must be modified, which is why it can be enlarged repeatedly til a transverse force that can be measured by a force measuring device is detected. In order to evaluate the force of friction, F in the linear meter checker, a spring balance is usually used to create an adjustable load, N, applied to the two connected objects. In general, as the standardized load cell is attached to the stator body as a force of friction measuring device. Subsequently, the friction factor is computed by separating the frictional force F by the normal load value.

2.1.2. Friction Behavior through Running-In of Sliding Contact

Running-in is the process of changing wear and\or friction in tribosystem before the stable status when the two contacted surfaces are contacted under the normal load and comparative movement. Some machines such as new engines expose to specific operating procedures after assembly in order to accomplish long-term life of service. Running-in behaviour shapes include eight popular shapes with metal contact of

sliding which are classified by Blau [47] Depending on the literature studies of tribology tests performed in the 1980s as shown in Fig.2.3 [48]. Some of the possible causes of each type of curves are shown in Table 2.1. The results of Blau [47] studies proposed that there is no indication that these eight curves are illustrative of certain contact circumstances [48].

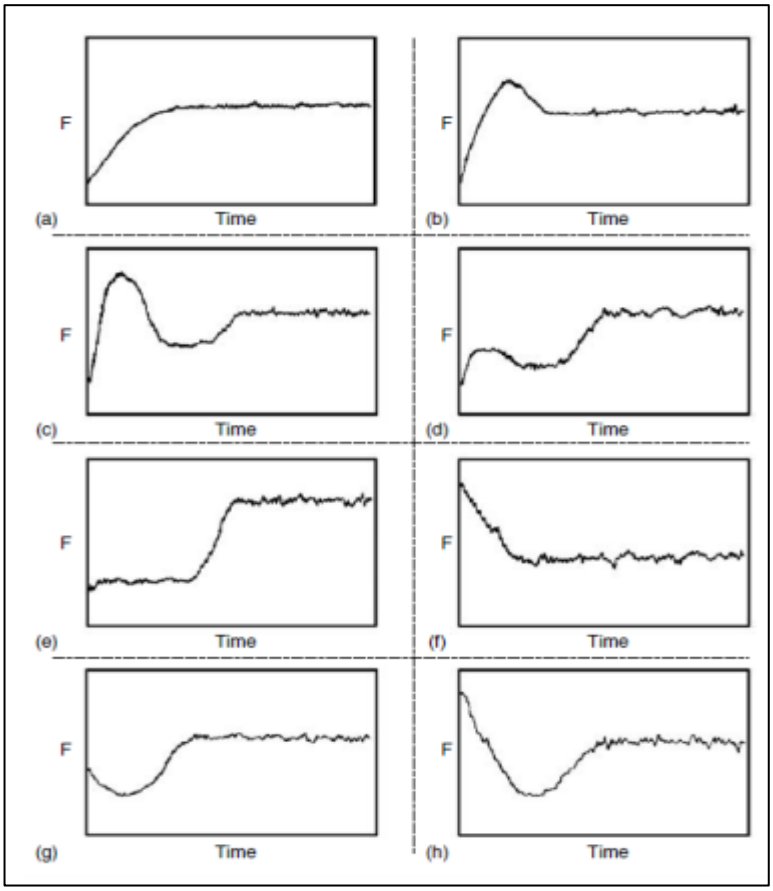

Figure 2.3. Eight distinctive formulas of primary friction behavior through the running-in process [48].

Table 2.1. Probable reasons of friction running-in behavior [48].

Type	Existence	Probable reason(s)
A	Pollutant surfaces	A light class of lubricious pollutant is removed from the sliding of surface [48]. Impacts of element heating emerges due to the friction of sliding [49]. Mechanical disturbance of surface oxide class with rising the metallic contact [50]. (iv) The changes of contact geometry [51].
B	Boundary-lubricated metals	Surfaces wear-in; primary wear ratio is great until the severest asperities are worn off and surface is become glibber [52].
c	Unlubricated oxidized metals, usually perceived in ferrous or nonferrous/ferrous combines	Wear-in, as in category (b), but with the succeeding growth of a debris layer (debris gathering) or extreme transfer of metal [52]
d	Same as (c) section	Like section (c), but the primary oxide film perhaps more determined and protecting [52].
e	Coated systems where they are controlled in wear by process of subsurface fatigue.	Coating wear-through or cracks in subsurface fatigues grow until debris is first generated. Then, debris generates three bodies that lead to quick change in friction. Occasionally a little preliminary spikes of the friction refer to the beginning of that change [53].
f	Pure and clean metals.	Crystallographic redirection of zones near the surfaces layers decrease their friction and strength of shear [54]. Instead, the preliminary roughness is removed and separating smoother surface [48].

g	Metal of graphite and graphite of graphite;	Create a tinny class through the transfer operating or debris creates a succeeding friction increase [48].
h	Hard coatings on ceramic	Roughness changes, later a fine-grained debris layer is formed [55]

2.1.3. Increase of Contact Temperature and Frictional Heating

Some of the mechanical energy that employ in moving material in frictional contacts scatters as a heat energy. This dissipation of energy is called frictional temperature that could work in increasing the heat of the two sliding bodies. Increasing the frictional heating of sliding contacts may effect on the tribological behavior and sliding elements failures. Sometimes increasing the temperature of surface is efficient bring about material melting, oxidation of surface and can be change to the structure and properties of materials in the zone of contacts [56].

The temperature of the surface in sliding of bodies may be gauged experimentally or assessed by computation. The whole reach temperature at a specific point can be assessed depending on the gathering of three elements as follows (Eq. 2.7). [56]:

$$Tc = Tb + \Delta Tnom + \Delta Tf \tag{2.7}$$

Where Tb represents the temperature of the bulk material, $\Delta Tnom$ represents the average contact temperature and ΔTf represents the increase in the flash temperature for a short period of time on severe contact. In terms of the fixed temperature source to move object (with a circular radius,), the highest flash overheat may be estimated as follows (Eq. 2.8). [56]:

$$\Delta Tfmax = \frac{2qa}{K\sqrt{\pi(1.273 + Pe)}} \tag{2.8}$$

Where $q = \mu PU$ represents the ratio of temperature created per unit zone (W/m2), μ represents the factor of friction, P represents the touch pressure (N/m2), a represents the circular zone radius (m), k represents the thermal conductivity(W/mK), Pe

represents the Peclet number $= \frac{Va}{2k}$, V represents the speed (m/s) and $K = \frac{k}{pc}$ represents the current diffusivity (m2 /s).

The increase of insignificant surface heat represents an extra heat because of the temperature source which passes repetitively through the same point on the surface. The increase of nominal surface temperature of a moving body can be measure as follows (Eq. 2.9). [56]:

$$\Delta Tnom = qnom = \frac{lb}{K} \quad (2.9)$$

Where $qnom$ = q$\frac{Ar}{A}$ q, Ar represents the real contact zone (m2), $A = \pi a$ 2 represents the nominal contact zone (m2), l b= $\frac{a}{a\pi 1/2}$ $\left[\frac{2\pi K}{av}\right]^{\frac{1}{2}}$ = a π1/2 tan−1 [$2\pi K$ aV] 1 2 represents the efficient length of diffusion (m).

2.2. WEAR

Wear may be described as the gradual lack of material from the body's effective surface due to the comparative movement on the surface [57]. Where the basic mathematical model of the relationship between the ratio of wear and normal load can be calculated by the following equation (Eq. 2.10). (Archard Equation for Corrosion):

$$Q = \frac{KN}{H} \quad (2.10)$$

Where Q represents the volume removed from a surface each unit a sliding distance (m3 / m), N also represents the normal load applied to the surface, while H represents the depression stiffness of the wear surface (N / m2) and K represents the wear constant.

Equation of Archard can be applied only on the wear volume, sliding distance, material hardness and linear relationship between the normal loads. It must be mentioned that the values of $K, N$and $H$are still constant through the test of wear while the volume of

material lost from the surface is directly related to the distance of sliding and experiment time [57].

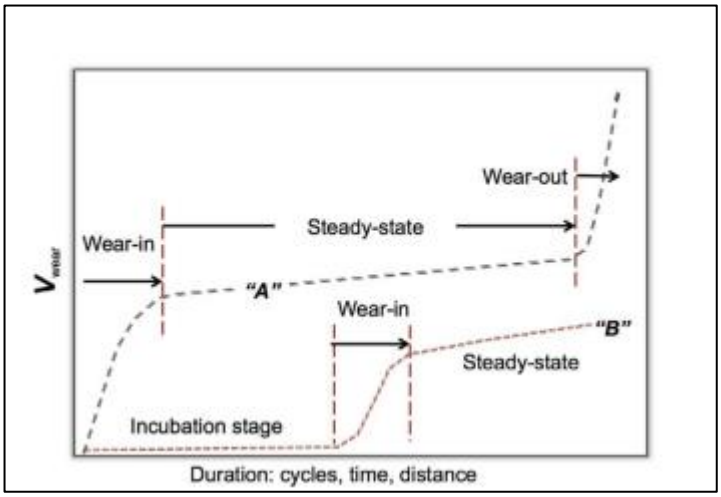

Figure 2.4. Popular curves of non-linear sliding wear behavior [58].

Figure 2.4 shows the distinctive wear behavior of sliding contact for non-induced wear change. Where they may be effected by choosing the material in a 21 tribosystem [58]. It presents that the wear growth (Curve "A" in Figure 2.4) happens in different phases, wear rapidly increases during the wear-in process, period growth of stable wear and wear increase again through the wear-out phase. In terms of mild wear at the start of sliding process (Curve "B"), at a minor normal load, the primary wear change is similarly to stay slower before the beginning of the wear-in process.

Study the wear change needs an accurate approach to measure the wear in location. In many tests where the constant measurement of wear is unreasonable (because of the inadequacy in test rigs), many researchers select to stop the test rig occasionally for the purpose of measuring the wear [59]. Nevertheless, the approach is vulnerable to the probability of convincing an arrangement error in the contact zone when resembling the samplings for second time. Therefore, develop a device to measure a wear in location is still representing a significant field in wear researches.

2.2.1. Wear Measurement Approaches

Wear includes progressive material loss and therefore, mass loss is regularly utilized as wear measure. This is conducted by determining the specimen mass prior and after the experiment. Other than mass loss measurement, the computation of wear volume may similarly be conducted depending on the wear scar geometry of worn specimen (width and length) that can be dignified by using a profilometer. For instance, Figure 2.5 shows the distinctive view of wear scare on flat specimen in case of ball-on-flat linearly countering sliding wear experiment. Total wear volume (Vw) is then computed by the following formula [60]:

$$Vw = L\ \{r\ 2\ \sin{-1}\ (2r) - w\ 2\ \sqrt{r\ 2 - w2\ 4}\} + \pi\ 3\ \{2r\ 3 - 2r\ 2\sqrt{r\ 2 - w2\ 4} - w\ 2\ 4\ \sqrt{r\ 2 - w2\ 4}\}$$

$$Vw = L\left\{r^{2sinsin\,-1\ \left(\frac{w^2}{2r}\right)} - \frac{w}{2}\ \sqrt{r^2 + \frac{w^2}{4}}\right\} \quad + \frac{\pi}{3}\left\{2r^3 - 2r^2\sqrt{r^2 - \frac{w^2}{4}}\ \frac{w^2}{4}\ \sqrt{r^2 - \frac{w^2}{4}}\right\}$$

Where w represents the width of wear scar (m), L represents the length of wear scar (m) and r represents the ball radius (m)

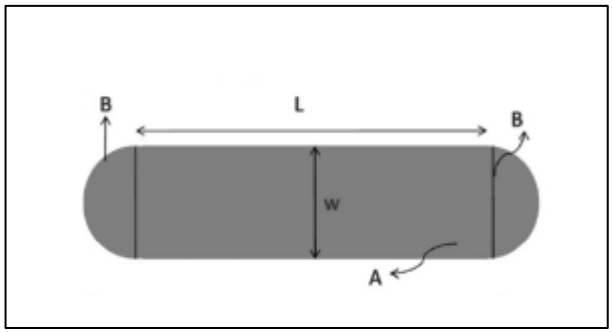

Figure 2.5. Upper assessment of distinctive wear scar created on flat specimen by ball-on-flat linearly responding wear test. The computation of wear volume depending on dividing the scar of wear zone for A and B [60].

By the use of other equipment with the help of program may lead to simplify the measurement of wear scare geometry. For instance, Sharma et al (2013 suggested an approach to calculate the volume of wear for a ball-on-flat responding sliding wear test by an optical microscopic method [60]. In this method the geometry in various

locations of the worn division has been measured by defocusing and focusing on the sample flat surface. Despite of numerous approach to measure wear, wear volume computation accuracy is restricted to wear scars of ‘uniform’ form. In case of non-uniform shape of wear scar created on the surface, the mass measurement loss approach is an improved selection.

2.2.2. Wear Mechanisms

The wear is caused when there is inadequate shield between the two contacted surfaces. The reason behind the occurrence of wear on surface is properly known as wear mechanism. Before taking a step to control the wear, it is necessary to understand and identify the wear mechanism. Generally, wear mechanism consists four main classes including adhesive wear, abrasive wear, chemical wear and surface fatigue wear.

2.2.2.1. Adhesive Wear

At this mechanism, the material is replaced during the sliding process when the asperities contact of surface under the normal load. The transition of material is started by a micro-welding process arising in two contacted asperities when efficient heat is created and monitored by the material shearing process as shown in Figure 2.6.

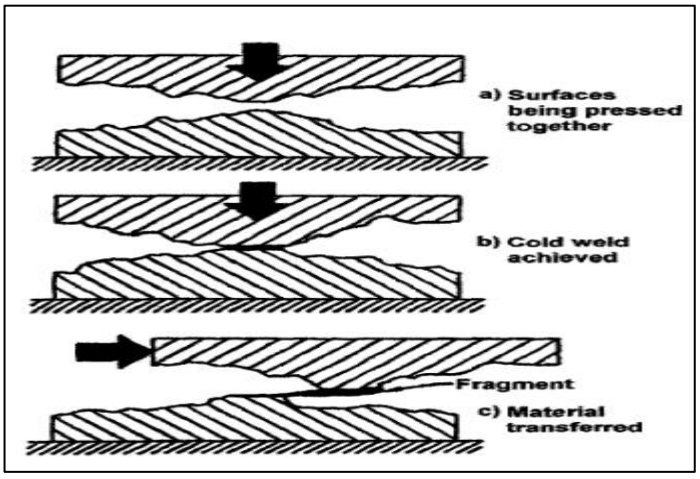

Figure 2.6. The adhesive wear mechanism [61].

The adhesive wear occurs when the fracture arises in subsurface at one of the materials as shown in (Figure 2.7). Forming the transfer films is typical properties of adhesive wear where the material convoys from one of the surfaces to other before unrestricted as a particle of wear as shown in (Figure 2.8.)

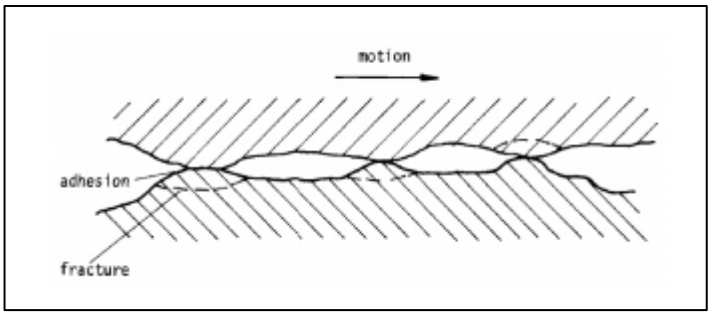

Figure 2.7. Formation of fracture in the materials subsurface because of the adhesive wear [62].

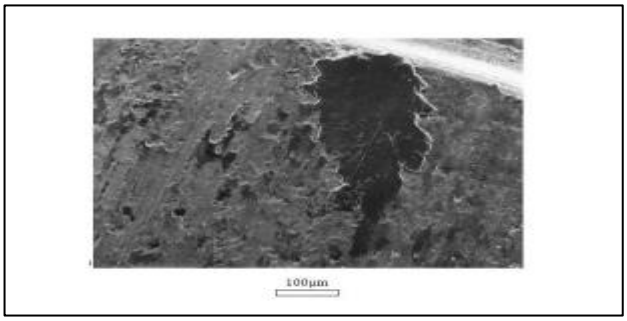

Figure 2.8. An example of adhesive wear presence (Al-Si alloy transfer film into the piston ring) [44].

2.2.2.2. Abrasive Wear

This type of wears happen when the hard protuberances or hard particles are enforced to slide on the contacted surface. It is named three-body abrasive when the abrasive wear is created by the hard particles whereas the two-body abrasive is produced by the harder asperities piercing to the softer material as clarified in (Figure 2.9.)

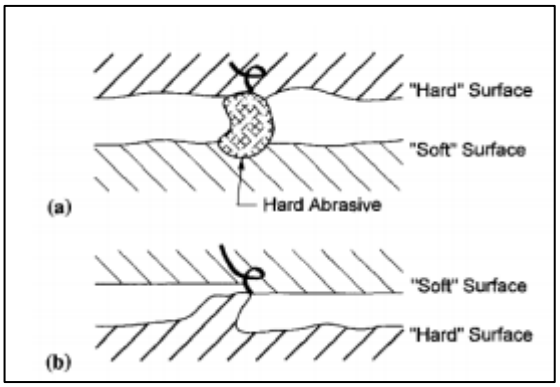

Figure 2.9. A diagram of three-body and two-body abrasive wear model [61].

In this type of wear, the material is removed by the cultivating or micro cutting process that is effected by many elements including material hardness, shape and particle size. (Figure 2.10) shows the distinctive presence on the worn surface which caused by the abrasive wear.

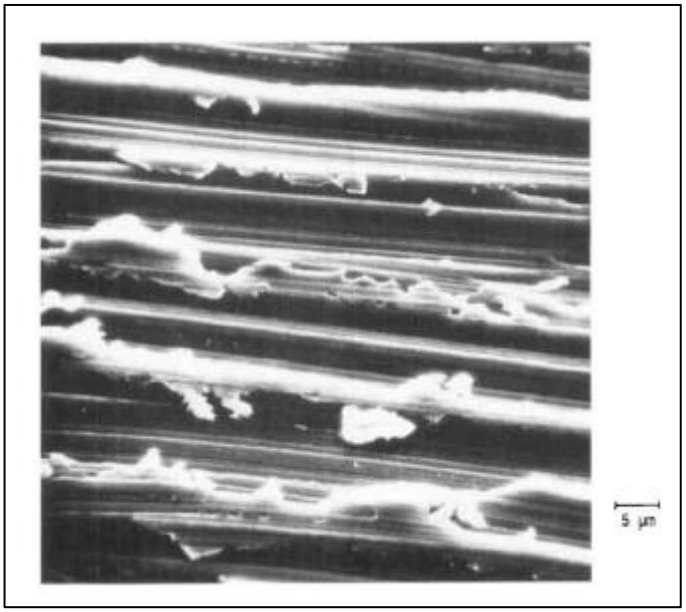

Figure 2.10. An example for the presence of abrasive wear [62].

2.2.2.3. Fatigue Wear

On surfaces, this type of wear happens when repetitive stress cycling occurs in a sliding or rolling interaction. Fractures or fractures, as explained in (Figure 2.11), are formed after an effective number of fluctuating strains and stresses. Microscopically,

fatigue wear is visualized by surface spalling and pitting caused by sub-surface shear stresses that exceed shear material power, as shown in(Figure 2.12).

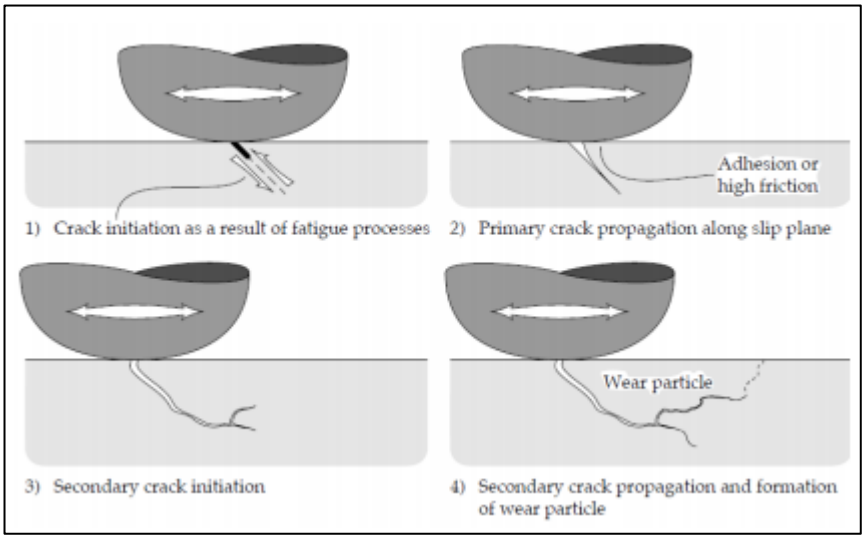

Figure 2.11. Surface crack instigation and proliferation process [44].

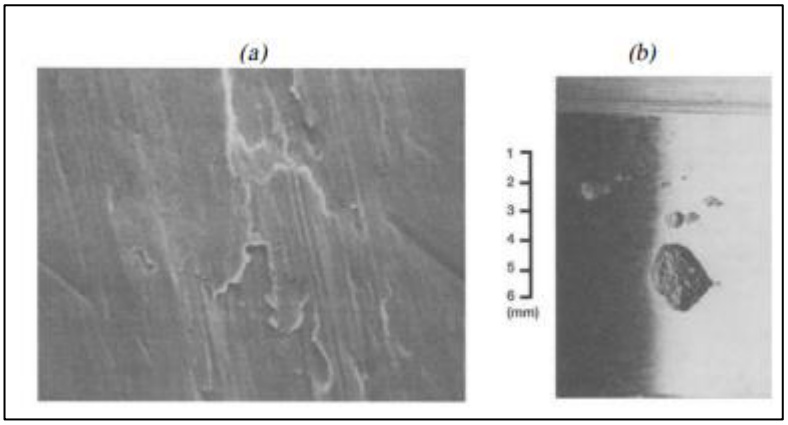

Figure 2.12. Examples of wear scar presences because of fatigue wear technique. (a) Spalling wear and (b) Pitting wear [61].

Delamination wear is a distinct kind of wear that can be defined as a sub-set of stress wear induced by cracks under the surface. Suh (1973) suggested the theory of discharge and claimed that turbulence occurs below the surface because of continuous loading. [63]. Then, due to the restricted impurities in most engineering materials, dislocations accumulate and cause voids to form. Parallel cracks on the surface were caused by the merging of the voids(Figure 2. 13) . This ends up in the form of sheet-

like particles, replacing the thin layer of material. The characteristic appearance of delamination wear on a worn out surface is clarified in Figure 2.14. [52].

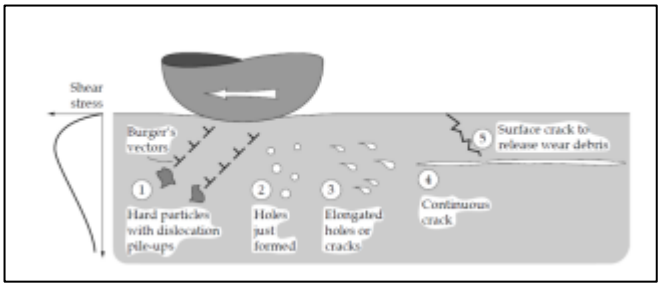

Figure 2. 14. Creation of crack in subsurface by link up and growth of voids [44].

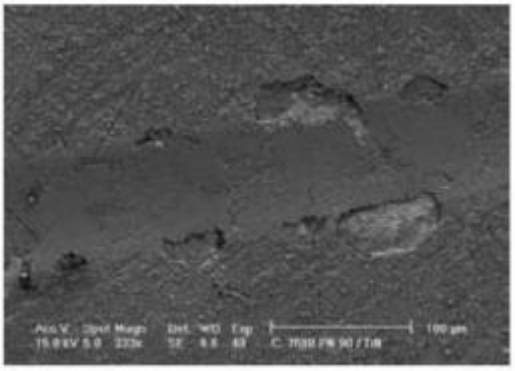

Figure 2.15. The appearance of delamination wear [52].

2.2.2.4. Chemical Wear

Corrosive wear or chemical wear happen when the sliding process occurs at the corrosive environment. Chemical wear happens due to electrochemical or chemical reaction on the metal surface from the corrosive or lubricant contaminates including acids, water and salts.(Figure 2.15) shows corrosive wear mechanism where pitting is typically created on the worn surface. In general, the chemical wear is named oxidative wear because the oxygen is considered most prevailing corrosive medium. This type of wear can be controlled by using a suitable constraining additives.(Figure 2.16) shows a worn surface example because of the chemical wear.

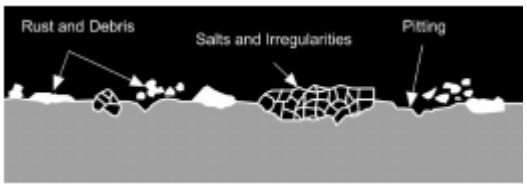

Figure 2.16. The corrosive wear mechanism of [64].

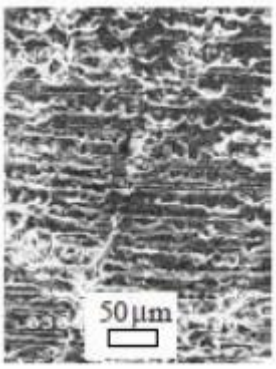

Figure 2.17. Chemical wear instance for cast iron because of the sulphuric acid [44].

2.3 LUBRICATION

The lubrication is applied between two contacted materials with a view to decrease the friction and minimize the wear between them. Lubrication decreases the friction by delivering a low snip strength layer among both surfaces that is less than the material shear strength [44]. In addition, it has another important role including heat transferability, removes the contaminants and decreases the corrosion. There are two types of lubricants, Solid lubricants and liquid lubricants. Solid lubricants are also found in powdery lubricants for example graphite and molybdenum disulfide. Liquid lubricants are usually those derived from the base oil and adding an additive with a view to improving their performance.

2.3.1. Lubrications Regimes

As we stated above that the main function of lubricant is to deliver protection layer which decrease the friction and wear between tow contacted surfaces. However, the standard load size between the two contact surfaces imposes different lubrication requirements that can classify the lubricant into different regimes of lubrication. Three

popular lubricating systems consisting of boundary, mixed and hydrodynamic lubrications operate under lubricants. A description of the lubrication regimes (Figure 2.17) is clarified by the Stribeck curve that is a plot of a fluid-lubricated bearing system which provides a friction factor versus N/P, where N represents the viscosity of the lubricant, N represents the rotating velocity and P represents the load per expected bearing zone unit.

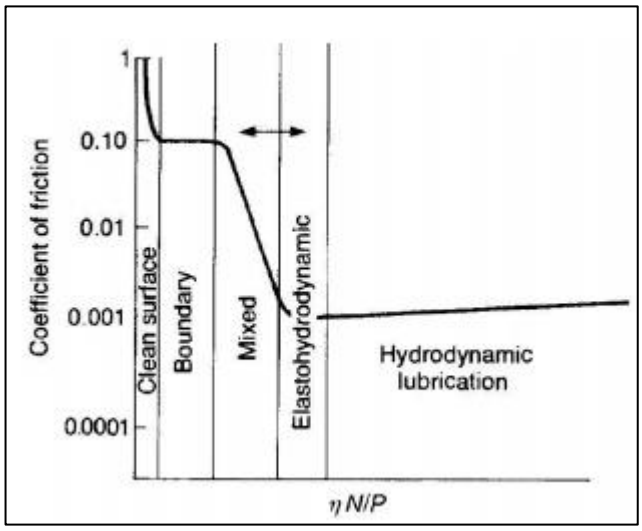

Figure 2.18. Stribeck curve shows different lubrication systems that associate with friction element, speed and lubricant thickness [56].

Full film lubrication is known as hydrodynamic and is the state under which a relatively thick film between them completely supports the contact load between the sliding surfaces. (> 0.25 μm) [56]. The interaction between the metal is circumvented through this lubrication which make the friction element only depending on the lubrication thickness (with continuous speed and load). Elastohydrodynamic is a hydrodynamic lubrication sub-set through which the contact load is efficiently effective for hydrodynamic action to distort surfaces flexibly. The lubrication film is usually very thin compared to the thickness of the film created by hydrodynamic lubrication. [56].

A higher temperature, higher load or lower speed is treated by the mixed lubrication system that expressively reduces lubrication viscosity. With this state, the touch surface wounds in certain areas may be in contact with each other. In the case of

borders, the thickness of the lubricating film is thinner (1-3 nm) than the thickness of other wounds, and touch is very sensitive. [56]. When the load is raised or the speed is decreased, this occurs. As opposed to other forms of lubrication systems, border lubrication is a more dangerous contact condition. During the first half of the power stroke, it is present in the armature contacts (i.e. between the cylinder liner and the piston ring) when the crank angle is 0 to 90 °, as shown in(Fig.2.18) [65]. The chemical and physical properties of thin surface films are important under these lubricating conditions.

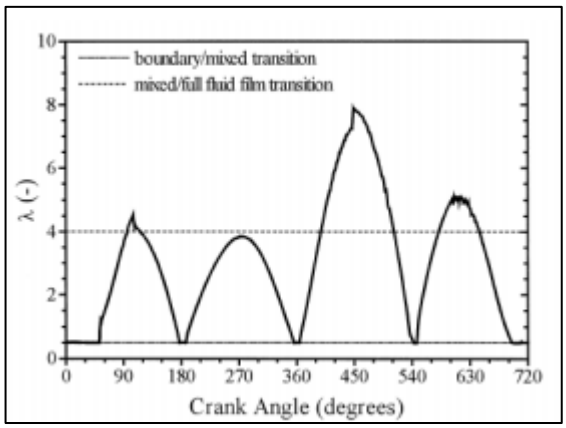

Figure 2.19. Cyclic difference of certain film wideness among a top compression ring and the cylinder wall show the lubrication system [65].

2.3.2. Mineral Oil Based Lubricants

The most popular lubricants used in the industry are the mineral oil lubricants created by the iteration process of rough oil.The main use of mineral oils are in the turbines and engines In light of the chemical composition of mineral oils, can classify them into three types consisting of paraffin (branched and straight hydrocarbons), naphthenic (recurring carbon particles) and aromatic (benzene-type composites) as shown in (Figure 2.19). The presence of various particle structure in the mineral oils could effect on the lubricant characteristics. For instance, the viscosity-temperature properties between the naphthenic and paraffinic oils are expressively different [44]. The oils of traditional engines are those oils mixed with additives. Additives are artificial chemicals that severe to enhance the present characteristics or add new features to base oil. The percentage of additives to lubricant is surrounding between 1 to 25%.

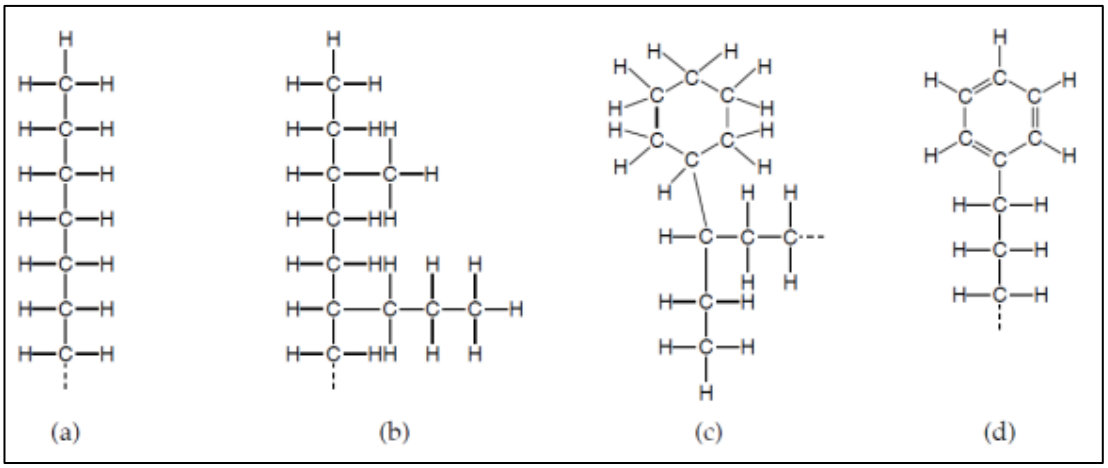

Figure 2.20. Mineral oils categories that consist (a) straight paraffin, (b) branched paraffin, (c) naphthene and (d) aromatic [44].

Table 2.2 shows the categories of additives that used in lubricating oil.

Table 2. 2. Categories of additives used in lubricating oil [108].

Categories of additive	**Purpose**	**Example**
Anti-oxidants	In order to delay the process of oil ageing	zinc dialkyl dithiophosphates
Viscosity Modifiers	In order to give a required thickness index	olefin copolymers, polyalkylmethacrylates
Detergents and Dispersants	In order to keep oil-insoluble burning by-products in postponement and inhibit the accumulation of the oxidation products in the hard elements	calcium phenates, polyisobutene succinimide
Anti-foam Agents	In order to inhibit foaming of lubricants	polydimethylsiloxanes
Anti-wear and Extreme Pressure Additives	In order to decrease wear	zinc dialkyldithiophosphates
Friction Modifiers	In order to decrease the element of friction	Molybdenum disulfide

Corrosion Inhibitors	In order protect the metal surface from the attack because of the moisture and oxygen	petroleum sulfonates
Pour-point Depressants	In order to allow a lubricant to flow at low temperatures	polymethacrylates

2.3.3. Lubricant Additives

The lubricant additives are chemical materials which can added to the base oil to offer many features to the finished oil. The limitations of features present in basic oils caused them the incapability to fulfill the requirement of high performance lubricant. They provide benefits in many ways such as improve the features of present base oil, destroy undesirable characteristics and add new properties to the base oil. The correct formation of lubricant additives and base oil are responsible to improve the tribological performance of oil particularly in boundary lubrication application. Therefore, additives are generally mixed with base oil in order to increase viscosity, enhance viscosity index, enhance wear resistance, decrease corrosion, enhance stability of oxidation, increase the life span, decrease the pollution and decrease the friction. The overall categorization of lubricant additives consists anti-oxidants, pollution control additives, viscosity reformers, pour point depressants, anti-wear and extreme pressure additive, corrosion control additives, foam inhibitors and friction modifiers. The scope of this study will only include the above three mentioned additives (friction modifiers, antiwar and extreme pressure additives and anti-oxidants) to be mentioned and clarified in this part.

2.3.3.1. Friction Modifiers

This is a significant kind of additives in frontier lubrication which work below the absorption mechanism (chemical or physical adsorption) to practice a “carpet” of particles on the substrate surface as shown in (Figure 2.20). They are used to decrease the friction of surface and inhibit the phenomena of stick-slip [44]. In general, they are

polar chemical combinations which characterize by a high similarity for metal surfaces and enjoying by long alkyl chains. In base oil, the friction modifiers are classified into three classes including nanoparticles, oregano-molybdenum compounds and organic friction modifiers [66].

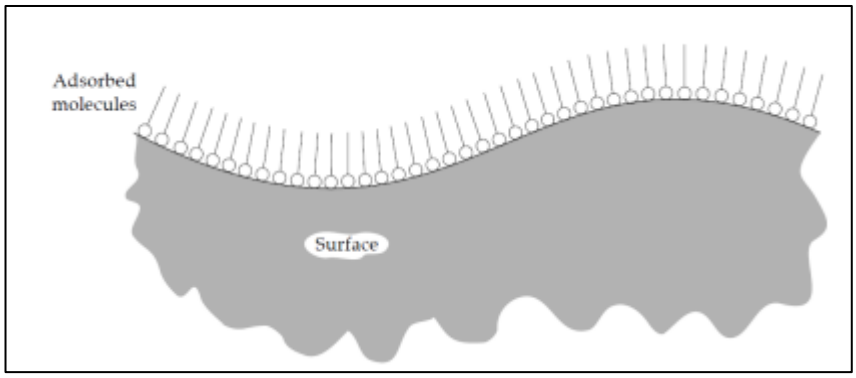

Figure 2.21. Adsorption lubrication technique by boundary additives [44].

A hundred years ago, organic friction modifiers were invented which are usually long-chain hydrocarbons with polar end groups [67]. It is composed of carboxylic acids [68, 69], esters [70], alcohols [71], amines [72], polymers [66, 73], etc. Where the polar end groups are inserted to the metal surface friction rates either by chemical reaction or Psychological absorption whereas hydrocarbon chain includes lubricants. Fatty acids are distinct additives that have been used in the carboxylic acid group. It was found that the friction behaviour of the hexadecane solution by using the ball scale on the disc is affected by the types of acids where the submerged fatty acid (fatty acid) gives less friction compared to its unsaturated counterpart (oleic acid) as we have shown in Fig. 2.21 [74]. It has been suggested that the behaviour of saturated fatty acids as a linear formation favours the formation of a more coherent monolayer on the surface [68] that contributed to a slight friction result [74]. Nevertheless,, uses of carboxylic acids as auxiliary engine oil transfer oil are currently declining as they are found to be wear bearings for engines [75].

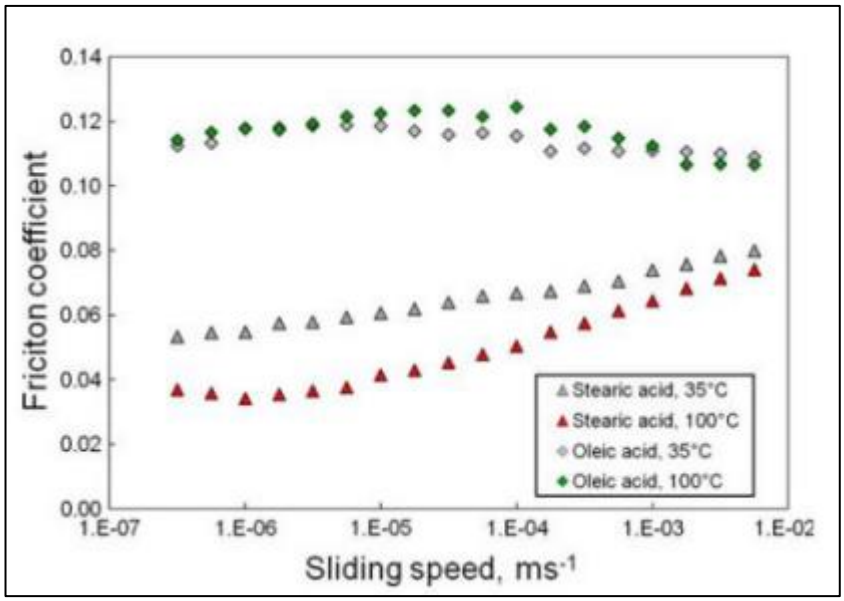

Figure 2.22. Friction against sliding velocity of 0.01 M fatty acids in hexadecane solution at 35 °C and 100 °C [74].

A sufficient additive was discovered in the 1980s to reduce wear and friction in the boundary lubrication system and are organic molybdenum formulations [76,78].Where it consist of three groups (Fig. 2.22) including sulfur and phosphorous free compounds including molybdates, sulfur Which contains phosphorous-free compounds, specifically molybdenum bicarbonate molybdenum (MoDTC) and compounds comprising sulfur and phosphorous, specifically dicalkyl molybdenum. [79]. The reduction of friction at the friction surface was associated with the formation of small molybdenum disulfide (MoS2) nanostructures with a distinctive laminate structure [67] which creates a low shear strength material [66, 80]. For instance, it is informed that the MoS2 was cofngiured with molybdenum oxides from MoDTC degradation on the contact surfaces by means of a triple chemistry reaction [81]. Organo-molybdenum compounds have another interesting advantage as it has been found that instead of acting as a friction modifier, they can also be used as anti-corrosion additives because both MoDTP and MoDTC have been discovered to reduce wear and friction [82]. Moreover, it has been found that MoDTP has good anti-corrosion features in mineral oil [83] whereas molybdate and MoDTC show better corrosion resistance synergism with zinc dimethyphosphate (ZDDP) [78, 79].

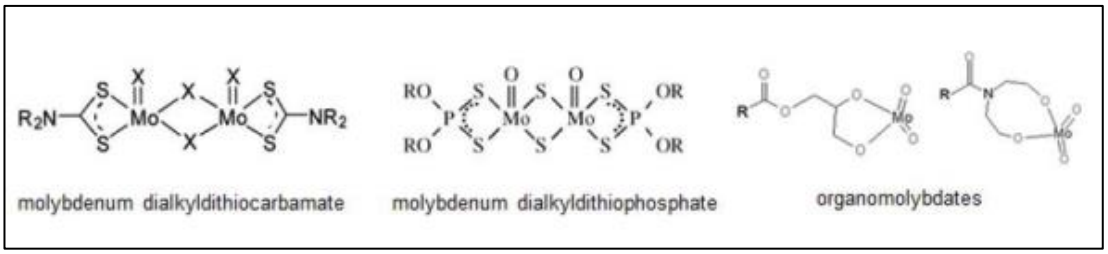

Figure 2.23. Three categories of organ-molybdenum friction modifiers [67].

Recently, numerous research, development and studies have been presented in the fields of nanotechnology and chemistry, the probability to produce a friction rate dependent on nanoparticles [84]. Nanoparticles are elements ranging in the size from 2–120 nm [66] which generally include metallic oxides (such as TiO2, CuO, titanium dioxide, and copper oxide), fullerenes, borates and phosphates, metals (such as copper and copper), and mineral fullerenes or oxides. We want boron [67]. They were added to lubricating oils as friction transformers to decrease the friction and wear [84-86]. It has been discovered that the tribological performance as a friction modifier is effected by elements including concentration, size, nanoparticle structure and shape [87]. There are three techniques through which nanoparticles can decrease the applied pressure, as mentioned by Julie et al. (Figure 2.23) [88]. Particle progressing may arise at low pressure subject to particle hardness and shape. At medium pressure, the particles stay intact but slide over the surrounding surfaces. At high pressure, the particles are creased to form a mesh layer with low shear resistance and, thus, give less friction factor [88].

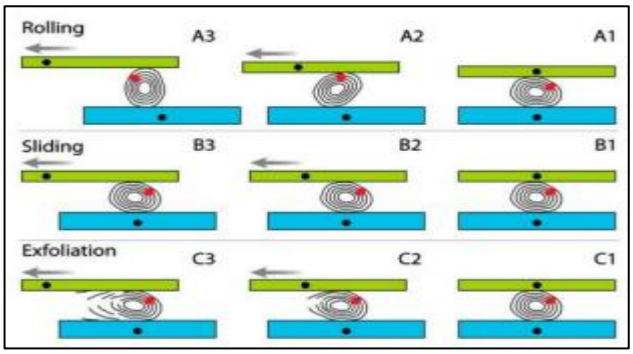

Figure 2.24. The three main techniques of friction: rolling (A), sliding (B) and exfoliation (C). The minor substrate is immovable whereas the higher substrate is slit to the left. The red sign refers to the point of a nanoparticle [88].

2.3.3.2 Anti-wear and Extreme-pressure Additives

These types of additives shield rubbing surfaces from interaction between metal and metal, thereby preventing seizures and minimizing wear under minimal lubrication conditions. Anti-wear additives work to minimize the wear ratio by shaping films, whereas extreme pressure additives are projected to respond quickly to a surface under high distress to avoid more disastrous impairment, including galling, seizure and scuffing. [89]. Many extreme pressure additives incline to be so powerful that they can affect oil oxidative stability [90], others are metal corrosive [91, 92] and may decrease the machine modules life [93]. In general, in engine oils, extreme pressure additives are not normally used. They are used only when the lubricant, for example in a gear tooth contact, is subjected to high stress conditions. Sulfurized olefins (EP additives), phosphates, phosphate esters, metal dithiocarbamates, metal thiophosphates and borates [94] are available in a variety of forms. Zinc dialkyldithiophosphates (ZDDP) are still commonly utilized in oils of engine among the collection of additives mentioned above, despite being the first additive produced in the forties of the last century. [95].

ZDDP is made by alcohols response with phosphorus pent sulfide (P2S5) to create dialkyldithiophosphoric acid. Later, it is neutralized by the zinc oxide to produce the invention as clarified in (Figure 2.24) [96]. The lubrication mechanism conducted by ZDDP has been studied by many researchers in order to be comprehended [95, 97, 98]. The mechanism begins by forming the layer that includes the compound of organic iron and ZDDP corrosion element and metal oxides diversified with the metal substrate on the surface of metal as shown in (Figure 2.25) [99]. The ZDDP is analyzed by sliding to create an iron polyphosphate and glassy zinc that mixes with the OMM layer and delivers the wear-resistant action. Later, at high loading and temperature, the organic ZDDP element will produce the concurrent development of OIC and OMM layers. Anti-wear iron phosphate pads and a solid anti-wear film comprising higher P, Zn and S concentrations are then created (known as OIC-Zn film). The OIC-Zn films form a strong protective layer from wear during continuous sliding, while the OMM layers can wear out. The OIC-Zn films can also promote metallic iron, iron carbide and iron oxide film formation.

These ZDDP brought films enjoy by high loading capacity and operate as an anti-scuffing film and an anti-wear in protecting the steel substrates [99].

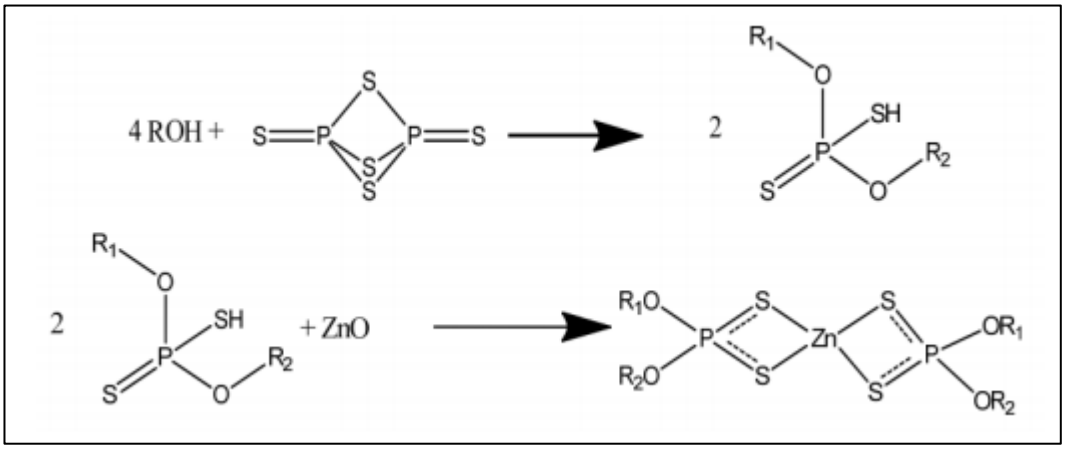

Figure 2.25. Approach to prepare the zinc dialkyldithio-phosphate (ZDDP) [96].

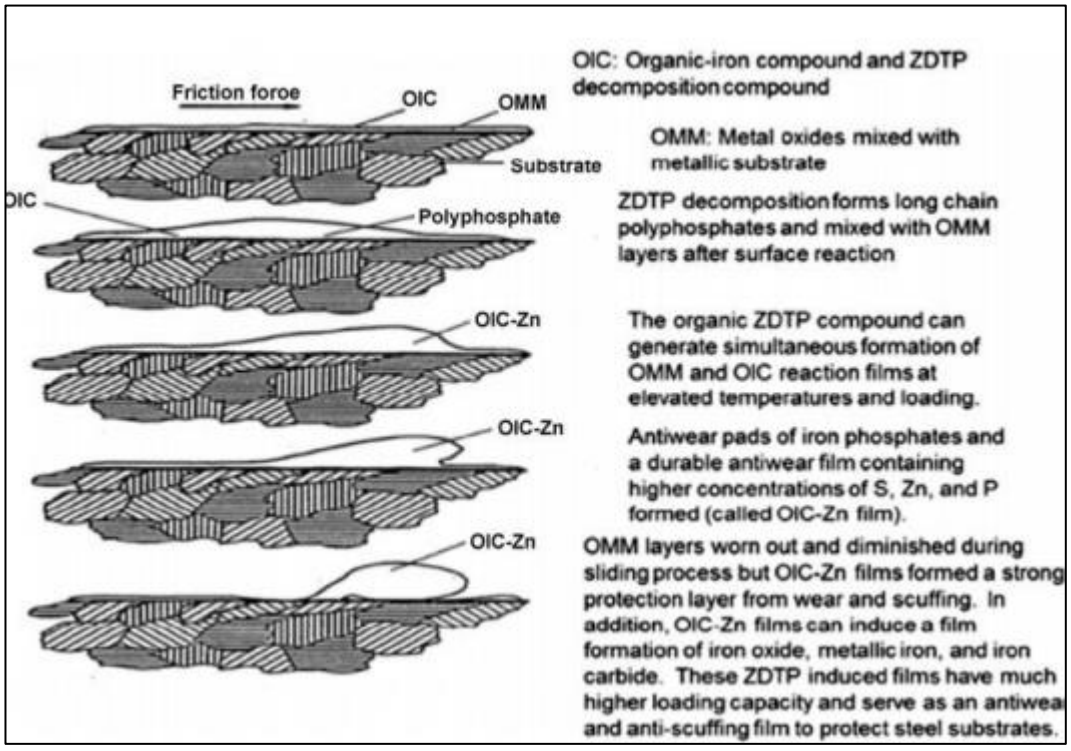

Figure 2. 26. Antiwar film formation technique by ZDDP [99].

2.4. SILVER NANOPARTICLES

Nanoparticles silver use started by the glass founders from the Roman Empire time where it includes efficient optical properties. This is proven by the purported Lycurgus

cup (4th century AD) which is presented currently in the British Museum. Studies on the configuration of its bronze-mounted inclusions of stained glass performed later of last century detected the existence of metal nanoparticles (the average diameter of 40 nm) which includes alloys of gold by 30% and alloy and silver by 70% [80]. This illustrates an extraordinary characteristic of this bowl to change its color from the red color in convoyed light to the grayish green color in reflected light. In order to prepare this glass, it is required the formation of silver in the same location. Before the eighties of last century, there were practical and scientific interest in silver nanoparticles due to the ability to be used as dispersed supports to improve the signals from the organic particles in the Raman spectroscopy [81].

Preliminary studies performed in the last few decades showed that the silver nanoparticles show a rare mixture of value properties and they are the unique optical proprieties related to the well-built surfaces, catalytic action, high electrical dual layer capacitance, surface Plasmon resonance (SPR), etc.[82]. This is the reason behind their work as materials to develop the new generation of sensor, optical and electronic devices. During the last two decades, the efforts of reducing and the significance to modernize the technical process led to high increase in the number of practical researches and studies dedicated to the combination and features of silver nanoparticles. Currently, the synthesis of these combinations is considered of the most developed trends in colloid chemistry. The silver is commonly used to oxidize the methanol to formaldehyde and ethylene to ethylene oxide [83]. Colloidal silver occupies great importance due to its typical characteristics including antibacterial activity chemical stability, good conductivity and catalytic [84]. For instance, it provides many benefits to surface improved spectroscopy because it partially needs for connected surfaces to electricity [85, 86].

2.4.1 Synthesis of Silver Nanoparticles

Currently, scientists in the field of materials perform studies and researches to develop new materials with better features, functions and less cost than the existed ones. Many biological, physical and chemical production approaches were developed to improve the nanoparticles performance presenting enhanced features which work to include

good control through the morphology, distribution and particle size [87, 88]. Mixture of nanoparticles to include good control through the size, quality, purity, morphology quantity and distribution of particles by the use of environment friendly economic process are the main obstacles for researchers [89]. The most commonly used method to prepare the nanoparticles of silver as stable, colloidal scatterings in water or organic solvents is the chemical decrease [90, 91]. The most frequently used reductants are borohydride, elemental hydrogen, ascorbate and citrate [81, 87]. In general, the colloidal silver is usually created by decrease the silver ions (Ag+) in aqueous solution with particle diameters of numerous nanometers. If the colloidal particles are slightly less than the wavelength of visible light, the solutions will consist of a brown yellow color with a large band ranging between 380-400 nm and other less or less effective bands in the captivation spectrum at longer wavelengths [85, 86].

The combined excitation of the electron gas in the elements is supported by this band with a steady change in electron density at the surface (absorption of surface Plasmon) [82]. The literature indicates that using a strong reductant, like borohydride, can produce small particles which are rather monodispersed, but it is difficult to regulate the formation of larger particles. The use of weaker reducing agents, like citrate, would lead to a slower reduce ratio, but the size of distribution was far from constrained. The controlled mixture of Ag NPs depends on a two-step decreasing process. A strong reduction element is used in this mechanism to produce small Ag particles that expand in the subordinate step by reducing more with a weaker reduction element. [81]. In the secondary process, several researchers explored the expansion of particles from approximately 20-45 nm to 120-170 nm [86]. In addition, the primary condition was not reproducible and it required particular equipment. Thus, in the presence of stabilizers, the synthesis of nanoparticles by chemical reduction approaches is typically carried out to avoid undesired aggregation of the colloidal silver solution of the nanoparticle.

2.4.2. Biochemical Synthesis of Ag Nanoparticles

The most common methods to prepare the nanoparticles are the chemical methods. Nevertheless, many chemical approaches cannot avoid using the toxic chemicals in the

synthesis protocol. As nobles nanoparticle metals including platinum, gold and silver nanoparticles are commonly used in human contacting regions, there is increasing interest to develop globally approachable operations of nanoparticles mixture which do not utilize toxic chemicals. Many organic methods of nanoparticles mixtures have been suggested by the use of plant or plant extract [87], microorganism [92] and enzyme [91] as possible sustainable substitutes to chemical and physical approaches. The use of plant nanoparticles may provide many benefits over other biological operations by removing the intricate operation to maintain cell cultures [93]. It can also be better improved for important nanoparticle mixtures. It is normal that several metal or metal which consist of particles in the nanometer size scope can be offered by the biological system. The mixture of magnetite nanoparticles by magneto tactical bacteria, silica materials by diatoms, and layers of gypsum and calcium carbonate by S-layer bacteria are some typical examples. The assembly and synthesis of nanoparticles can be helpful in the production of "green chemistry "procedures that are clean and environmentally safe and involve species ranging from bacteria to fungi and even plants [94, 87]. Multicellular and unicellular species are also well known for creating both intra- and extracellular inorganic materials. The sp. of Verticillium. Bare to aqueous AgNO3 solution fungal biomass resulted in the intracellular formation of silver nanoparticles, while extracellular silver nanoparticles were caused by Fusarium oxysporum biomass [95]. Microorganisms such as actinomycetes, fungi, bacteria and yeast have been suggested for the development and application of nanoparticles. [87, 96].

2.5 APPLICATION OF SILVER NANOPARTICLES

Silver nanoparticles include many use in many sciences such as materials science, catalysis and biomedical. The reason behind this is the unique features they enjoy if compared with their bulk solid. At this section of our study, we will result in a brief review of these applications.

2.5.1 Human Health

Nanoparticles include several impacts on human health based on the bulk materials through which they are created [97]. Increasing the biological activity of nanoparticles man provide benefits, damages or both on human health. Some of the nanoparticles are adequately small to reach to the brain, lungs and skin [98,99]. Exposing to metal comprising nanoparticles of human lung epithelial cells create reactive oxygen species that cause cells damage and oxidative stress [100,60]. A research on toxic impact of silver nanoparticles has been implemented on zebrafish as a model because of its rapid expansion and apparent structure of body. The result of the research showed particles deposition on organs and high expansion impacts. The toxicity and biocompatibility of silver nanoparticles have been shown by perceiving single silver nanoparticles within embryos in every development phase. The categories of abnormalities in zebra fish were highly depended on the silver nanoparticles dose [101].

2.5.2 Environmental

Silver nanoparticles configure great fear to the biological systems and wastewater treatment services. The inhibitory impacts of silver nanoparticles on microbial growth have been assessed in a treatment facility by the use of extant respirometer mechanism. The nitrifying bacteria is vulnerable to reserve by silver nanoparticles that may configure harmful impacts on microorganisms in the wastewater treatment. In recent years, the environmental threat of silver nanoparticles have been studied by identifying the released silver of traditional clothing. The wash water and sock material included silver nanoparticles of 10–500 nm diameter.

2.5.3 Catalytic Action

High surface energy and high surface zone determine metal nanoparticles of being efficient catalytic medium. It is noticed that the growth of small silver particles is resulted in more efficient catalyst than the particles of stable colloidal. These emergent particles are catalyzed the borohydride decrease of numerous organic dyes. The decrease ratio catalyzed by growing particles is particularly quicker compared with

large and steady particles that considered the final product of growing particles. Catalysis is because of the effective particle-mediated electron transfered from the BH4 - ion to the dye. The activity of catalytic particles is based on the dye-particle interaction, E1/2 of the dye and size [102].

2.5.4 Antimicrobial

Silver is considered antibacterial, non-toxic and safe agent. It has been used for many centuries to kill 650 microorganisms which cause disease [103]. It was described as being ‘oligo dynamic’, which is able to cause bacteriostatic (growth reserve) or even a bactericidal (antibacterial) effect. So, it enjoys by the ability to use bactericidal impact with high absorption. Silver has high importance for many applications including prevent infections, healing injuries antibacterial agents for antibiotic resistant bacteria and anti-inflammatory. Silver ions (Ag+) and its composites configure great toxic on organisms where it may exhibit high biocidal impact on many types of bacteria but with low toxicity to animal cells. So, solver ions (Ag+) as antibacterial element is employed to formulate coatings, dental resin composites, ion exchange fibers and bone cement for medical devices.

The bactericidal activity of nanoparticles is related to the existence of electronic impacts which acquired due to smaller size changes in the local electronic surface structure. These impacts contribute in enhancing the silver reactivity of nanoparticles surface. It must be mentioned that silver in ionic shape highly interact with thiol groups of vital enzymes and inactivates them. It is proposed that when bacteria are preserved with silver ions, the DNA loses its ability to replicate [103]. Silver nanoparticles threaten the future plasma membrane and deplete intracellular adenosine triphosphate (ATP) levels by pointing to the membrane of bacteria that result in the death of bacterial cells. In burn treatment, sterilization and drinking water, conventional silver compounds, including silver sulfadiazine and silver nitrate, are used to prevent the growth of bacteria. For antibacterial functionality, silver is economically merged into polymers, catheters, fabrics and composites.

PART 3

NANO MATERIALS

3.1. NANO MATERIALS SCIENCE

In general, nonmaterial particularly graphite have been used only as dry lubricants in very hard circumstances such as high temperature where it is supposed that organic lubricants are inappropriate [28]. Many studies and researches have proven the ability to organize size, shape and surface practical nanoparticles groups [23]. This has increased the possibility of the use of nanoparticles in colloidal structures in related fields, including science and technology such as grease [129,130], oil [131], biomedicine [132,133], etc. There are nanofluids called colloidal nanoparticle suspensions. Choi initially projected nanofluids in 1995. It must be understood that the nanoparticles features have a great effect on the nanofluids existence. Metals (Cu, Ag, Au, etc.) [134,135], metal oxides (TiO_2, ZrO_2, Al_2O_3, SiO_2, etc.) [136,137], carbon (graphene, carbon nanotubes, diamonds, etc.) [138] are the most widely used and researched nanoparticles so far [138]. Adding nanoparticles to lubricants considerably decrease interfacial friction and increases component which carry capacity [139,140]. The effect of SiO_2 nanoparticles and diamonds on the tribological features of paraffin has been investigated by Peng et al [141]. It is discovered that the varying factor of friction depends not only on the nanoparticles concentration but also on the time of contact among two steel bearing surfaces. As pure liquid paraffin is used, the factor of friction increases with time, as shown by the bond between the contact surfaces. Nevertheless, as the testing time increases, it is found that when SiO_2 nanoparticles or diamonds are applied to the main fluid, the friction factor decreases monotonically and becomes stable after a definite period of time. In order to clarify the technique of the impact of nanoparticles on the tribological characteristics of lubricants, several theories were proposed by the researchers, such as the impacts of 'ball bearing'[142,143], 'protective film', 'mending'[144] and 'polishing'[143].

It must be mentioned that the nanoparticles introduction to lubricants is a complex issue because nature, size, concentration, shape, etc. are very significant elements that affect the performance of the lubricant. Stachowiak et al. [145] and Martin and Ohmae [146] mentioned that because of the high surface energy despite the size, nanoparticles tend to collective, agglomerated or syrupy after being entered to most of the liquids particularly when these are bare to change in temperature or pressure. Some nanoparticles configure a problem to spread in a liquid stage (base oil). Inorganic fullerenes, for example, reflect spherical or cylindrical mineral particles with a particle size varying from 50-150 nm. They have no preference of oils and without the use of surfactants, their dispersion is difficult. The nanoparticles concentration is thought would be no less significant. It is noted that the friction factor depends on additive concentration. Nonetheless, it must be mentioned that several researches were carried out under many circumstances [147, 148] that referred to a reduction in friction and a claim about the ability to carry parts when adding nanoparticles at a b1 %. Struggles are being made to study nanoparticles as lubricant additives, taking these details into account.

Nanotechnology requires the ability to monitor nanoscale features (10-9 m), and a number of mechanism have recently been created which offer this ability to humanity. The problems of chemistry and physics should be discussed on these scales from a basic science perspective. The response can be controlled by surface and boundary effects. "In this length scales range, several of the classical variations between mechanics, materials and physics vanish, and a new form of thought arises that is generally called nanoscience (occasionally funnily translated as "so few science"). The last quick growth of nanoscience, combined with the development of computational technologies that are most successful on small scales is resulting a newly discovered ability to perceive and monitor the structure in small time scales and length. By differentiating between what we can influence and what we can understand, one method to differentiate between nanoscience and nanotechnology. Much of whatever we deal with as humans has a nanoscale structure, that is, most materials have a nanoscale substructure. The center of nanoscience understands what the nanoscale structure acts (in terms of phenomena and action). The essence of nanotechnology is to monitor nanoscale structure so that a desired end can be achieved. Nanotechnology

cannot prosper without nanoscience, and when the requisite nanoscience is already available, the most effective development of nanotechnology (and growth with low risk) arises.

Currently, the science of nanomaterials is the science which allow much nanotechnology (indeed in the widest sense, nanotechnology is not be possible without nanomaterials). That very many nanoscale phenomena are either modulated or controlled from a punitive point of view, so nanomaterials play a critical role in the science of mechanics. Nanomechanics regulates phenomena as directly evident as the interaction of Nano size interfaces of crystal and as understated as protein folding (organizing and governing the living cell).

A nanomaterial is a substance in which there is an order of 100 nm or less of some controllable related dimension. In order to describe a nanomaterial, the mere existence of nanoscale structure only is not efficient, as all of the materials include structure in this collection. On this scale, the ability to monitor the structure is important. In this context, one might discuss that several of the traditional alloys and structural materials comprising nanoscale elements could be considered nanomaterials by nature (for instance alloys of ODS Oxide- and Dispersion-Strengthened). Conventionally, however, classical structural materials are not included in the current use of the term. Nanomaterials are newly designed materials in modern use, where the structure of nanoscale which is being monitored has a main influence on the material or device's desired behavior.

3.2. THE DIFFERENT CLASSES OF NANOMATERIALS

Three distinct types of nanomaterials exist discrete nanomaterials, materials for nanoscale applications, and bulk nanomaterials shown in (Table 3.1). Discrete nanomaterials or dn materials are freestanding material components in at least one dimension and 1-10 nm in scale (examples consist nanoparticles and nanofibers including carbon nanotubes). Materials of nanoscale devices or materials are components of nanoscale material found inside devices, typically as thin films (for

example of material may be the thin film of metal oxide utilized inside some semiconductor fabrication).

Table 3.1. A wide category of nanomaterials based of dimensionality and morphology.

Type of nanomaterial	Dimensionality	Morphology	Characteristics	Remarks
Discrete nano (dn) materials	0D or 1D	Particles, fibers	Large surface functionalization	Potential health hazard
Nanoscale device (nd) materials	Usually 2D, occasionally 1D	Thin films, sometimes wi	Functionalization, electrical/thermal characteristics	Semicond uctor fabrication
Bulk (nc or ns) nanomaterials	3D	Minimum mm3	Mechanical and structural applications	-

3.2.1. Characteristics of 2D Materials

If only one of its dimensions is nano-sized, materials may be properly described as 2D material or nanosheet, typically resembling a big sheet with one or little layers of atomic thickness (more such as a paper sheet). Because of their wonderful range of chemical properties optical, physical and electronic that are lacking in their bulk complements [17]. They characterize by certainly attracted important industrial and academic interest since their discovery. [20,21]. In order to determine the true contact zone and the frictional pinning probable, the high flexibility degree related to 2D materials when they are in contact with close objects plays a significant role[22,23]. In addition, the dispersion of 2D materials in aqueous solution is an appropriate prerequisite for the design of 2D-based films [24], and because the entire atoms of 2D materials are surface atoms, this delivers an appropriate means of altering the material properties by means of surface functionalization and alteration. [25, 26].

Current nanoscale investigations have detected that the layered materials, down to one atomic layer, similarly present exceptionally low surface friction if they were slid against other counter surfaces [27, 28]. Standard atomic arrangements, in addition to

poor interlayer interaction, are also recognized to affect those materials with the ability to accomplish super-low friction, otherwise known as super lubricity. [29,30]. In addition, it has been clarified that the static frictional force steadily raises for a little primary atomic cycles before accessing into a steady value with regard to few-layered 2D materials. When the number of 2D layers increases, the fleeting activity and the related enhancement of the steady-state of friction reduces and was only noticed when the 2D material was insecurely attached to a substrate [23, 31]. Li et al. replicate the experimental outcomes on layer-dependent friction and transient frictional consolidation on graphene Nano sheets by the use of atomistic replications. [23]. The analysis of atomic force proved that the development of static friction is a protest of the innate propensity for thinner and less-constrained graphene in order to re-arrange its shape as a direct elect in its higher suppleness. The tip atoms become more resolutely pinned and detect higher synchrony in their stick-slip attractiveness. Atomic force study has clarified that static friction development is a demonstration of the intrinsic propensity of thinner and less limited graphene to re-arrange its structure as a direct e-impact of its higher flexibility. In its stick-slip character, the tip atoms become more firmly pinned and present high synchrony. Although the amount of atomic-scale contacts that are the real contact area increases, in frictional sliding on graphene nanosheets, the local pinning status of individual atoms and the comprehensive commensurability also rises. From Lee et al. [31] the nanotribological properties of some chosen 2D materials, including graphene, MoS2, h-BN and niobium dieseline (NbSe2), which were isolated by mechanical exfoliation from their bulk origins, were analyzed. Friction on all the four 2D materials has been shown to be greater than that of their bulk sources. Their research suggests that the higher friction is correlated with the thinnest layers known as the puckering e-low ect's bending stiness. In order to understand the mechanism of sheet sti-ness in friction, they used a simple model of a tip sliding over an elastic membrane. Here, there is normally a local puckering due to adhesion when the tip comes in contact with the top surface [32]. This is due to the sheet's low bending sti-ness compared to its in-plane sti-ness. By tip-sheet friction, the puckered geometry can be adjusted at the front edge. Since the result rise in the tip-sheet contact zone, this out-of-plane puckering could clarify the raised friction. In addition, it could be because of the extra work needed to transfer the puckered area. The puckering e-ect becomes more substantial as the layer becomes thinner. In

comparison, graphene, MoS2 and h-BN have much lower friction (~1 nN) compared to NbSe2 (~7 nN). From Zhou et al. [33]

This is due to the sheet's low bending sti-ness compared to its in-plane sti-ness. By tip-sheet friction, the puckered geometry can be adjusted at the front edge. Due to the resulting rise in the tip-sheet contact area, this out-of-plane puckering could explain the increased friction. In addition, it could be because of the extra work needed to transfer the puckered area. The puckering e-ect became more substantial as the layer becomes thinner. In comparison, graphene, MoS2 and h-BN have very lower friction (~1 nN) compared to NbSe2 (~7 nN). From Zhou et al. which being said, as sliding continues and more heat is produced, the tribochemical reaction of the contact surfaces between the lubricants and the substrate is triggered, leading to the breakdown of the protective film and the improvement of the new film[4]. It is understood that this new film enhances tribological behavior significantly [38]. In addition, the high temperature produced through sliding could melt the nanosheets, allowing them to fill the contact surfaces with micro-holes, gaps and concave zones, thereby reducing friction and wear. [39].

3.3. APPLICATIONS AS LUBRICANT NANO-ADDITIVES

The use of nanomaterials as greater solid lubricants or nano-additives was recently attracted tremendous interest because of their specific characteristics, such as smaller scale, chemical and thermal stability [149,150]. At the sliding contact interface, these nanomaterials can easily form a shearing thin film giving rise to low friction, can also fill and/or fix the micro/nano cracks formed on the worn surfaces, demonstrating comprehensive benefits to improve lubricant oils' tribological performance [151]. In order to minimize wear and friction of hydrogenated steel diamond-like-carbon (H-DLC) contacts working at high contact pressures and sliding speed, Mutyala and coworkers [152] used a composite combination of graphene and MoS2 as a solid lubricant. Compared to Steel vs H-DLC (baseline) studies, the sliding friction tests carried out under dry nitrogen conditions showed a reduction of friction by 16 times and wear by 29 times as clarified in(Figure 3.1). In addition, a decrease in friction by a factor of 43 and wear by a factor of 434 compared with self-made steel against steel

experiments was observed. The TEM images confirmed the deposition of the tribolayer on the ball and disc and the amorphous carbon mixed with graphene layers consists of the wear debris. Tribochemistry results in the formation of amorphous carbon by the active disintegration of MoS2 at the tribological interface under the influence of high contact pressure. The primary mechanism is assigned.

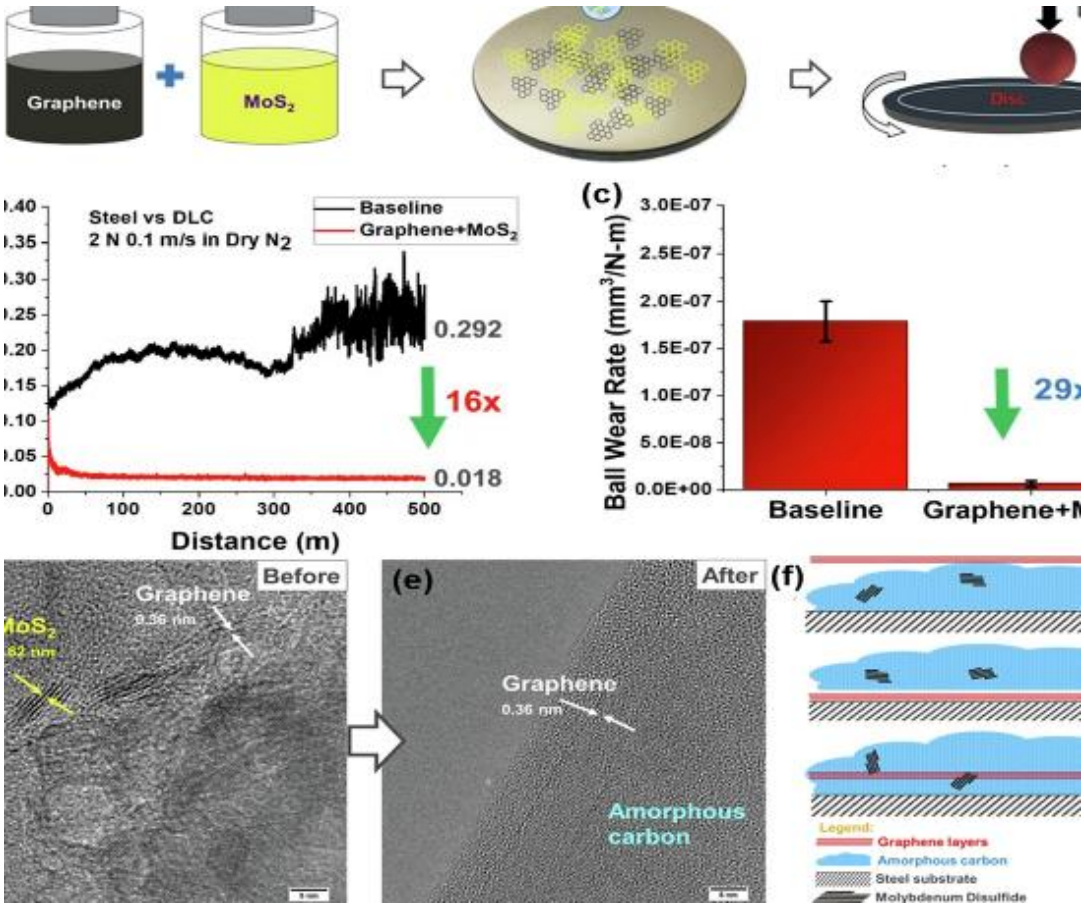

Figure 3.1. Graphene + MoS2 solid lubricant via drop-casting method: (i) Mixing of the solution-processed graphene andMoS2, (ii) Drop-casted onto steel disc and (iii) Ballon-disc configuration.

Test. (b) Baseline and Graphene + MoS2 test COF graph, (c) Baseline and Grapehene + MoS2 ball wear rate comparison. TEM images presenting (d) the existence of Graphene and MoS2 prior to testing in the as-prepared solid lubricant and (e) the wear debris consisting of graphene layers mixed with amorphous carbon. (f) Mechanistic model that describes graphene mixed amorphous carbon in partially disintegrated MoS2 layered di-erent configurations. Reproduced with authorization from. [153].

3.4. FUNCTIONAL LUBRICANT ADDITIVES

Base oils (as a lubricant base) play a significant role to lubricate motion surfaces, thus minimizing surplus heat, decrease wear and contamination of system. However, sufficient additive materials must be applied to the lubricant materials in order to enhance their basic properties, including anti-corrosion safety, anti-friction and anti-wear protection, oxidative stability and biodegradation resistance. Their classification defines the function of the additives [153] (Table 1). Figure 5.2 demonstrates how nanoparticles work in lubricants. As shown in Table 1, a wide number of lubricant additives are properly used by the industry. Around the same time, it must be noted that the process of creating new additives continues, as both environmental services and equipment manufacturers are gradually hardening the specifications of lubricants. It is also necessary to gain a good edge in operative efficiency.

3.4.1. Nanoparticle parameters affecting the tribological properties of lubricants

The ability of nanoparticles is influenced by the tribological properties of lubricants. This is attributable to many properties and their extraordinary scale is the most significant of them. It was noted that the structure, scale, functional surface groups, shape and nanoparticles concentration are the most significant factors that affect nanoparticle tribological characteristics depending on lubricants [154,152].

3.4.2. Nanoparticle Size Effect

The internal mechanical and physic-chemical properties are determined by the size of nanoparticles which in turn effect their tribological characteristics shown in (Figure 3.2.) For example, Hall-Petch mentioned that nanomaterials solidness increases when the grain size of 100 nm are increased [155,156] and basically their elasticity increases at values 10 nm [157,158]. Nevertheless, if nanoparticles are solder than the surfaces of rubbing, this may cause wear. Therefore, this must be taken into consideration.

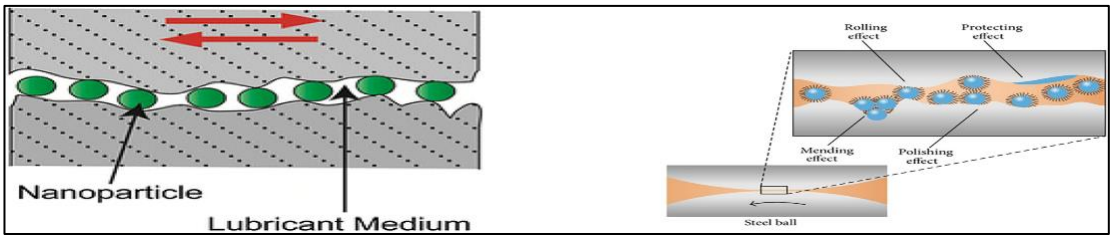

Figure 3.2. Working of nanoparticles in lubricant

Roughness of rubbing surfaces is an important issue which must be taken into account because if the nanoparticle radius is bigger than the irregularities size, tribological features will not follow from the nanoadditive. Nevertheless, if the roughness of surface is much greater than the radius of nanoparticles, the nanadditive will fill the irregularities. Thus, artificially levelling the surfaces of friction and, consequently, leading to an enhancement in the tribological characteristics [159]. The lubricant composition similarity relies upon the size of nanoparticle. Stokes [160] mentioned that probable enhancement in the depression solidity happens with reduce in the nanoparticle size.

3.4.3. Nanoparticle Form Effect

Another important factor which must be taken into the shape of nanoparticles is the explanation for the creation of nanomodified lubricants. For example, as compared to nanoplatelets, nanospheres would be subject to higher pressure at a particular load because the contact surface zone of the previous one is often smaller. Therefore, the use of amellar nanoparticles, distortion of rubbing surfaces is at least possible.

3.4.4. Internal Nanostructure Effect

The mechanical properties and therefore tribological properties can be effected by the internal structure of nanoparticles. For instance, vacancies (the pretended Schottky defect) in nanomaterials prevent the dislocations motion, thus, increasing the mechanical strength [161,162]. So, the existing of a few number of atomic vacancies may increase the mechanical strength of nanomaterials. Thus, this may affect

positively on the topological properties. Nevertheless, high amount of shortcomings may decrease the mechanical strength of nanomaterials. For example, Young's modulus and tensile strength will regularly decrease with every atomic shortcoming of a nanotube [163].

3.4.5. Surface Functionalization Effect

In the developmental sense of nano-modified lubricants, surface function plays an important role. Because of their bonding by strong van der Waals forces [164], non-functionalized nano-particles typically appear to combine. For example, nano-particles coated with surfactants enjoy higher tribological characteristics because of the following issues:

1) Surfactant molecules are bound to the nano-particles, therefore generating a buffer around them and that and thus weakening the powers of van der Waals as the distance between these particles increases, thus inhibiting agglomeration;
2) The nanoparticles are bound to surfactant molecules, so their internal polarity becomes the same across the entire external surface. Because we know that the shells are similarly charged for all nanoparticles, they repel each other and thus agglomeration is avoided.
3) The nanoparticle surface is shielded from direct interaction with surfaces by the surfactant;

By the way, in a case where increased colloidal strength and homogeneous distribution of nanoparticles in the base oil are needed, surface functionalization is a significant event.

3.4.6. Nanoparticle concentration effect

Researches and studies referred that the amount of nanoparticle in base oils highly effect tribological features of lubricants [165]. Nevertheless, it is necessary to consider

the entire operating system variables in order to consider the optimal focus of the lowest friction element.

3.5. PHYSICAL AND CHEMICAL ASPECTS OF SURFACES DURING FRICTION

The most important issues to validate durability and quality stability when using tribotechnical materials are the establishment of frequencies of conjugated solids wear over the action of friction forces. Because of the permanent changes in the operational features of surface layers, the wear phase is an integral process. This ensures that the effects of several processes occurring at local surface microsites over time are explained. The homogeneity of the processes taking place at the interface and the machineries of friction surface wear can be measured by regulating the chemical and physical phases of surfaces by friction. And as such, if the interatomic distance between two surfaces is reached, the same striking forces operate between them as in the bulk of the material. In several ways, comparable powers exist as follows:

1) Ionic bonding occurs between electromagnetic force held together through cations and anions. Ion bonded solids possess high strength, like alumina;
2) Covalent (homopolar) bonding takes place between neutral atoms by overlapping their electronic fields, resulting in a very deep connection (e.g., diamond);
3) Metallic bonding is common for two metals and is due to the ability of electrons to pass freely between the ionic lattice nodes. Only in the absence of films on their surfaces does a similar bond take place between some of the rubbing surfaces;
4) Bonding of Van-der-Waals can occur between any molecules or atoms due to dipole-dipole interaction. The physical adsorption of environmental elements on the solid surface is responsible.

3.6. SURFACE MECHANICAL ATTRITION TREATMENT

By hitting the surface repeatedly with hardened materials, large plastic deformations can also be achieved on the surface (as in shot peening). The standard method involves seating the sample inside a chamber filled with a large number of hardened steel balls, then using a vibration generator to shake the entire chamber [166]. The steel balls can be induced to impact the specimen at relatively high velocities by careful tuning of the frequencies and produce reasonably high strains on the sample in a surface layer. Continued vibration may lead to the surface layer's microstructural refinement. This method is very close to the mechanical attrition process in order to produce nanoparticles in ball milling; since it is restricted to a surface, the process is called the treatment of surface mechanical attrition or SMAT. The difference is the nature of a surface layer and associated brush strokes of strain and microstructural gradients. Atmosphere regulation in the chamber, vibration frequency and temperature enables one to control the produced microstructures.

PART 4

MATERIAL AND METHOD

4.1. SYNTHESIS, CHARACTERIZATION OF NANO SILVER PARTICLES

Within the scope of this study, nano-silver particles were produced by Tollens' method. In this method, for the synthesis of nanoparticles, a salt containing silver (Ag +) ion must be dissolved in a suitable solution and Ag + ions must be reduced (Figure 4.1). $AgNO_3$, which is determined as the silver salt, can form a solution by dissolving in H_2O. It is necessary to add a base to the solution in order to reduce Ag ions from the soluble $AgNO_3$ salt and to be dispersed in solution in a smaller form. With the addition of the basic $NaBH_4$ compound to the solution, Ag ions, which are reduced in size, are distributed among oxygen ions. A stabilizing ligand must be added to the mixture to prevent Ag ions from re-combining with NO_3 and precipitating. In order for the + ion element Ag to interact with the ligand, a - charged ligand must be used. Gelatin, which can be used as a ligand material, is a very strong coating thanks to the nitrogen, phosphorus and oxygen it contains. The concentration of gelatin should be sufficient to cover the Ag ions, but at high concentrations it tends to associate with each other. Additionally, polymer-based coatings can be used such as PVA and PVP. The chemicals convoluted in this study were all analytically pure and none of them have been treated with a second purification. Particles obtained by nano-silver synthesis are characterized by UV test, zeta potential, TEM and PSA analysis. While the UV test determines the absorbance of the particles, the width of the curve obtained gives information about the size of the particles. It is understood that the particle size decreases as the area scanned by the curve gets narrower. The absorbance value may increase depending on the concentration of the test sample prepared. In the literature studies, it is seen that the samples give absorbance between 0.6 - 2 values.

In addition, spherical nanosilver particles were found to peak around 390-450 nm. Nanoparticle sizes can be determined visually by TEM analysis and numerically by PDA analysis. Particle sizes ranging from 10 ~ 100 nm are subject to growth if they lose their stability. Its colloidal stability is linked to the stability of the ligand applied to the particles. Ligand stability is determined by the zeta potential test. If the zeta potential test result of nanoparticles is higher than +30 mV or lower than -30 mV, it means that it has a high degree of stability.

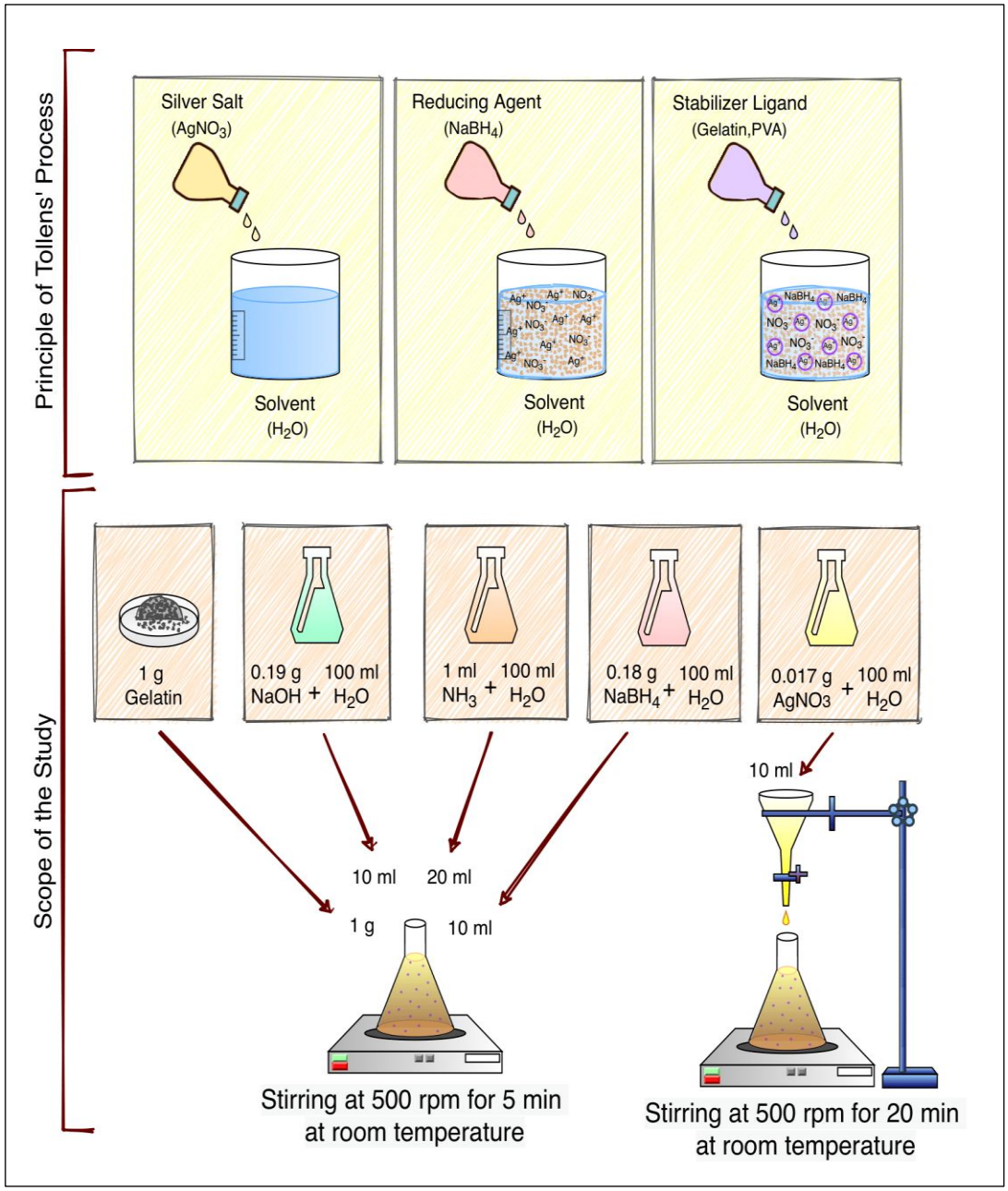

Figure 4. 1. Production of nano silver particles by Tollens' method.

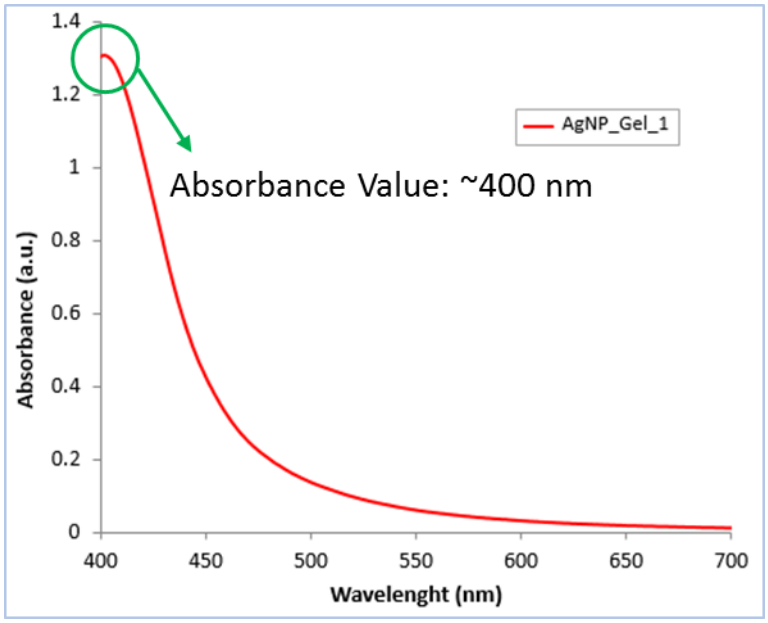

Figure 4.2. Absorbance graph for gelatin coated AgNP.

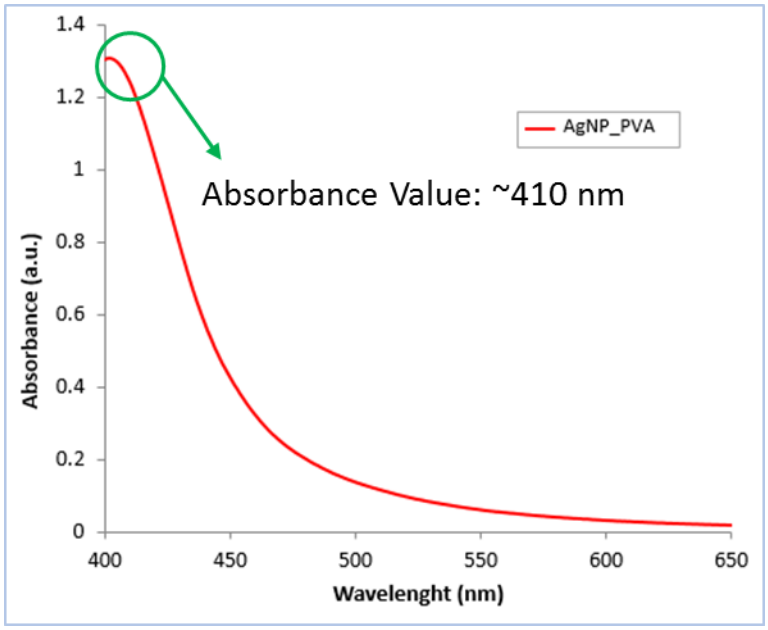

Figure 4.3. Absorbance graph for PVA coated AgNP.

In this study, 0.19 g NaOH (Merck; 5x10-2 M), 0.18 g $NaBH_4$ (98.0%, Sigma-Aldrich; 0.1 M), 0.017 g $AgNO_3$ (99.0%, Sigma-Aldrich; 2.5x10-3 M) and 1 ml of NH_3 (25-30%, Sigma-Aldrich; 1.25x10-2 M) in 100 ml of purified water were mixed separately to prepare solutions (Figure 4.1). After adding 1 g of coating material (Gel, PVA) to the mixing bowl at room temperature, 10 ml of NaOH solution was added from the prepared mixtures and magnetic stirring was started. 20 ml of NH_3 and 10 ml of

$NABH_4$ were added to the solution, which was stirred for 5 minutes at 500 rpm, and stirring was continued. Then, the prepared 10 ml $AgNO_3$ solution was dropped into the mixture as 1 drop per second. The chemical reaction continued at 500 rpm for 20 minutes. The colloidal suspension obtained after filtration was kept in the dark. The results of the UV analysis performed for the characterization of the particles produced are given in Figure 4.2 and 4.3. According to the UV-Vis graph, the particles gave an absorbance of ~ 400-410 nm (Figure4.3). Zeta potential test values show that colloidal stability is ensured (Figure 4.5). In Figure 4.4 and 6.5, when using Gel and PVA, the result of the Zeta test for nano-particles was higher than 30 mv, which means a stability, the result was -32 and -38 mv as shown in the figures above. As a result of the PSA (Figure 4.7) and TEM (Zeiss – EM900) (Figure 4.9) analysis, the particle sizes were determined as between 10-20 nm.

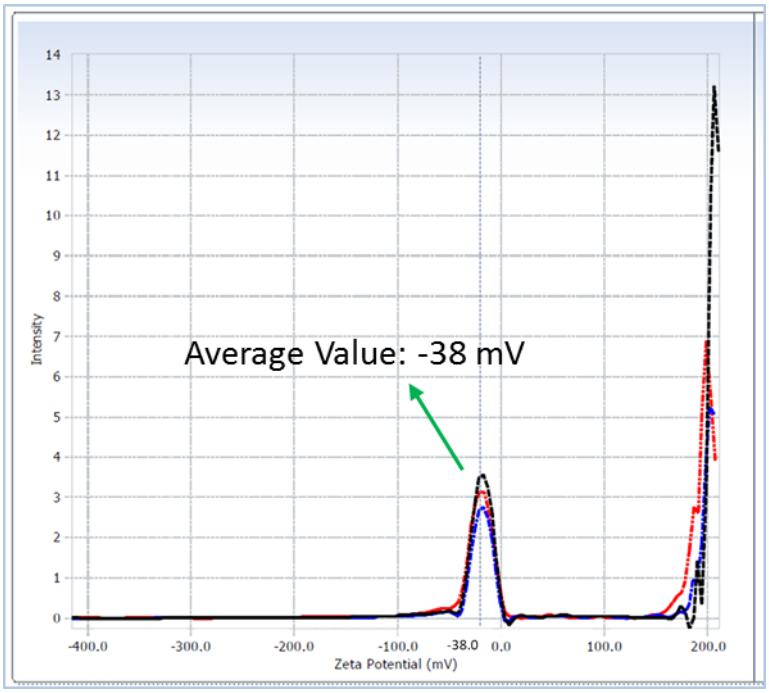

Figure 4.4. Zeta potential measurement for AgNP_GEL.

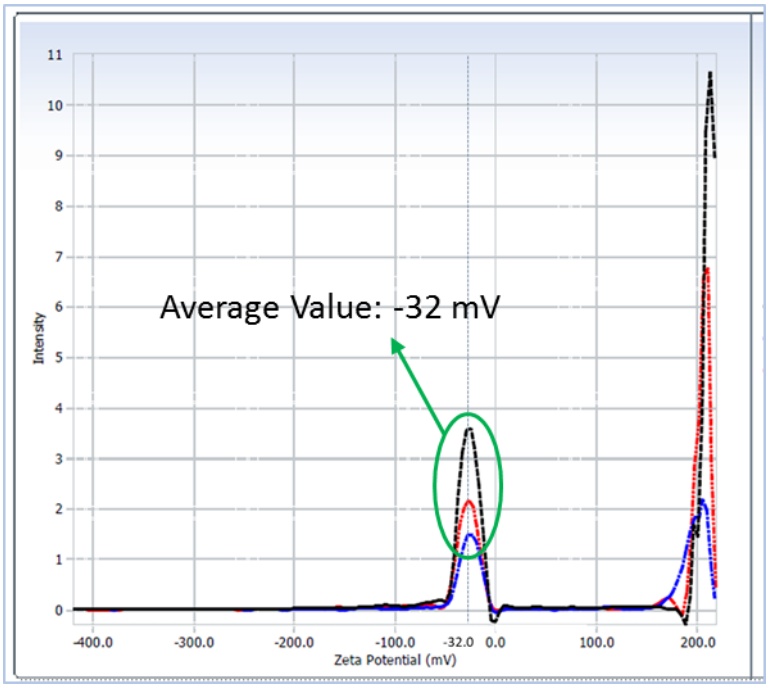

Figure 4.5. Zeta potential measurement for AgNP_PVA.

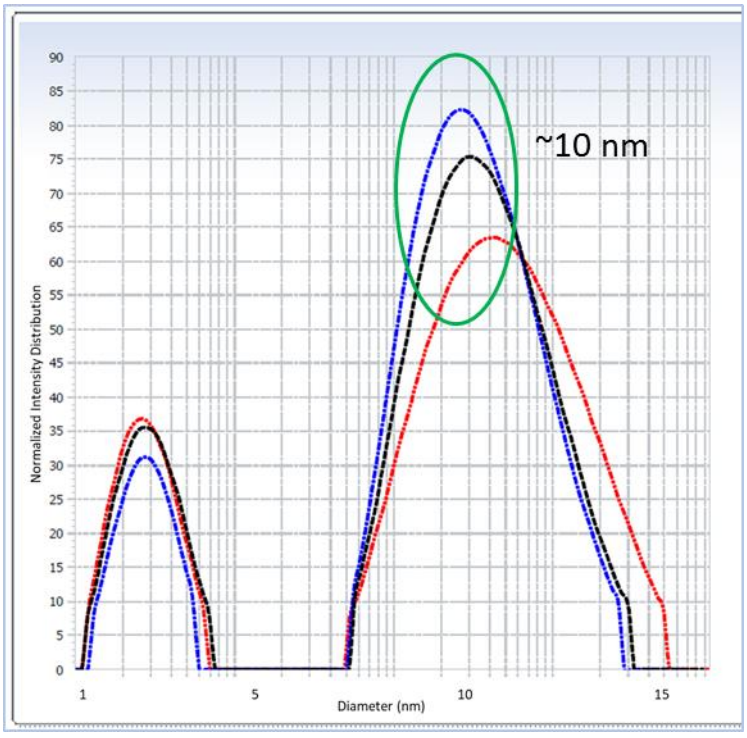

Figure 4.6. Particle size distribution measurement for AgNP_GEL

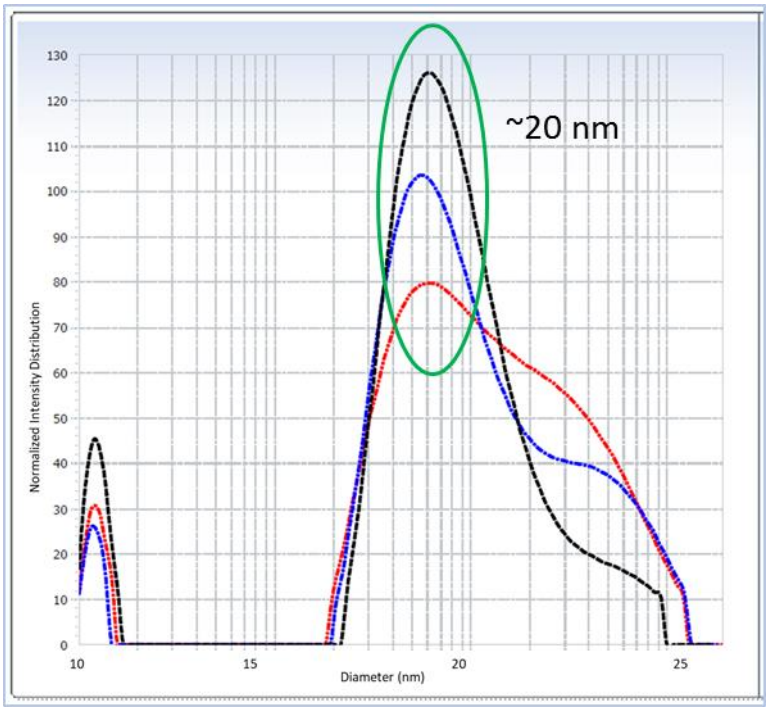

Figure 4.7. Particle size distribution measurement for AgNP_PVA.

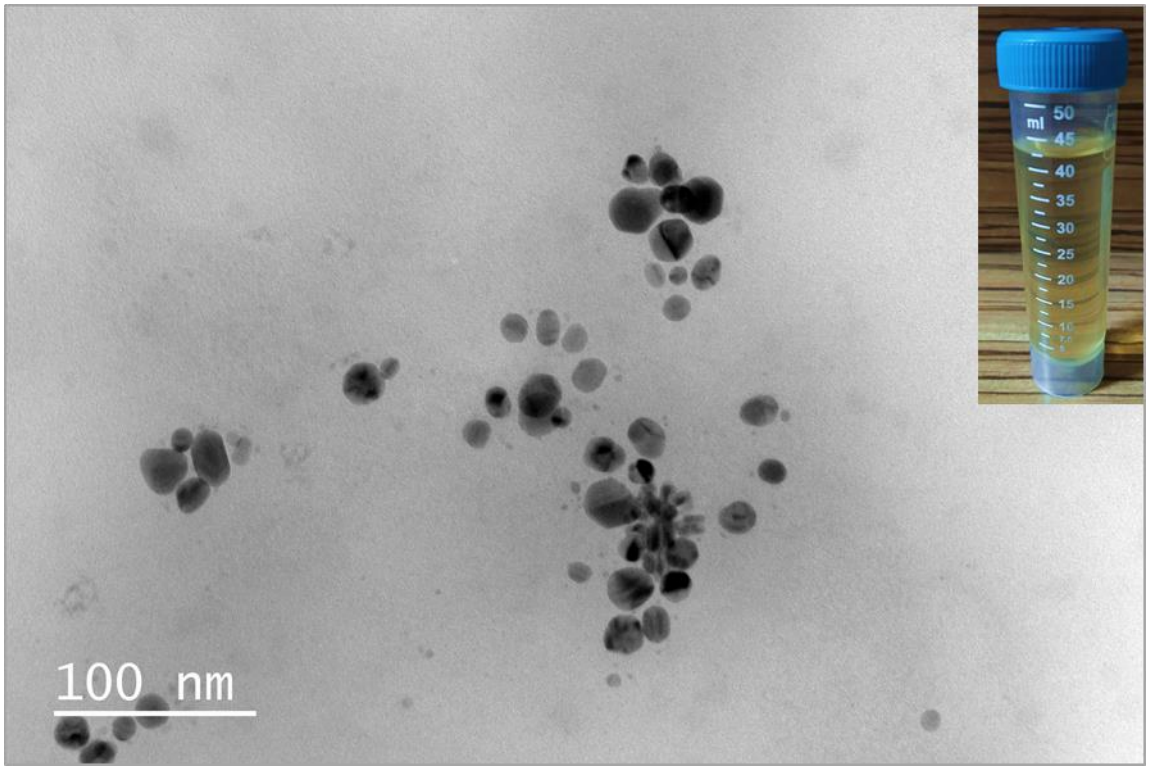

Figure 4.8. Tem image of AgNP_GEL.

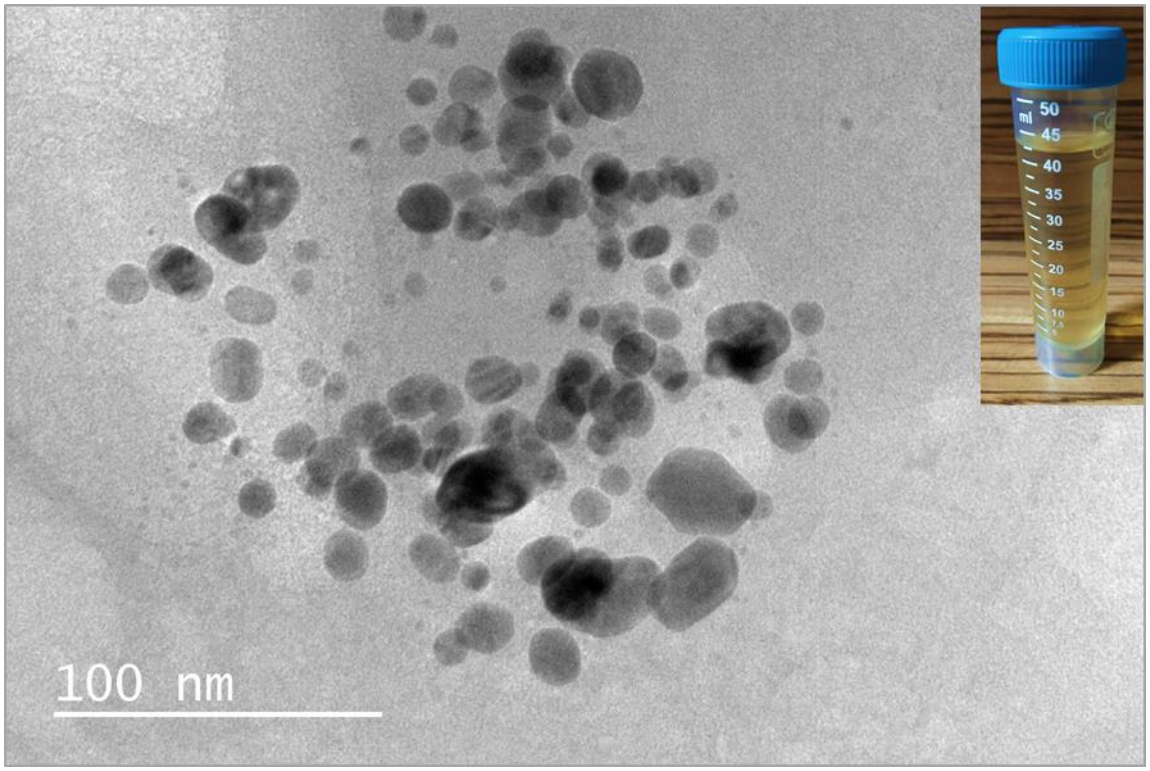

Figure 4.9. Tem image of AgNP_PVA.

4.2. PREPARATION OF LUBRICANTS

Wear tests were carried out under dry, ethylene glycol (EG), EP added ethylene glycol and nano silver + EP added ethylene glycol lubrication conditions. Additives are added to ethylene glycol according to certain concentrations. In the first stage of the study, it was carried out under dry, EG and EG with different EP concentrations (5%, 10%, 15%). By choosing the lubrication condition that gives the best results, wear test was carried out with combinations of gelatin coated nano silver (AgNP_Gel) and PVA coated nano silver (AgNP_PVA) fluids prepared in different concentrations (2%, 5%, 8%). The fluids were mixed homogeneously at room temperature by mechanical mixing method. Mixing ratios of the prepared fluids are given in Table 4.1. Before the experiments, the surface tension (ST) and the wettability angle (WD) of the prepared liquids were examined (Figure 4.10).

Table 4.1. Mixing ratios of lubricants.

Experiment Stages	**Lubricated Conditions**
1. Phase	Dry
	EG
	EG + 5% EP
	EG + 10% EP
	EG + 15% EP
Optimum Lubrication Condition as a result of 1st Stage: EG + 5% EP	
2. Phase	EG + 5% EP + 2% AgNP_Gel
	EG + 5% EP + 5% AgNP_Gel
	EG + 5% EP + 8% AgNP_Gel
	EG + 5% EP + 2% AgNP_PVA
	EG + 5% EP + 5% AgNP_PVA
	EG + 5% EP + 8% AgNP_PVA

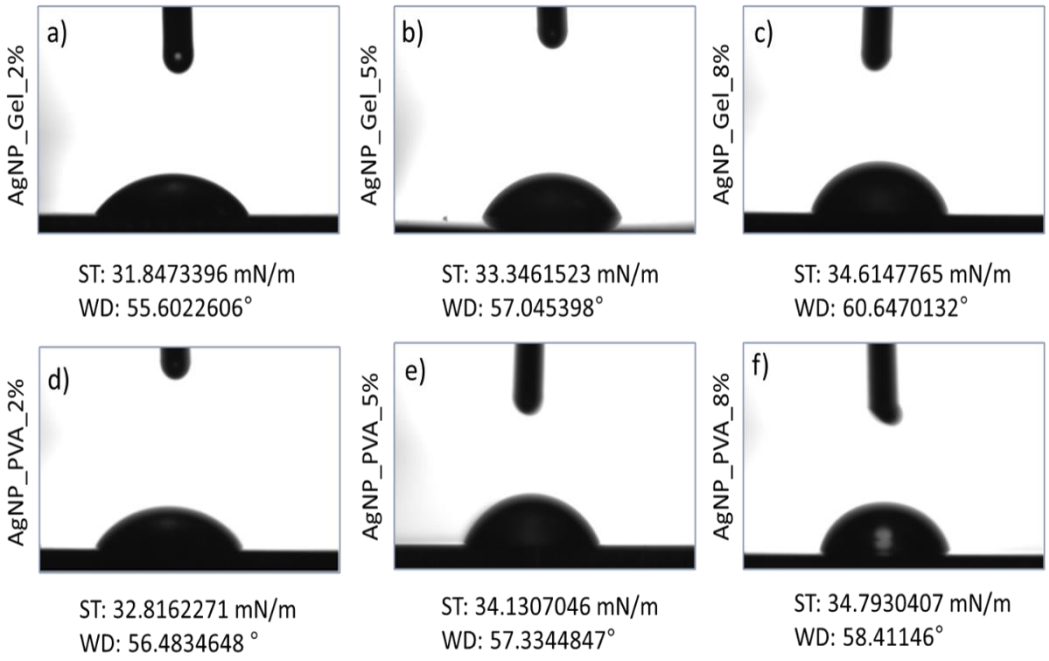

Figure 4.10. Surface tension and wettability angle results of prepared liquids: a) AgNP_Gel_2%, b) AgNP_Gel_5%, c) AgNP_Gel_8%, d) AgNP_PVA_2%, e) AgNP_PVA_5%, f) AgNP_PVA_8%.

4.3. EXPERIMENTAL SET-UP

Experiments in this study were carried out with a ball-on-plate wear tester. The schematic view of the system and the experimental setup are given in Figure 4.11 and 4.12, respectively. CuSn10Zn tin bronze was used as the wear sample and a 6 mm diameter 100Cr6 (AISI 52100) alloy was used as the abrasive. Wear material sample and chemical composition of abrasive ball are given in Tables 4.2 and 6.3. Wear test parameters were carried out under constant load (20 N) and sliding speed (40 rpm) conditions. Parameter selection was determined according to the pre-tests and the literature [7,22]. Experimental results were evaluated according to SEM (Carl Zeiss Gemini FESEM), 3D topography analysis, 2D volume loss and friction coefficient data.

Table 4.2. Chemical composition of CuSn10Zn alloy.

Element	Cu	Sn	Zn	Pb	Ni	P
Yüzde Ağırlığı (%)	86.0 – 89.0	9.0 – 11.0	1.0 – 3.0	1.5 (max)	2.0 (max)	0.05 (max)

Table 4.3. Chemical composition of AISI 52100 alloy.

Element	C	Si	Mn	P_{max}	S_{max}	Cr	Mo
Weight (%)	1.02	0.27	0.32	0.025	0.015	1.53	≤0.1

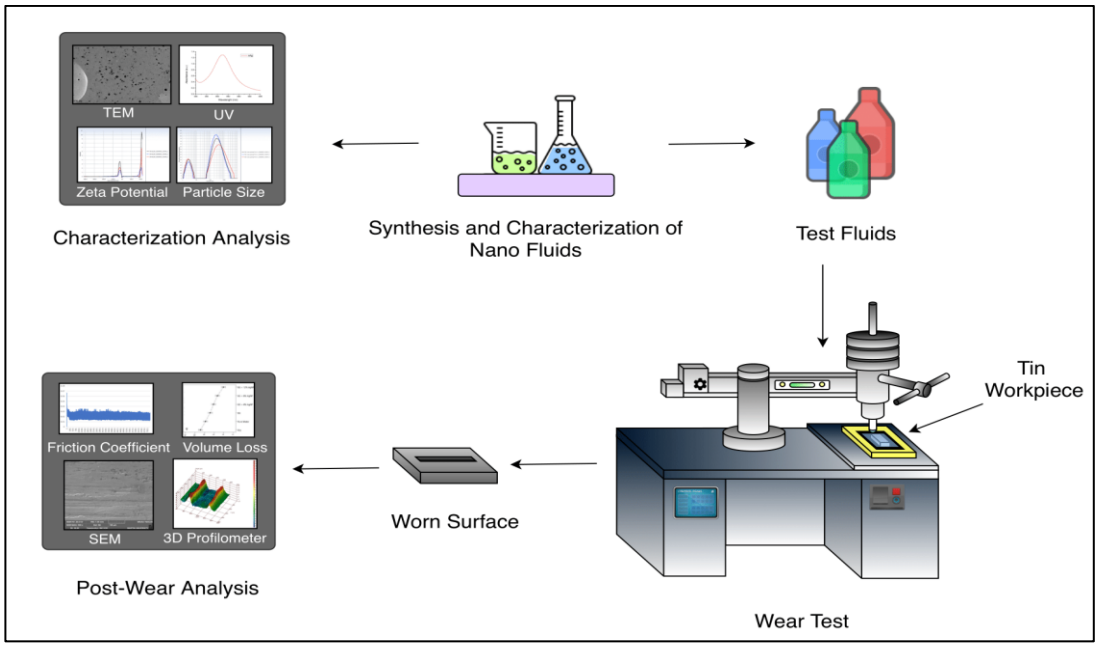

Figure 4.11. Experimental Set-up.

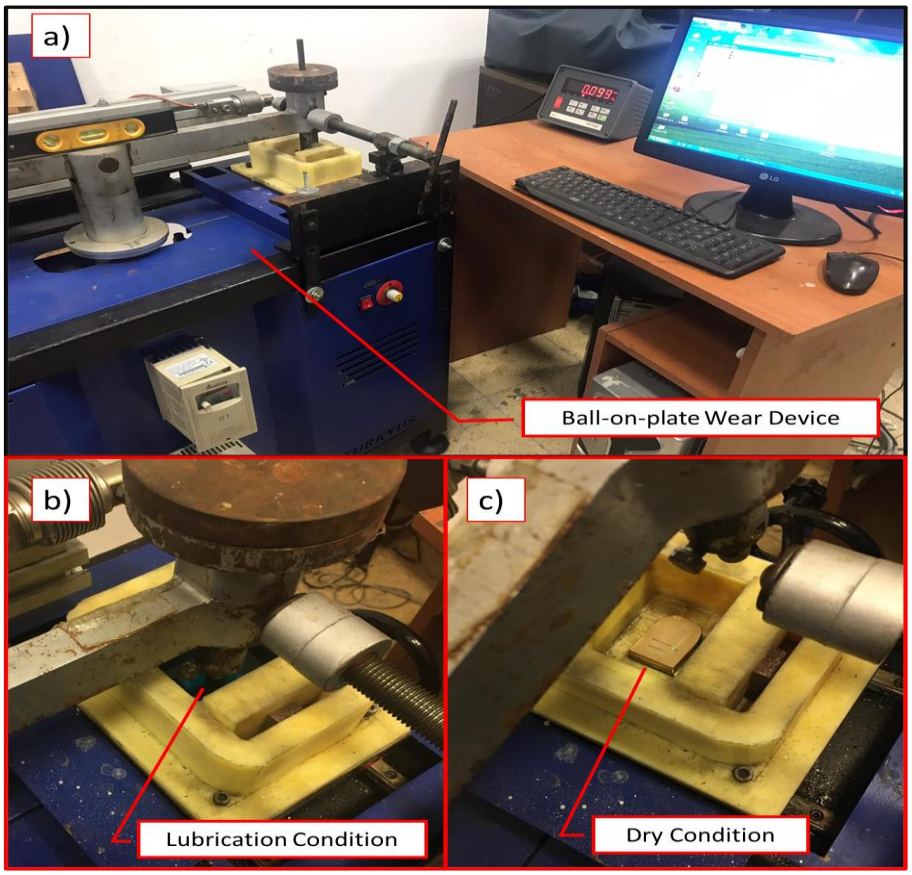

Figure 4.12. Wear equipment: a) Ball-on-plate Wear Device, b) Wear Under Lubrication Condition, c) Wear Under Dry Condition.

Friction coefficients were measured with a single axis dynamometer with an accuracy of ± 0.5 N. The friction coefficients were obtained graphically as seen in Figure 4.13. Steady-state coefficients were determined by considering the arithmetic mean of the graph values. As a result of the experiments, the length of the abrasion trace was determined with a 1/10 caliper, and the depth and width of the abrasion scar were determined with a 2D profilometer device. An example of the size chart, which is the output of the 2D profilometer device, and the wear sample are given in Figure4.14. Volume loss data are calculated according to the equation in Equation 1 and the volume loss graph is formed. The a, b and c values are given in Equation 1 refers to the width, depth and stroke distance of the wear scar, respectively.

$$V = \frac{2}{3} * a * b * c \qquad (1)$$

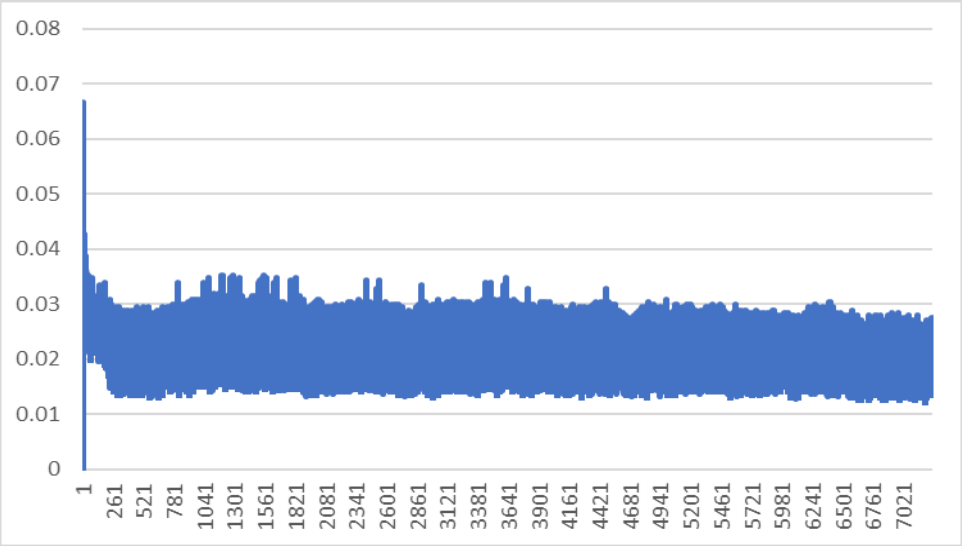

Figure 4.13. Friction Coefficient Graph.

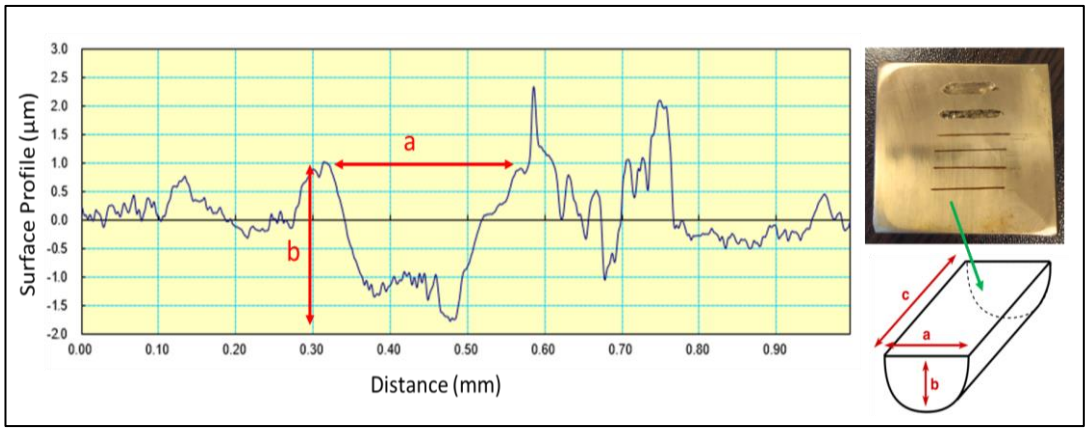

Figure 4.14. 2D Volume Loss Graph

PART 5

RESULTS AND DISCUSSIONS

The methodology determined for the analysis of experimental results is given in Figure 5.1. The study was carried out in two stages. the Firstly, in order to determine the optimum EP ratio, the lubricants obtained by adding EP to EG fluid in different proportions were subjected to wear tests at the parameter of 20 N load and 40 rpm. In order to determine the optimum EP additive ratio, abrasion tests were carried out under dry, pure EG, EG + 5% EP, EG + 10% EP and EG + 15% EP conditions. According to the results obtained from the abrasion tests, it was determined that the optimum results were obtained at 5% concentration. In the second stage, 6 different liquids were prepared by mixing the AgNP additive in different proportions and with different coaters, with the EP additive at the specified optimum ratio. Colloidal suspensions prepared by adding 2%, 5% and 8% nanosilver particles were used in the experiments and the optimum nanosilver concentration was determined. Abrasion tests were applied separately for gelatin and PVA coated nanosilver particles, thus the effect of different coating materials was also analyzed. Experimental results were determined by analyzing friction coefficient values, wear volume values, SEM and 3D topography images for both stages.

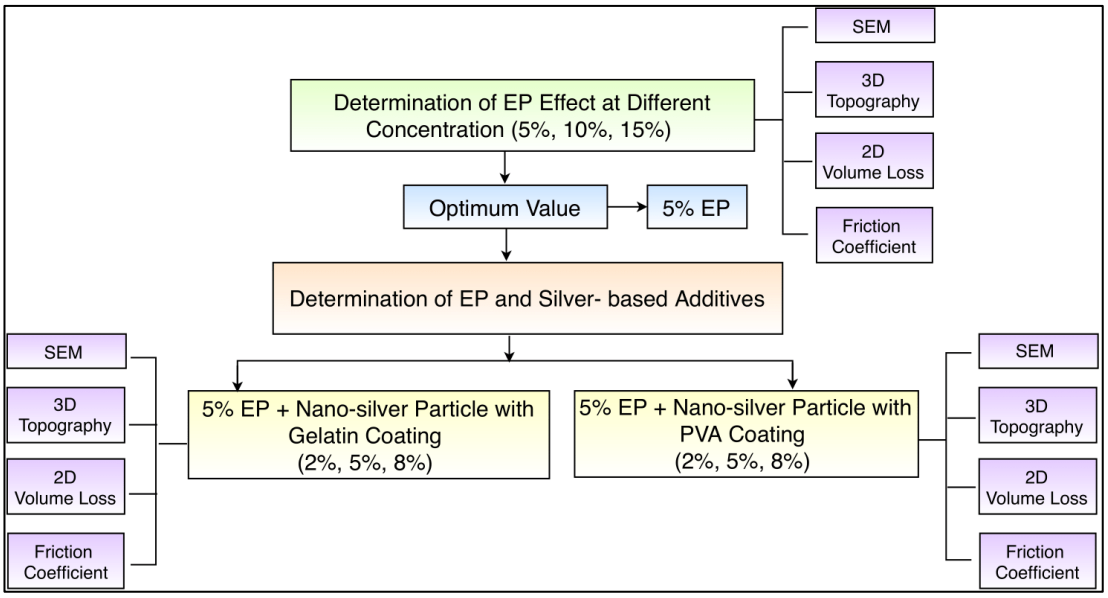

Figure 5.1. Experimental Process.

5.1.1 Determination of Optimum EP Additive Ratio

Until the lubricant film is formed in systems operating under hydrodynamic lubrication conditions, high values of friction coefficient occur depending on the metal-metal contact between the bearing material and the shaft material. This increase in the friction coefficient increases the wear on the bearing materials and this causes the service life of the bearing materials to shorten. For this reason, the friction coefficients need to be analyzed. In order to determine the optimum EP concentration, the friction coefficient values obtained from the experiments carried out under 20 N load and 40 rpm speed parameters under dry, EG, EG + 5% EP, EG + 10% EP and EG + 15% EP conditions are given in Figure 10. According to Figure 10, it was determined that the friction coefficient values decreased by 68.71%, 77.86%, 77.23%, 77.30% in EG, EG + 5% EP, EG + 10% EP and EG + 15% EP conditions, respectively, compared to dry environment conditions. According to these values, it is concluded that EG + 5% EP fluid is the lubricant that has the highest effect on the friction coefficient. By creating a stable oil film on the surface, EP additive [5] reduced the friction coefficient by ~ 77.7% according to dry conditions and ~ 28.7% compared to pure EG lubricant. The best EP additive ratio was found to be 5%. There is no significant difference in terms of friction coefficient in lubricants obtained with 10% EP and 15% EP ratios.

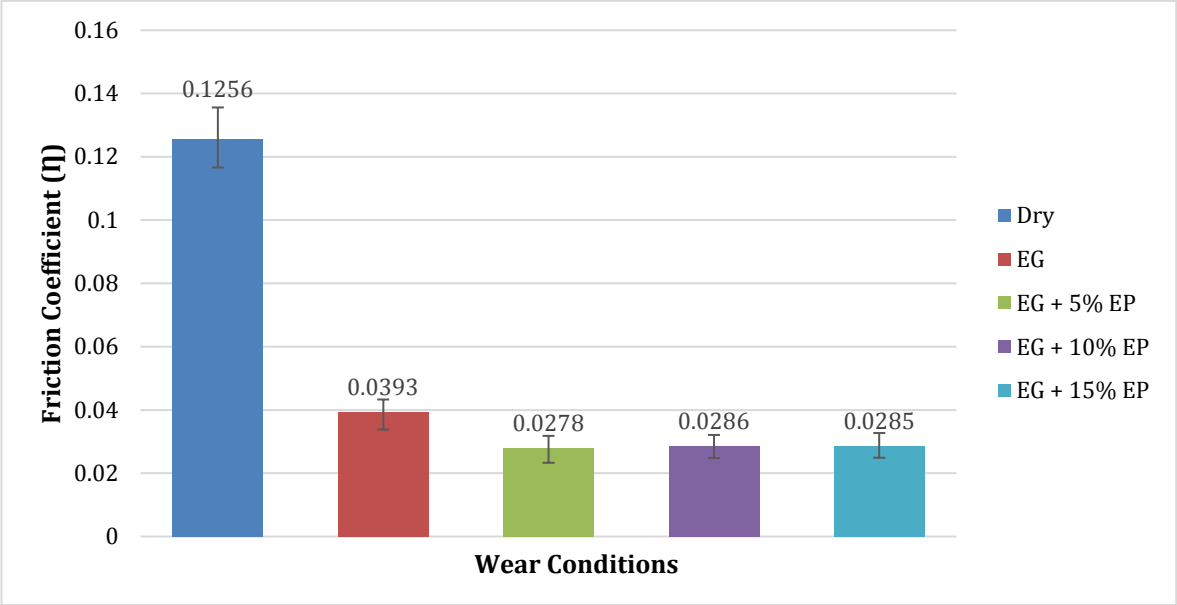

Figure 5. 2. Friction coefficient values of the abrasion test.

Due to the increase in the friction coefficient, wear mechanisms occur in the bearing material and the amount of particles detached from the surface of the material increases. The wear increase in the bearing material negatively affects the system performance in terms of dimensional integrity and fatigue strength. For this reason, wear volume values need to be analyzed. Abrasion volume values obtained from the measurement results with 2D profilometer as a result of the experiments carried out under dry, EG, EG + 5% EP, EG + 10% EP and EG + 15% EP conditions are given in Figure 5.3 . It was determined that the wear volume values decreased by 17.06%, 76.55%, 39.92% and 7.15%, respectively, in the conditions of EG, EG + 5% EP, EG + 10% EP and EG + 15% compared to dry ambient conditions. The amount of wear increases due to the increase in the friction coefficient on the contact surfaces. However, when 2D volume loss data were examined, it was determined that, unlike the friction coefficient results, EG + 15% EP environment gave values close to dry conditions. This shows that the high amount of EP additives negatively affects the tribological performance. According to the volume loss data, the optimum EP additive ratio was found to be 5%. EP additive of 5% reduced the volume loss by ~ 76.5% for dry conditions and ~ 71.7% for pure EG conditions.

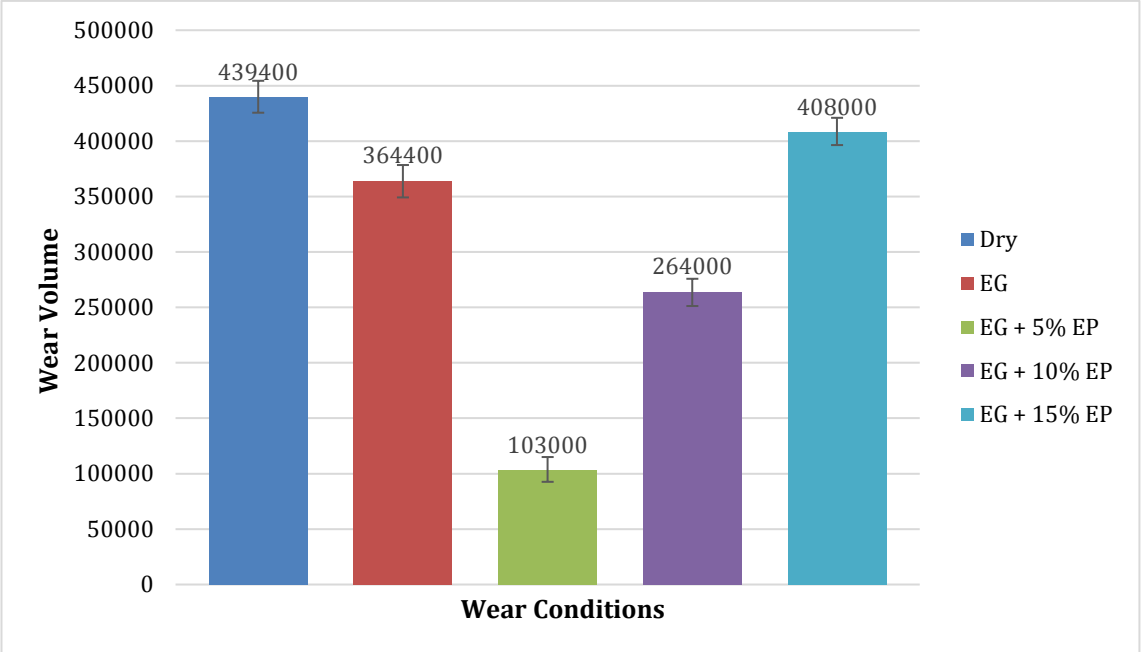

Figure 5.3. Volume Loss Data of the 1st Abrasion Test.

5.1.2.Sem Analyses

Surface morphology deteriorates as a result of the particles broken due to the abrasion mechanisms occurring on the material surface. This situation negatively affects the dimensional change and surface quality of the material. For this reason, SEM images should be analyzed in order to analyze the wear mechanisms occurring on the material surfaces. In Figure 5.4, SEM images of the samples obtained from the experiments performed in dry, EG and EG + 5% EP (optimum EP concentration) ambient conditions are given. When SEM images are examined, it is seen that the surface that is worn in dry conditions is quite rough (Figure 5.4 a). The absence of an oil film on surfaces subject to wear increases the friction coefficient. As the friction continues, the particles detached from the worn surface cause abrasive wear by scratching the surfaces. In addition, with the effect of the heat released, micro-source formation occurs on the surface. In dry environment conditions (Figure 5.4 a), it is seen that the material ruptures from the surface of the material in layers and the delamination mechanism occurs. In addition, deep wear marks and pits were formed on the surface. This situation disrupts the morphology of the contact surface. The presence of an oil film between the surfaces prevents metal-metal contact and reduces the friction coefficient. In addition, it prevents the adhesion mechanism by reducing the

temperature occurring in the friction area. The decrease in cracks, scratches and adhesion layers on the abraded surface under pure EG conditions is an indicator of this situation (Figure5.4 b). In EG ambient conditions compared to dry conditions, abrasion scar depths decreased and surface defects were significantly minimized. With 5% EP additive, micro-welding formation and scratches on the surface have been minimized and the abrasion scar has been considerably reduced compared to pure EG media. In the condition of EG + 5% EP, it is seen that the amount of defects in the wear zone and the depth of existing defects decrease and the surface quality increases visibly. This situation can be explained by the stable oil film formation created by the EP additive on the surface (Figure 5.4 c).

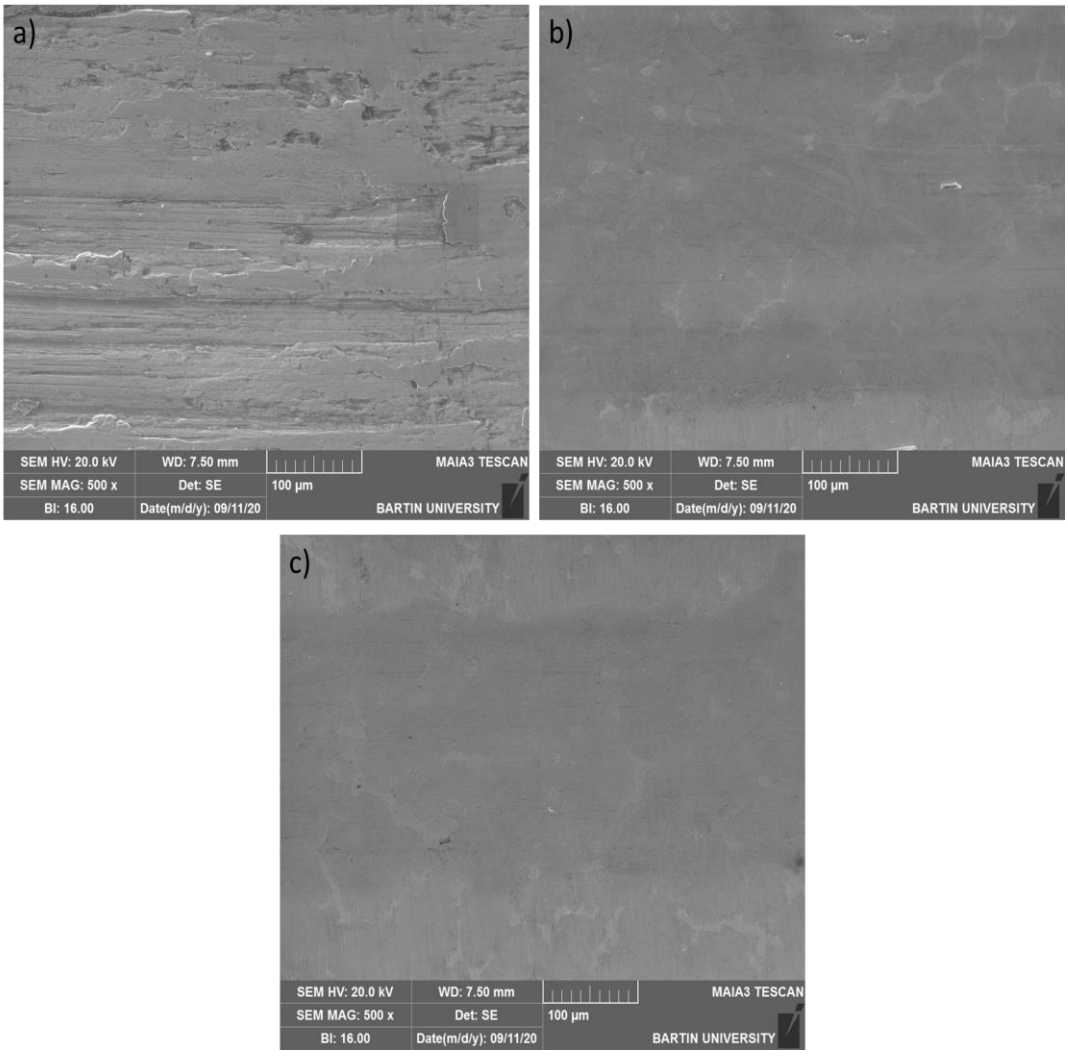

Figure 5.4. SEM Images of Abrasion Test: a) Dry, b) EG, c) EG + 5% EP.

5.1.3. 3D Topography

Due to the deterioration of the surface morphology as a result of the wear mechanisms seen in the SEM images, the surface form also changes. The 3D topography images obtained from the wear zones for the analysis of the form changes of the samples subjected to the abrasion test under dry, EG and EG + 5% EP conditions are given in Figure 5.5 . In the topography images given in Figure5.5, blue tones indicate abrasion scar depth, red tones indicate the excess surface roughness and yellow and green tones indicate less surface roughness than red tones. According to Figure 5.5a, it is seen that blue and red tones are intense in dry environment condition. The intensity of the red and blue colors indicates the presence of peaks and troughs on the surface. Considering the area where the blue color is intense, it is seen that the wear scar width is high. . The color distribution in the topographic image indicates that the wear scar depth, width and surface roughness are high. As can be seen in the SEM images of dry conditions, the adhesive wear mechanism has created micro-sized peaks and pits on the surface (Figure 5.4 a). In addition, the absence of an oil film in the contact area caused the temperature not to be distributed homogeneously and the surface form to deteriorate. With the use of pure EG, the yellow and green colors expressing flatness on the surface have increased compared to dry conditions, but the presence of red colored peaks indicates that the surface has a wavy form (Figure 5.5 c). By creating a thin film layer on pure EG contact surfaces, it ensured a homogeneous distribution of temperature and protection of surface form compared to dry conditions. In EG + 5% EP conditions, a smoother surface morphology was obtained compared to dry and pure EG conditions (Figure 5.5 b). When the surface is examined, it is seen that yellow and green colors are dominant. This shows that the roughness on the surface is at minimum level. EP additive increased the load carrying capacity of the oil film, separating the surfaces from each other, ensuring a homogeneous distribution of temperature and achieving a smooth surface morphology. The surface roughness values obtained confirm these findings.

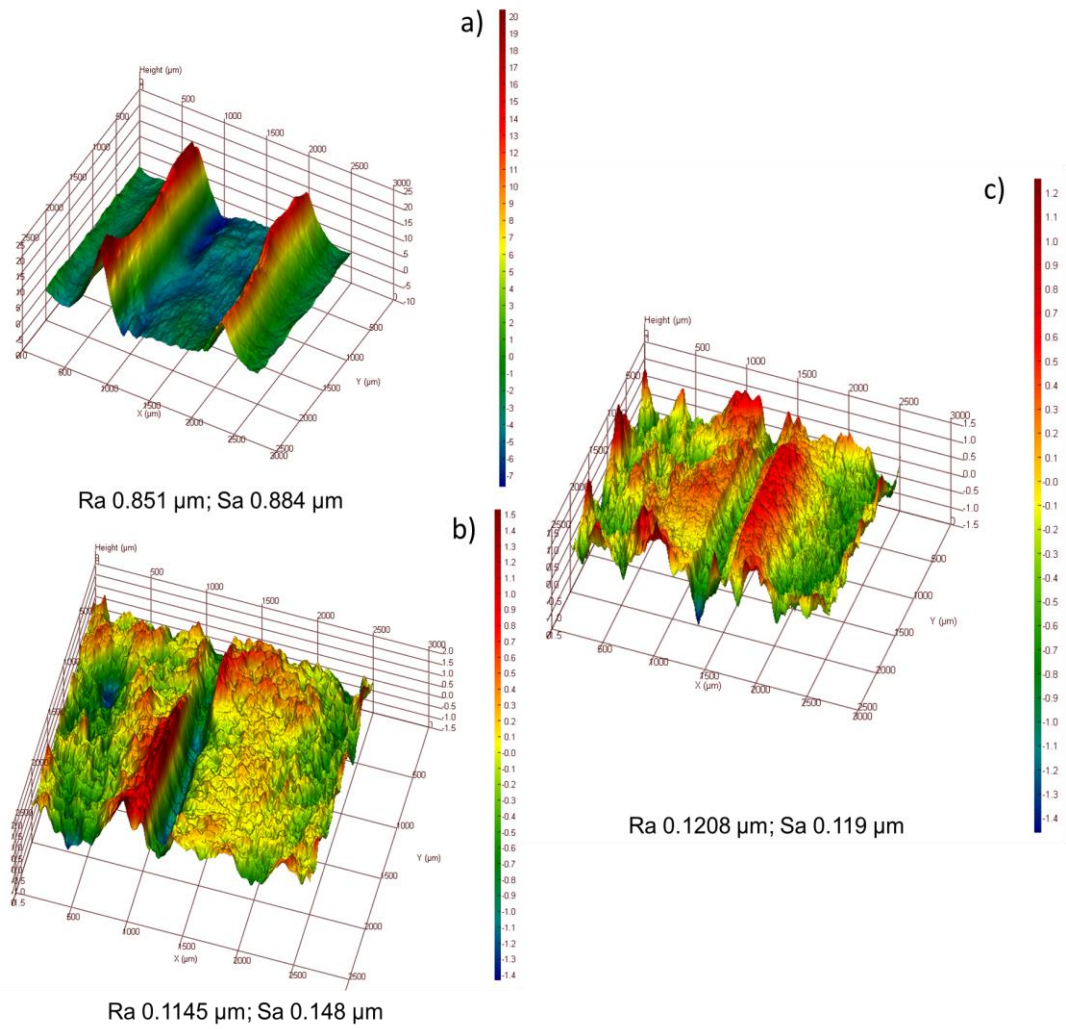

Figure 5.5. 3D Topograpy Results of Abrasion Test: a) Dry, b) EG + 5% EP, c) EG.

According to the abrasion tests performed in the first stage of the study, the best lubricating medium was found as EG + 5% EP. When the friction coefficient, 2D volume loss, SEM and 3D topography images were examined, it was observed that the friction coefficient decreased and the surface quality increased thanks to the stable oil film created by the EP additive. Optimum additive rate was determined as 5% in terms of EP additive fulfilling its lubricating function. As a result of the first phase of this study, it is thought that the use of EG + 5% EP fluid in the plain bearings will increase the surface quality and consequently the wear fatigue resistance will increase. In the next step, the interaction of AgNP additive produced with different proportions and coaters with EG + 5% EP fluid will be examined.

5.2. INVESTIGATION OF INTERACTION OF EP AND SILVER BASED ADDITIVES

5.2.1. Friction Coefficient

In order to determine the optimum nanosilver concentration and coating material, the friction coefficient values obtained under colloidal suspension conditions prepared by adding 2%, 5% and 8% gelatin and PVA coated nanosilver particles to the EG + 5% EP liquid are given in Figure 5.6 . According to the friction coefficient data of the wear tests performed, the lubricants giving the highest values are respectively EG + 5% EP + 8% AgNP (PVA), EG + 5% EP + 5% AgNP (PVA), EG + 5% EP + 2% AgNP (PVA).), EG + 5% EP + 8% AgNP (Gel), EG + 5% EP + 5% AgNP (Gel) and EG + 5% EP + 2% AgNP (Gel). According to Figure 7.6, it was determined that EG + 5% EP + 2% AgNP suspension decreased the friction coefficient by 7.55% and 14.33%, respectively, compared to EG + 5% EP + 5% AgNP and EG + 5% EP + 8% AgNP. . When a comparison is made between PVA and gelatin coatings, the friction coefficient of gelatin coated nanosilver particles for EG + 5% EP + 2% AgNP, EG + 5% EP + 5% AgNP and EG + 5% EP + 8% AgNP conditions compared to PVA coated nanosilver particles 12.06%, 14.03% and 17.33% respectively. According to the results, it was determined that PVA coated nanoparticles were insufficient to reduce the friction coefficient compared to gelatine coated nanoparticles. The rate of additive giving the best friction coefficient for both types of coaters was found to be 2%.

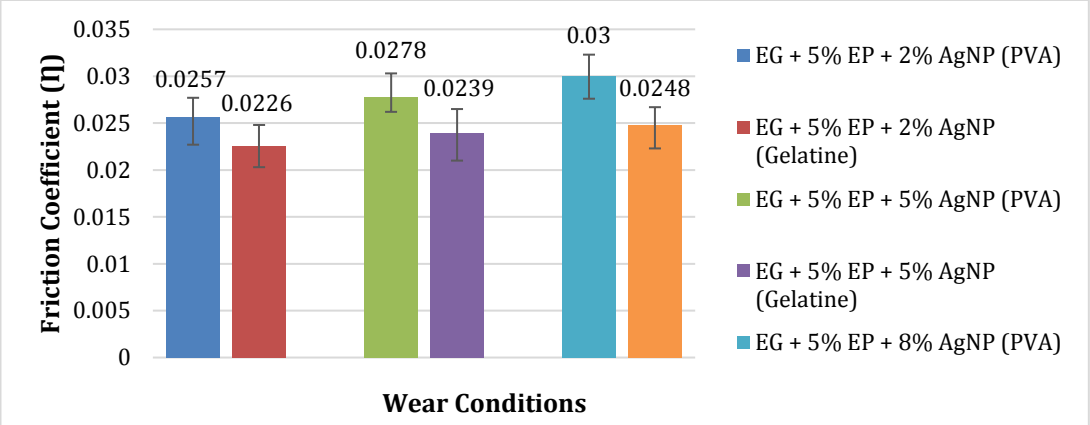

Figure 5.6. Friction coefficient results of abrasion test.

5.2.2. Wear Loss

For the analysis of the effect of nanosilver reinforcement and coating materials on the abrasion volume, the wear volume values formed in the material as a result of the abrasion experiments performed with the nanosilver colloidal suspensions prepared by reinforcing 2%, 5% and 8% with PVA and gelatin coating (Figure5.7). According to 2D Volume loss data, the lubricant that gives the best results is EG + 5% EP + 2% AgNP (Gel), EG + 5% EP + 5% AgNP (Gel), EG + 5% EP + 8% AgNP (Gel), EG + 5% EP + 2% AgNP (PVA), EG + 5% EP + 8% AgNP (PVA) and EG + 5% EP + 5% AgNP (PVA). According to Figure x, it was determined that EG + 5% EP + 2% AgNP suspension decreased the abrasion volume by 6.38% and 42.28%, respectively, compared to EG + 5% EP + 5% AgNP and EG + 5% EP + 8% AgNP. When compared between PVA and gelatin coatings, the friction coefficient of gelatin coated nanosilver particles compared to PVA coated nanosilver particles for EG + 5% EP + 2% AgNP, EG + 5% EP + 5% AgNP and EG + 5% EP + 8% AgNP conditions It was found that it decreased by 53.36%, 67.29% and 41.16%, respectively. As in the friction coefficient data, the gelatine coating gave a better result than the PVA coating and the optimum contribution ratio was determined as 2%.

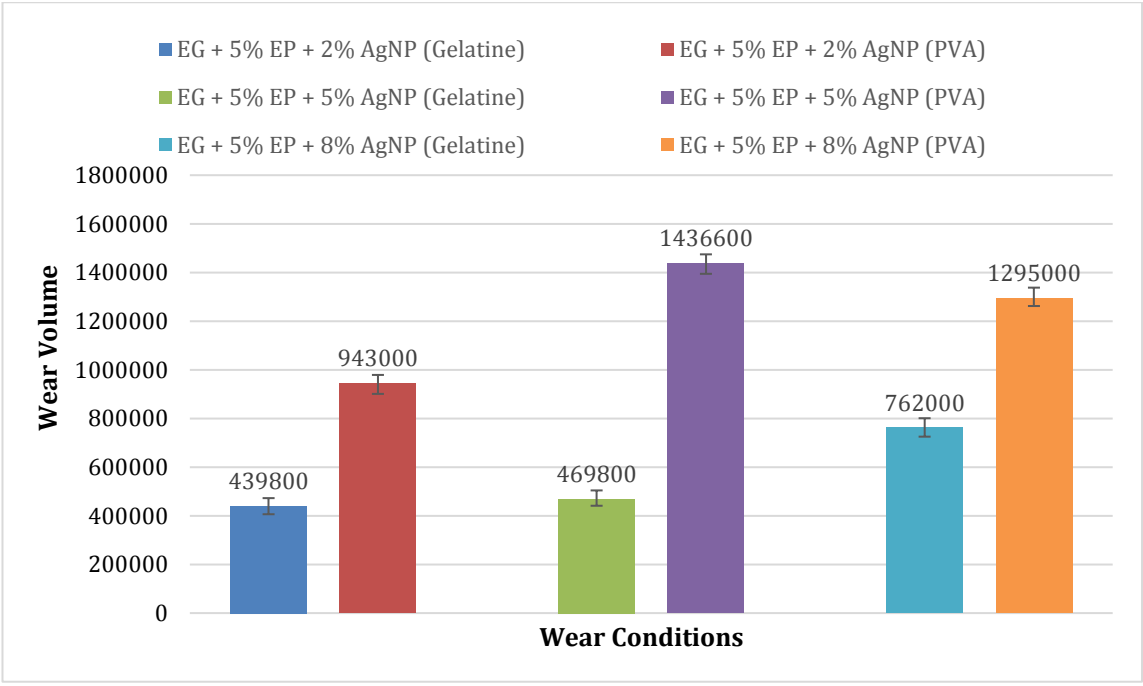

Figure 5.7. Volume loss results of abrasion test.

5.2.3. SEM

According to SEM data, it is seen that the best surface images were obtained under EG + 5% EP + 8% AgNP (Gel) and EG + 5% EP + 5% AgNP (Gel) conditions. According to the friction coefficient and volume loss data, AgNP (Gel) gave a better result by 2%, but there was no visible difference in SEM images. It is seen that the surfaces obtained under the conditions of EG + 5% EP + 8% AgNP (PVA) and EG + 5% EP + 5% AgNP (PVA) give similar results. It is observed that there are roughness and cracks on the wear surfaces obtained with 8% AgNP additive for both coatings. When the friction coefficient and volume loss data were examined, it was determined that 8% AgNP additive was insufficient to minimize wear and friction compared to other concentrations. The increase in nanoparticle concentration and the difficulty in penetration of the liquid into the wear surface can be shown as the reason for this situation.According to the data obtained during the characterization phase, the fact that the 8% AgNP additive has the highest wetting angle confirms this situation (Figure 6.10 4). According to the results, it was determined that 2% and 5% AgNP additives gave better results for both coating materials. The friction coefficient, volume loss and wettability data can be taken as reference to make a comparison between 2% and 5% AgNP additive rates. Based on these results, the optimum concentration ratio can be determined as 2%. When the images were compared, it was determined that gelatine coating gave better results in all concentrations than PVA coating. This shows that gelatin is a more stable coating on nanoparticles, and it ensures colloidal stability by preventing the agglomeration of nanoparticles.

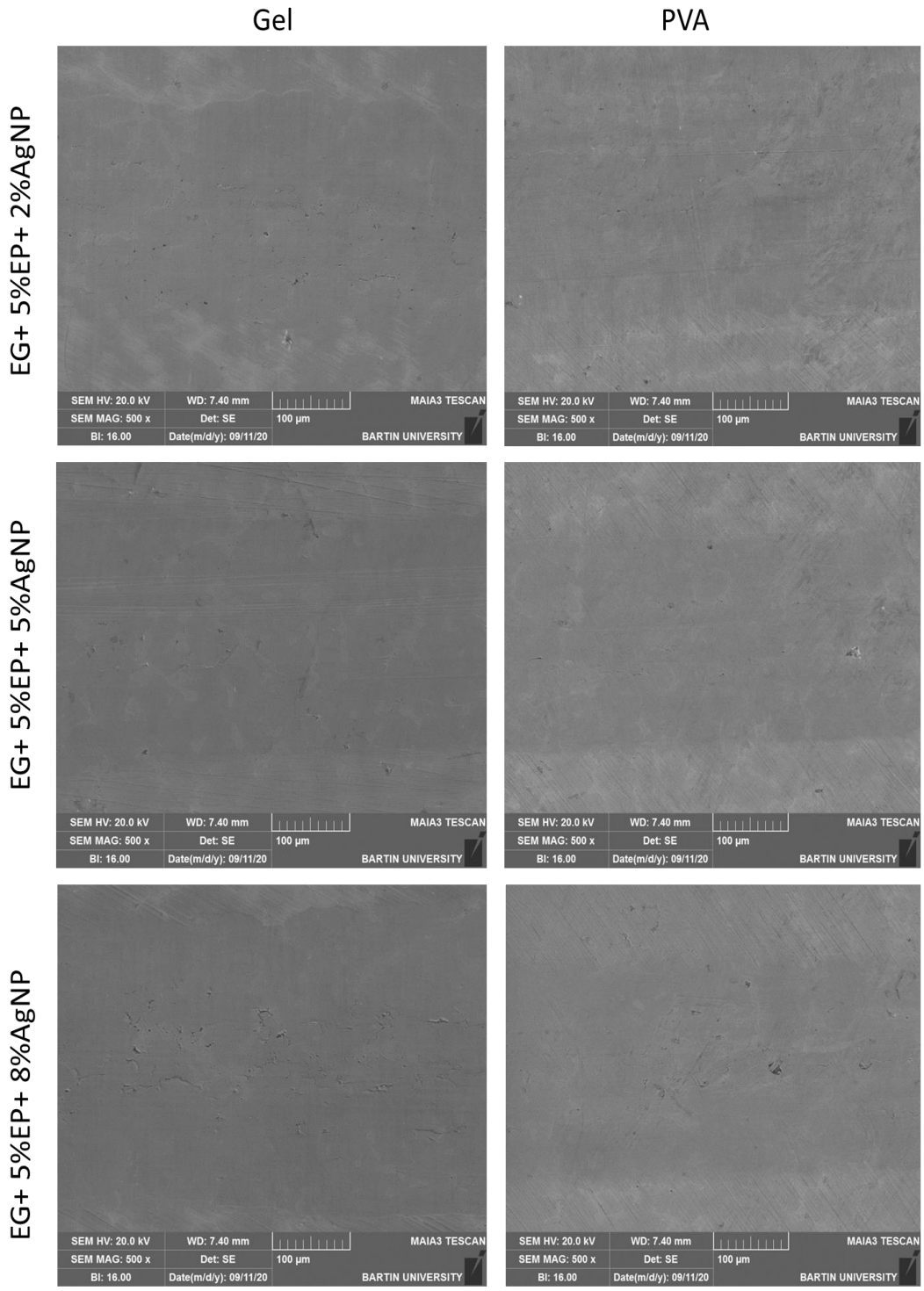

Figure 5.8. SEM images of eroded surfaces in nano-fluid environment prepared with different ratios and coaters3D Topography.

3D topography images obtained from wear zones are given in Figure 5.9 to examine the effect of colloidal suspensions prepared by reinforcing PVA and gelatin coated AgNP on surface form. In 3D topography images obtained under gelatin coated

nanosilver reinforced colloidal suspension conditions, the green tones of EG + 5% EP + 2% AgNP on the sample surface used compared to the conditions of EG + 5% EP + 5% AgNP and EG + 5% EP + 8% AgNP. It is seen that it is denser and a smoother surface form is obtained. Yellow and red tones are more intense in 3D topography images obtained under PVA coated nanosilver reinforced colloidal suspension conditions. When comparing the concentrations, it is seen that there is a similar situation with gelatin coated nanosilver particles. As the amount of concentration increased, the color tones became darker and the red tones spread over more areas. Depending on this situation, the surface roughness has increased and an inhomogeneous surface form has been formed. The difference between roughness values is negligible, but when the color distribution in the images is analyzed, it was determined that better surface quality was obtained at 2% concentration compared to 5% and 8% concentrations. As the concentration increases, the particle density of AgNP in the EG + EP mixture increases. Due to the increasing density, the movement of the particles in the liquid becomes difficult and the particles cannot penetrate the wear zone sufficiently. When the comparison is made between gelatin and PVA coated nanosilver particles, it is seen that the color distribution on the surface where gelatin coated AgNP is used is intensely green and the color distribution on the surface where PVA coated AgNP is used is yellow and red. In addition, a more homogeneous surface form was obtained on surfaces where gelatin coated AgNP was used compared to PVA coated AgNP. When the concentration rates and the effect of the coating materials were evaluated together, it was determined that the optimum surface form was obtained in EG + 5% EP + 2% AgNP environment.

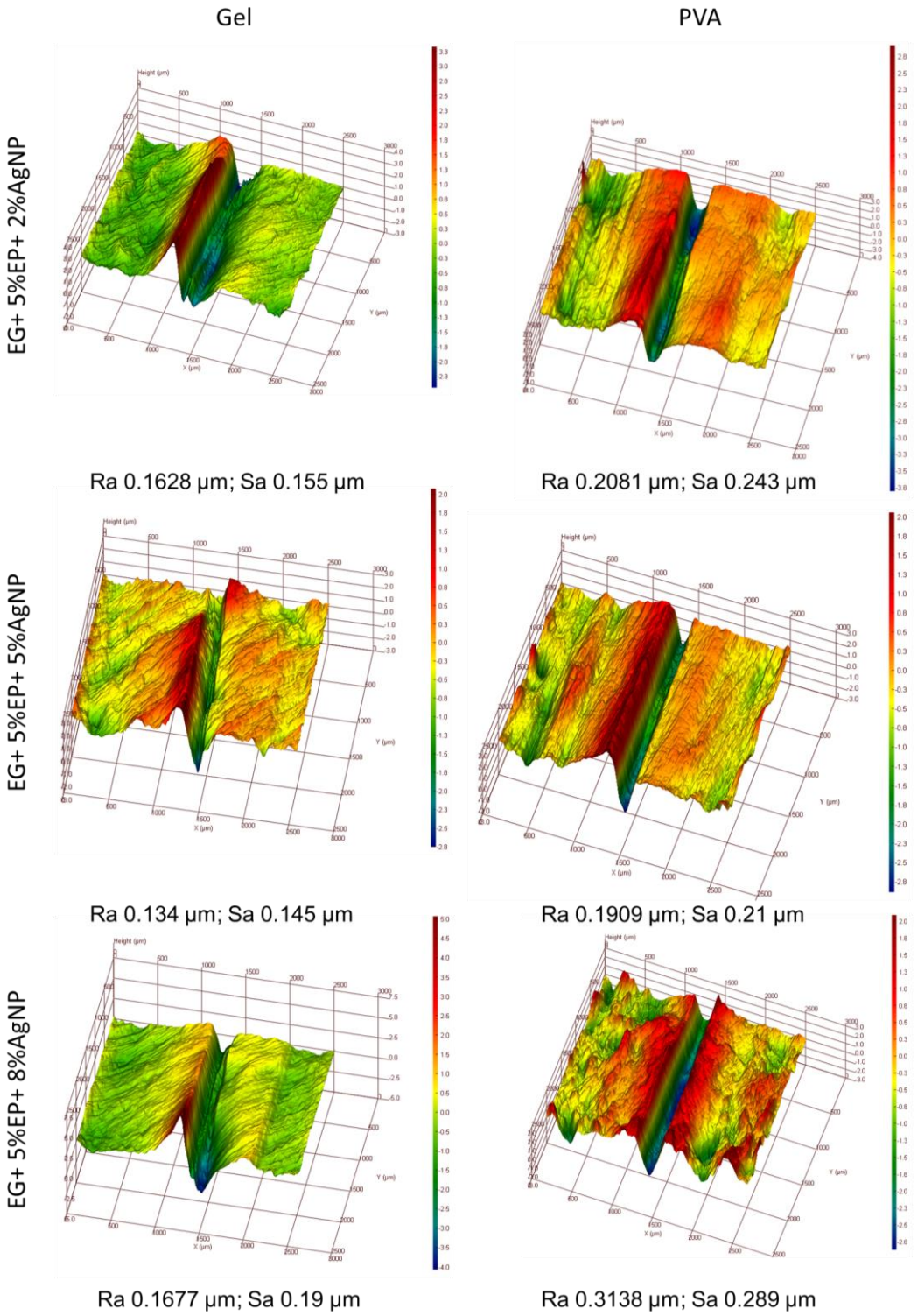

Figure 5.9. 3D topography images of eroded surfaces in nanofluidic environment prepared with different ratios and coaters.

PART 6

CONCLUSION

Tribology is a science that has a strong bond with mechanical growth. The nanoscale has already been interested in this thesis, all of which affect lubrication, friction, wear and sliding mechanisms. The tribological characteristics and the mechanism of lubrication of different forms of nanoparticles as lubricant additives have been investigated here.The specifications of nanoparticles affecting the tribological properties, the dispersion process, the techniques for increasing the reliability of dispersion, as well as the characterization of nano lubricants were also covered in the current review within the reach of this report. In this study, nano-silver particles were produced by Tollens' method. The chemicals included in this experiment are all analytically pure and none of them was treated with a second purification. Particles obtained by nano-silver synthesis are characterized by UV test. The optimum concentration of EP and AgNP were investigated comprehensively. The conclusion drawn from the present experiments are as follows:

- It is concluded that EG + 5% EP fluid is the lubricant that has the highest impact on the friction coefficient. By creating a stable oil film on the surface, EP additive reduced the friction coefficient by ~ 77.7% according to dry conditions and ~ 28.7% compared to pure EG lubricant. The best EP additive ratio was found to be 5%. There is no important difference in terms of friction coefficient in lubricants obtained with 10% EP and 15% EP ratios.
- The wear increase in the bearing material negatively affects the system performance in terms of dimensional integrity and fatigue strength. For this reason, wear volume values need to be analyzed.
- The volume of wear increases due to the increase in the friction coefficient on the contact surfaces. However, when 2D volume loss data were examined, it was determined that, unlike the friction coefficient results, EG + 15% EP

environment gave values close to dry conditions. This shows that the high amount of EP additives negatively affects the tribological performance.

- According to the volume loss data, the optimum EP additive ratio was found to be 5%. EP additive of 5% reduced the volume loss by ~ 76.5% for dry conditions and ~ 71.7% for pure EG conditions.
- EP additive increased the load-carrying capacity of the oil film, separating the surfaces from each other, ensuring a homogeneous distribution of temperature and achieving a smooth surface morphology.
- The best lubricating medium was found as EG + 5% EP. When the friction coefficient, 2D volume loss, SEM and 3D topography images were examined, it was observed that the friction coefficient decreased and the surface quality increased thanks to the stable oil-film created by the EP additive.
- PVA coated nanoparticles were insufficient to reduce the friction coefficient compared to gelatine coated nanoparticles. The rate of additive giving the best friction coefficient for both types of coaters was found to be 2%. The gelatine coating gave a better result than the PVA coating and the optimum contribution ratio was determined as 2%.
- It was determined that the gelatine coating gave better results in all concentrations than the PVA coating. This shows that gelatin is a more stable coating on nanoparticles, and it ensures colloidal stability by preventing the agglomeration of nanoparticles.
- It was determined that the optimum surface form was obtained in EG + 5% EP + 2% AgNP environment.

8.2. RECOMMENDATIONS FOR FUTURE WORK

Based on the outcomes of this study, silver particle-based additives coated with different ligands are indeed a potential candidate as alternative lubricants. Advantages that they have, like renewable base stocks. A study conducted by Prabu et al (2018) showed that silver present low modulus of solidity and elasticity, thus particles are deformed because of high pressure and friction force in the metal interface. It is noticed that the particles deformed because of sliding movement on the surface fill the eroded

surfaces. Yu et al (2018) mentioned that recently, researches and studies were performed to prepare thin films with superior tribological properties in a broad range of temperature. It has been mentioned that the most efficient method for this is to manufacture films which show self-lubricant properties with different temperatures. Researches detected that WCN-Ag films with some silver added may show self-lubricating properties in the temperature range of 25–600 ° C. Further research that confirms the capability of tribological performance of nanoparticles additives offers automotive engine must be conducted systematically. The findings of this study provide the basis for data on silver particle-based additives coated with various ligands and could also be used to help the establishment of other lubricants, in addition, to promote ongoing research on the use of alternative lubricants from renewable natural sources.

REFERENCES

1. Bağcı, M., & İmrek, H., "Effects of Sliding Speed in a CuZn10 Brass Material on Wear", ***Doctoral Dissertation, MS Thesis, Selçuk University, Institute of Sciences,*** Konya, Turkey 12-15 (2003).

2. Ünlü, B. S., Atik, E., & Meriç, C., "Effect of loading capacity (pressure–velocity) to tribological properties of CuSn10 bearings", ***Materials & Design,*** *28*(7): 2160-2165 (2007).

3. Ünlü, B. S., & Pinar, A. M., "CuSn10 Yatakların Farklı Yükleme, Hız Ve Ortamlarda Yüzey Pürüzlülüğü Ve Aşınmaya Etkisi", ***The International Advanced Technologies Symposium,*** Elazığ, Turkey, 16-18 (2011).

4. Zhu, J., Ma, L. & Dwyer-Joyce, R. S., "Friction and wear of Cu-15 wt% Ni-8 wt% Sn bronze lubricated by grease at room and elevated temperature", ***Wear***, *46(2):* 474 (2020).

5. Neely, A., "The evolution of performance measurement research", ***International Journal of Operations & Production Management.*** 25(12): 1228-1263 (2005).
6. Aytekin, V. "Metal yataklari," ***Bilim. Madencilik Derg.,*** 1(2): 79–97 (1961).

7. Huttunen-Saarivirta, E., Kilpi, L., Pasanen, A. T., Salminen, T., & Ronkainen, H., "Tribocorrosion behaviour of tin bronze CuSn12 under a sliding motion in NaCl containing environment: Contact to inert vs. reactive counterbody", ***Tribology International,*** 10(6): 389 (2020).

8. Kilincarslan, S. K., & Cetin, M. H., "Improvement of the milling process performance by using cutting fluids prepared with nano-silver and boric acid", ***Journal of Manufacturing Processes,*** 5(6): 707-717 (2020).

9. Almeida, M. R. D., Almeida, R. R. D., Oltramari-Navarro, P. V. P., Conti, A. C. D. C. F., Navarro, R. D. L., & Camacho, J. G. D. D., "Early treatment of Class III malocclusion: 10-year clinical follow-up", ***Journal of Applied Oral Science,*** 19(4): 431-439 (2011).

10. Reverberi, A. P., D'Addona, D. M., Bruzzone, A. A. G., Teti, R., & Fabiano, B., "Nanotechnology in machining processes: recent advances", ***Procedia CIRP,*** 7(9): 3-8 (2019).

11. Cetin, M. H., & Korkmaz, S., "Investigation of the concentration rate and aggregation behaviour of nano-silver added colloidal suspensions on wear behaviour of metallic materials by using ANOVA method", ***Tribology International,*** 14(7): 106-273 (2020).

12. Khan, M. S., Sisodia, M. S., Gupta, S., Feroskhan, M., Kannan, S., & Krishnasamy, K., "Measurement of tribological properties of Cu and Ag blended coconut oil nanofluids for metal cutting", ***Engineering Science and Technology, an International Journal,*** *22*(6): 1187-1192 (2019).

13. Lee, K., Hwang, Y., Cheong, S., Choi, Y., Kwon, L., Lee, J. & Kim, S. H., Understanding the role of nanoparticles in nano-oil lubrication", ***Tribology Letters,*** 35(2): 127-131 (2009).

14. Eltugral, N., Simsir, H., & Karagoz, S., "Preparation of nano-silver-supported activated carbon using different ligands", ***Research on Chemical Intermediates,*** 42(3): 1663-1676 (2016).

15. Simsir, H., Eltugral, N., & Karagoz, S., "The role of capping agents in the fabrication of nano-silver-decorated hydrothermal carbons", ***Journal of Environmental Chemical Engineering,*** *7*(5): 103-415 (2019).

16. Prabu, L., Saravanakumar, N., & Rajaram, G., "Influence of Ag Nanoparticles for the Anti-wear and Extreme Pressure Properties of the Mineral Oil Based Nano-cutting Fluid", ***Tribology in Industry,*** 40(3): 45-91 (2018).

17. Mražíková, A., Velgosová, O., Kavuličová, J., Krum, S., & Málek, J., "The influence of silver nanoparticles synthesis on their properties", ***Acta Polytechnica,*** *58*(6): 365-369 (2018).

18. Uysal, M., Akbulut, H., Tokur, M., Algül, H., & Çetinkaya, T., "Structural and sliding wear properties of Ag/Graphene/WC hybrid nanocomposites produced by electroless co-deposition", ***Journal of Alloys and Compounds,*** 65(4): 185-195 (2016).

19. Annaz, A. A., Irhayyim, S. S., Hamada, M. L., & Hammood, H. S., "Comparative study of mechanical performance between Al–Graphite and Cu–Graphite self-lubricating composites reinforced by nano-Ag particles", ***AIMS Materials Science,*** 7(5): 534–551 (2020).

20. Ahmed, S., & Ali, W., "Green Nanomaterials: Processing, Properties, and Applications", ***Springer Nature,*** New Delhi, 12-22 (2020).

21. Cetin, M. H., & Kilincarslan, S. K., "Effects of cutting fluids with nano-silver and borax additives on milling performance of aluminium alloys", ***Journal of Manufacturing Processes,*** 50(2): 170-182 (2020).

22. Sarafraz, M. M., Arya, A., Nikkhah, V., & Hormozi, F., "Thermal performance and viscosity of biologically produced silver/coconut oil nanofluids", ***Chemical and Biochemical Engineering Quarterly,*** *30*(4): 489-500 (2016).

23. Meng, Y., Su, F., & Chen, Y., "Effective lubricant additive of nano-Ag/MWCNTs nanocomposite produced by supercritical CO2 synthesis", ***Tribology International,*** 11(8): 180-188 (2018).

24. Yu, L., Zhao, H., & Xu, J., "Influence of silver content on structure, mechanical and tribological properties of WCN–Ag films", ***Materials Characterization,*** 11(4): 136-145 (2016).

25. Mate, C. M., "Tribology on the small scale: a bottom up approach to friction, lubrication, and wear", ***Oxford University Press,*** London, UK, 34-45 (2008).

26.

27. Bowden, F. P., Moore, A. J. W., & Tabor, D., "The ploughing and adhesion of sliding metals", ***Journal of Applied Physics,*** 14(2): 80-91 (1943).

28. Karthikeyan, K. M. B., Vijayanand, J., Arun, K. & Rao, V. S., "Thermophysical and wear properties of eco-friendly nano lubricants", ***Materials Today: Proceedings*** 2(4): 1-6 (2020).

29. Bowden, F. P., & Tabor, D., "The Friction and Lubrication Oil Solids", ***Oxford University Press,*** London, UK, 45-55 (1950).

30. Rohatgi, P. K., Tabandeh-Khorshid, M., Omrani, E., Lovell, M. R., & Menezes, P. L., "Tribology of metal matrix composites", **Springer,** New York, 233-268 (2013).

31. Soltani, M. E., Shams, K., Akbarzadeh, S., & Ruggiero, A., "A Comparative Investigation on the Tribological Performance and Physicochemical Properties of Biolubricants of Various Sources, a Petroleum-Based Lubricant and Blends of the Petroleum-Based Lubricant and Crambe Oil", ***Tribology Transactions,*** 63(6): 1121-1134 (2020).

32. Blau, P. J., "Friction science and technology: from concepts to applications", ***CRC press,*** Ohio, USA 32-37 (2008).

33. Furey, M. J., "Surface temperatures in sliding contact", ***ASLE Transactions,*** 7(2): 133-146 (1964).

34. Rabinowicz, E., "Lubrication of metal surfaces by oxide films", ***ASLE Transactions,*** 10(4), 400-407 (1967).

35. Mecklenburg, K. R., "The effect of wear on the compressive stress in the sphere-on-plane configuration", ***ASLE Transactions,*** 17(2): 149-157 (1974).

36. Ursachi, L., "Bibliografie titluri cărți de chimie", ***Universitatea Dunărea de Jos" din Galaţi Biblioteca, Galaţi,*** 78-101 (2015).

37. Buckley, D. H., "Possible relation of friction of copper-aluminum alloys with decreasing stacking-fault energy", ***National Aeronautics and Space Administration,*** Washington, USA, 43-55 (1967).

38. Rigney, D. A. & Hirth, J. P., "Plastic deformation and sliding friction of metals", ***Wear,*** *53*(2): 345-370 (1979).

39. Bhushan, B., "Modern tribology handbook, two volume set", ***CRC Press,*** Florida, USA, 23-33 (2000).

40. Stachowiak, G. W., "Wear: materials, mechanisms and practice", ***John Wiley & Sons,*** New York, USA, 56-77 (2006).

41. Blau, P. J., "How common is the steady-state? The implications of wear transitions for materials selection and design", ***Wear,*** 3(32): 1120-1128 (2015).

42. Ajayi, O. O., & Erck, R. A., "Variation of nominal contact pressure with time during sliding wear", ***International Joint Tribology Conference,*** San Francisco, USA, 12-29 (2001).

43. Sharma, S. S. K. M. S., Sangal, S., & Mondal, K., "On the optical microscopic method for the determination of ball-on-flat surface linearly reciprocating sliding wear volume", ***Wear,*** 300(2): 82-89 (2013).

44. Totten, G. E., Shah, R., & Forester, D., "Fuels and Lubricants Handbook: Technology, Properties, Performance and Testing 2nd Edition", ***ASTM International,*** Washington, USA, 56-61 (2019).

45. Czichos, H., "Tribology: a systems approach to the science and technology of friction, lubrication, and wear", ***Elsevier,*** Berlin, Germany 34-41 (2009).

46. Suh, N. P., "The delamination theory of wear", ***Wear,*** *25*(1): 111-124 (1973).

47. Bagi, S., Bowker, R., & Andrew, R., "Understanding chemical composition and phase transitions of ash from field returned DPF units and their correlation with filter operating conditions", ***SAE International Journal of Fuels and Lubricants,*** *9*(1): 239-259 (2016).

48. Priest, M., "Factors influencing boundary friction and wear of piston rings", ***Elsevier***, 3(2): 409-416 (2000).

49. Tang, Z., & Li, S., "A review of recent developments of friction modifiers for liquid lubricants (2007–present)", ***Current Opinion in Solid State and Materials Science,*** 18(3): 119-139 (2014).

50. Spikes, H., "Friction modifier additives", ***Tribology Letters,*** 60(1): 5 (2015)

51. Campen, S., Green, J. H., Lamb, G. D., & Spikes, H. A., "In situ study of model organic friction modifiers using liquid cell AFM; saturated and mono-unsaturated carboxylic acids", ***Tribology Letters,*** 57(2): 18 (2015).

52. Vilardo, J. S. & Mosier, P. E., "U.S. Patent Application No. 13/000,095", ***Google Patent,*** California, USA, 23-31 (2011).

53. DeBlase, F. J., Migdal, C. A., Mulqueen, G., & Madabusi, V. K., "U.S. Patent Application No. 12/371,872", ***Google Patent,*** California, USA, (2010).

54. Suen, Y. F., "U.S. Patent No. 8,703,680", ***Patent and Trademark Office,*** Washington, USA, 11-16 (2014).

55. Lundgren, S., "U.S. Patent No. 9,487,728", ***Patent and Trademark Office,*** Washington, USA, 31-35 (2016).

56. Holtmyer, M. D., & Chatterji, J., "Study of oil soluble polymers as drag reducers", ***Polymer Engineering & Science,*** 20(7): 473-477 (1980).

57. Campen, S., Green, J., Lamb, G., Atkinson, D., & Spikes, H., "On the increase in boundary friction with sliding speed", ***Tribology Letters,*** 48(2): 237-248 (2012).

58. Bray, U. B., Moore Jr, C. C. & Merrill, D. R., "Improvements in diesel-engine lubricating oils", ***SAE Transactions,*** 34(4): 35-42 (1939).

59. Mitchell, P.C., "Oil-soluble Mo-S compounds as lubricant additives", ***Wear,*** 100(3): 281-300 (1984).

60. Kasrai, M. J. N. K. G. G. M., Cutler, J. N., Gore, K., Canning, G., Bancroft, G. M., & Tan, K. H., "The chemistry of antiwear films generated by the combination of ZDDP and MoDTC examined by X-ray absorption spectroscopy", ***Tribology Transactions,*** 41(1): 69-77 (1998).

61. Feng, X., Jianqiang, H., Fazheng, Z., Feng, J., & Junbing, Y., "Anti-wear performance of organ molybdenum compounds as lubricant additives", ***Lubrication Science,*** 19(2), 81-85 (2007).

62. Miklozic, K. T., Graham, J., & Spikes, H., "Chemical and physical analysis of reaction films formed by molybdenum dialkyl-dithiocarbamate friction modifier additive using Raman and atomic force microscopy", ***Tribology Letters,*** 11(2): 71-81 (2001).

63. De Barros' Bouchet, M. I., Martin, J. M., Le-Mogne, T., & Vacher, B., "Boundary lubrication mechanisms of carbon coatings by MoDTC and ZDDP additives", ***Tribology International,*** 38(3): 257-264 (2005).

64. Yamamoto, Y. & Gondo, S., "Friction and wear characteristics of molybdenum dithiocarbamate and molybdenum thiophosphate", ***Tribology Transactions,*** 32(2): 251-257 (1989).

65. Parfenova, V. A., Belov, P. S., Duyanovskii, I. A., & Morozova, N. M., "Molybdenum-containing thiophosphates as multifunctional additives for mineral oils", ***Chem. Technol. Fuels Oils*** 22(2): 12-22 (1986).

66. Bakunin, V. N., Suslov, A. Y., Kuzmina, G. N., Parenago, O. P., & Topchiev, A. V., "Synthesis and application of inorganic nanoparticles as lubricant components–a review", ***Journal of Nanoparticle Research,*** *6*(2): 273-284 (2004).

67. Wu, Y. Y., Tsui, W. C., & Liu, T. C., "Experimental analysis of tribological properties of lubricating oils with nanoparticle additives", ***Wear,*** *262*(7): 819-825 (2007).

68. Sunqing, Q., Junxiu, D. & Guoxu, C., "A review of ultrafine particles as antiwear additives and friction modifiers in lubricating oils", ***Lubrication Science,*** *11*(3): 217-226 (1999).

69. Akbulut, M., "Nanoparticle-based lubrication systems", ***J. Powder Metall. Min,*** 1(1): 1-3 (2012).

70. Joly-Pottuz, L., Dassenoy, F., Belin, M., Vacher, B., Martin, J. M. & Fleischer, N., "Ultralow-friction and wear properties of IF-WS 2 under boundary lubrication", ***Tribology Letters,*** 18(4): 477-485 (2005).

71. Leslie,R. R., "Lubricant additives: chemistry and applications", **CRC Press,** Ohio, USA, 12-22(2003).

72. De Vries, L., & Kennedy, B., "U.S. Patent No. 3,753,908", ***Patent and Trademark Office***, Washington, USA, 12-17 (1973).

73. Wan, Y., & Xue, Q., "Effect of antiwear and extreme pressure additives on the wear of aluminium alloy in lubricated aluminum-on-steel contact", ***Tribology International,*** *28*(8): 553-557 (1995).

74. Anand, O. N., Kumar, V., Singh, A. K., & Bisht, R. P. S., "Anti-friction, anti-wear and load-carrying characteristics of environment friendly additive formulation", ***Lubrication Science,*** 19(3): 159-167 (2007).

75. Khorramian, B. A., Iyer, G. R., Kodali, S., Natarajan, P., & Tupil, R., "Review of antiwear additives for crankcase oils", ***Wear,*** 169(1): 87-95 (1993).

76. Spikes, H., "The history and mechanisms of ZDDP", ***Tribology Letters,*** 17(3): 469-489 (2004).

77. Johnson, D. W. & Hils, J. E., "Phosphate esters, thiophosphate esters and metal thiophosphates as lubricant additives", ***Lubricants,*** *1*(4): 132-148 (2013).

78. Zhang, Z., Yamaguchi, E. S., Kasrai, M., & Bancroft, G. M., "Tribofilms generated from ZDDP and DDP on steel surfaces: Part 1, growth, wear and morphology", ***Tribology Letters,*** *19*(3): 211-220 (2005).

79. Zhang, Z., Yamaguchi, E. S., Kasrai, M., & Bancroft, G. M., "Tribofilms generated from ZDDP and DDP on steel surfaces: Part 1, growth, wear and morphology", ***Tribology Letters,*** *19*(3): 211-220 (2005).

80. Wong, V. W. & Tung, S. C., "Overview of automotive engine friction and reduction trends–Effects of surface, material, and lubricant-additive technologies", ***Friction,*** 4(1): 1-28 (2016).

81. Barber, D. J., & Freestone, I. C., "An investigation of the origin of the colour of the Lycurgus Cup by analytical transmission electron microscopy", Archaeometry, *32*(1): 33-45 (1990).

82. Lee, P. C. & Meisel, D., "Adsorption and surface-enhanced Raman of dyes on silver and gold sols", ***The Journal of Physical Chemistry,*** 86(17): 3391-3395 (1982).

83. Henglein, A., "Small-particle research: physicochemical properties of extremely small colloidal metal and semiconductor particles", ***Chemical Reviews,*** 89(8): 1861-1873 (1989).

84. Nagy, A. & Mestl, G., "High temperature partial oxidation reactions over silver catalysts", ***Applied Catalysis A: General,*** 188(2): 337-353 (1999).

85. Frattini, A., Pellegri, N., Nicastro, D. D. & Sanctis, O., "First-principles study of the adsorption of NH3 on Ag surfaces", ***Mater Chem Phys,*** 9(4): 148-152 (2005).

86. Tessier, P. M., Velev, O. D., Kalambur, A. T., Rabolt, J. F., Lenhoff, A. M., & Kaler, E. W., "Assembly of gold nanostructured films templated by colloidal crystals and use in surface-enhanced Raman spectroscopy", ***Journal of the American Chemical Society,*** 122(39): 9554-9555 (2000).

87. Rosi, N. L., & Mirkin, C. A., "Nanostructures in bio diagnostics", ***Chemical Reviews,*** *105*(4): 1547-1562 (2005).

88. Shankar, S. S., Ahmad, A., & Sastry, M., "Geranium leaf assisted biosynthesis of silver nanoparticles", ***Biotechnology Progress,*** *19*(6): 1627-1631 (2003).

89. Shibata, S., Aoki, K., Yano, T., & Yamane, M., "Preparation of silica microspheres containing Ag nanoparticles", ***Journal of Sol-Gel Science and Technology,*** *11*(3): 279-287 (1998).

90. Hahn, H., "Unique features and properties of nanostructured materials", ***Advanced Engineering Materials,*** *5*(5): 277-284 (2003).

91. Ashe, B. A., "Detail investigation to observe the effect of zinc oxide and Silver nanoparticles in biological system", ***Doctorate Thesis, Department of Biotechnology & Medical Engineering National Institute of Technology Rourkela,*** Orissa, India, 34-51(2011).

92. Willner, I., Baron, R. & Willner, B., "Growing metal nanoparticles by enzymes", ***Advanced Materials,*** 18(9): 1109-1120 (2006)

93. Nair, B. & Pradeep, T., "Coalescence of nanoclusters and formation of submicron crystallites assisted by Lactobacillus strains", ***Crystal Growth & Design,*** *2*(4): 293-298 (2002).

94. Shankar, S. S., Rai, A., Ahmad, A., & Sastry, M., "Rapid synthesis of Au, Ag, and bimetallic Au core–Ag shell nanoparticles using Neem (Azadirachta indica) leaf broth", ***Journal of Colloid and Interface Science,*** 275(2): 496-502 (2004).

95. Baker, C. Pradhan, A. Pakstis, L. Pochan, D. J. and Shah, S. I. "Synthesis and antibacterial properties of silver nanoparticles," ***J. Nanosci. Nanotechnol.,*** 5(2): 244–249 (2005).

96. Ahmad, A., Mukherjee, P., Senapati, S., Mandal, D., Khan, M. I., Kumar, R. & Sastry, M., "Extracellular biosynthesis of silver nanoparticles using the fungus Fusarium oxysporum", ***Colloids and Surfaces B: Biointerfaces,*** *28*(4): 313-318 (2003).

97. Moores, A., & Goettmann, F., "The plasmon band in noble metal nanoparticles: an introduction to theory and applications", ***New Journal of Chemistry,*** 30(8): 1121-1132 (2006).

98. Albrecht, M. A., Evans, C. W., & Raston, C. L., "Green chemistry and the health implications of nanoparticles", ***Green Chemistry,*** *8*(5): 417-432 (2006).

99. Lockman, P. R., Koziara, J. M., Mumper, R. J. & Allen, D. D., "Nanoparticle surface charges alter blood–brain barrier integrity and permeability", ***Journal of Drug Targeting,*** 12(10): 635-641 (2004).

100. Oberdorster, G., Sharp Z, Atudorei V, Elder A, Gelein R, Kreyling W, Cox C., "Translocation of inhaled ultrafine particles to the brain", ***Inhal Toxicol,*** 1(6): 437-445 (2004).

101. Limbach, L. K., Wick, P., Manser, P., Grass, R. N., Bruinink, A. & Stark, W. J., "Exposure of engineered nanoparticles to human lung epithelial cells: influence of chemical composition and catalytic activity on oxidative stress", ***Environmental Science & Technology,*** 41(11): 4158-4163 (2007).

102. Asharani, P. V., Wu, Y. L., Gong, Z., & Valiyaveettil, S., "Toxicity of silver nanoparticles in zebrafish models", ***Nanotechnology,*** 19(25): 255 (2008).

103. Jana, N. R., Sau, T. K., & Pal, T., "Growing small silver particle as redox catalyst", ***The Journal of Physical Chemistry B,*** 103(1): 115-121 (1999).

104. Morones, J. R., Elechiguerra, J. L., Camacho, A., Holt, K., Kouri, J. B., Ramírez, J. T., & Yacaman, M. J., "The bactericidal effect of silver nanoparticles", ***Nanotechnology,*** 16(10): 23-46 (2005).

105. El Baradie, M. A., "Cutting fluids: Part I. characterization", ***Journal of Materials Processing Technology,*** 56(4): 786-797 (1996).

106. Manolov, N., & Kandeva, M., "Overall Tribology, Ed, House", ***Sv. Ivan Rilsky–Sofia,*** Bulgaria, Sofia, 100-110 (2010).

107. Manolov, N., Assenova, E., & Kandeva, M., "Conception for the Development of Tribology in Bulgaria", ***Sv. Ivan Rilsky–Sofia,*** Bulgaria, Sofia, 34-38 (2005).

108. Zadorozhnaya, E., Levanov, I., & Kandeva, M., "Tribological Research of Biodegradable Lubricants for Friction Units of Machines and Mechanisms: Current State of Research", ***In International Conference on Industrial Engineering***, Cham, 939-947 (2018).

109. Adhvaryu, A., Erhan, S. Z., & Perez, J. M., "Tribological studies of thermally and chemically modified vegetable oils for use as environmentally friendly lubricants", ***Wear,*** *257*(4): 359-367 (2004).

110. Alves, S. M., Barros, B. S., Trajano, M. F., Ribeiro, K. S. B., & Moura, E. J. T. I., "Tribological behavior of vegetable oil-based lubricants with nanoparticles of oxides in boundary lubrication conditions", ***Tribology International,*** 6(5): 28-36 (2013).

111. Quinchia, L. A., Delgado, M. A., Reddyhoff, T., Gallegos, C. & Spikes, H. A., "Tribological studies of potential vegetable oil-based lubricants containing environmentally friendly viscosity modifiers", ***Tribology International,*** 6(9): 110-117 (2014).

112. Hidayu, A. R., Mohamad, N. F., Matali, S., & Sharifah, A. S. A. K., "Characterization of activated carbon prepared from oil palm empty fruit bunch using BET and FT-IR techniques", ***Procedia Engineering,*** *68*(2013): 379-384 (2013).

113. Jeevan, T. P., & Jayaram, S. R., "Tribological Properties and Machining Performance of Vegetable Oil Based Metal Working Fluids—A Review", ***Modern Mechanical Engineering,*** *8*(1): 42-65 (2018).

114. Rabinowicz, E., & Tanner, R. I., "Friction and wear of materials", ***Journal of Applied Mechanics,*** 33(2): 479 (1966).

115. Zeren, A., "Embeddability behaviour of tin-based bearing material in dry sliding", ***Materials & Design,*** 28(8): 2344-2350 (2007).

116. Alp, A., Erdemir, A., & Kumar, S., "Energy and wear analysis in lubricated sliding contact", ***Wear,*** 191(2): 261-264 (1996).

117. Khonsari, M. M., & Booser, E. R., "Bearing design and Lubrication", ***John Wiley& Sons*, *Inc,*** New York, USA, 385-414 (2001).

118. Lakshminarayanan, P. A., & Nayak, N. S., "Critical component wear in heavy duty engines", ***John Wiley & Sons,*** New York, USA, 45-52 (2011).

119. Lancaster, J. K., "ASM handbook, volume 18, friction, lubrication and wear technology: Volume chairman", ***Elsevier,*** Berlin, Germany, 23-31 (1993).

120. Totten, G. E., "ASM Handbook: Friction, Lubrication, and Wear Technology", ***ASM International,*** Washington, USA, 23-31 (2017).

121. Pochaiah, S., Raju, V. P., Ahirwar, Y., & Venkatesh, R., "Production and Wear Characterization of Leaded Aluminium Alloys for Sliding Bearing Applications", ***Journal of the Gujarat Research Society,*** 21(7): 300-319 (2019).

122. Buschow, K. J., Cahn, R. W., Flemings, M. C., Ilschner, B., Kramer, E. J., & Mahajan, S., "Encyclopedia of materials", ***Science and Technology,*** 1(11): (2001).

123. Stolarski, T. A. "Tribology in machine design, 2000.", ***Butterworth-Heinemann,*** UK, 23-34 (2000).

124. Neale, M. J., "Bearings: a tribology handbook", **Elsevier,** Berlin, Germany, 45-53 (2013).

125. Lepper, K., James, M., Chashechkina, J., & Rigney, D. A., "Sliding behavior of selected aluminum alloys", ***Wear,*** 20(3): 46-56 (1997).

126. Xiao, L., Rosen, B. G., Amini, N., & Nilsson, P. H., "A study on the effect of surface topography on rough friction in roller contact", ***Wear,*** 254(11): 1162-1169 (2003).

127. Szeri, A. Z. "Fluid film lubrication," ***Cambridge University Press,*** UK, 10-15 (2011).

128. Akbarzadeh, S., & Khonsari, M. M., "On the prediction of running-in behavior in mixed-lubrication line contact", ***Journal of Tribology***, 132(3): 123-137 (2010).

129. Woydt, M., & Wäsche, R., "The history of the Stribeck curve and ball bearing steels: The role of Adolf Martens", ***Wear,*** 268(12): 1542-1546 (2010).

130. Buongiorno, J., Venerus, D. C., Prabhat, N., McKrell, T., Townsend, J., Christianson, R. & Zhou, S. Q., "A benchmark study on the thermal conductivity of nanofluids", ***Journal of Applied Physics,*** 106(9): 312 (2009).

131. Friedman, H., Eidelman, O., Feldman, Y., Moshkovich, A., Perfiliev, V., Rapoport, L., & Tenne, R., "Fabrication of self-lubricating cobalt coatings on metal surfaces", ***Nanotechnology,*** *18*(11): 115-703 (2007).

132. Chaudhury, M. K., "Spread the word about nanofluids", ***Nature,*** *423*(69): 131-132 (2003).

133. Elechiguerra, J. L., Reyes-Gasga, J. & Yacaman, M. J., "The role of twinning in shape evolution of anisotropic noble metal nanostructures", ***Journal of Materials Chemistry,*** 16(40): 3906-3919 (2006).

134. Pilkington, G. A., & Briscoe, W. H., "Nanofluids mediating surface forces", ***Advances in Colloid and Interface Science,*** 17(9): 68-84 (2012).

135. Daniel, M. C., & Astruc, D., "Gold nanoparticles: assembly, supramolecular chemistry, quantum-size-related properties, and applications toward biology, catalysis, and nanotechnology", ***Chemical Reviews,*** 104(1): 293-346 (2004).

136. Ali, I., & Aboul-Enein, H. Y., "Instrumental methods in metal ion speciation", ***CRC Press,*** Florida, USA, 21-23 (2006).

137. Agista, M. N., Guo, K., & Yu, Z., "A state-of-the-art review of nanoparticles application in petroleum with a focus on enhanced oil recovery", ***Applied Sciences,*** 8(6): 871 (2018).

138. Fan, Z., & Lu, J. G., "Zinc oxide nanostructures: synthesis and properties", ***Journal of Nanoscience and Nanotechnology,*** *5*(10): 1561-1573 (2005).

139. Ali, I., "New generation adsorbents for water treatment", ***Chemical Reviews,*** 112(10): 5073-5091 (2012).

140. Ali, I., "Water treatment by adsorption columns: evaluation at ground level", ***Separation & Purification Reviews,*** 43(3): 175-205 (2014).

141. Ali, I., Mukhtar, S. D., Hsieh, M. F., Alothman, Z. A., & Alwarthan, A., "Facile synthesis of indole heterocyclic compounds based micellar nano anti-cancer drugs", ***RSC Advances,*** 8(66): 37905-37914 (2018).

142. Peng, D. X., Kang, Y., Hwang, R. M., Shyr, S. S., & Chang, Y. P., "Tribological properties of diamond and SiO2 nanoparticles added in paraffin", ***Tribology International,*** 42(6): 911-917 (2009).

143. Rapoport, L., Leshchinsky, V., Lvovsky, M., Nepomnyashchy, O., Volovik, Y., & Tenne, R., "Mechanism of friction of fullerenes", ***Industrial Lubrication and Tribology,*** 54(4):171-176 (2002).

144. Ali, I., Alharbi, O. M., Alothman, Z. A. & Alwarthan, A., "Facile and eco-friendly synthesis of functionalized iron nanoparticles for cyanazine removal in water", ***Colloids and Surfaces B: Biointerfaces,*** 17(1): 606-613 (2018).

145. Liu, G., Li, X., Qin, B., Xing, D., Guo, Y., & Fan, R., "Investigation of the mending effect and mechanism of copper nano-particles on a tribologically stressed surface", ***Tribology Letters,*** *17*(4): 961-966 (2004).

146. Stachowiak, G., & Batchelor, A. W., "Experimental methods in tribology", ***Elsevier,*** Berlin, Germany, 34-36 (2004).

147. Martin, J. M., & Ohmae, N., "*Nanolubricants*", ***John Wiley & Sons,*** New York, USA, 23-34 (2008).

148. Rapoport, L., Feldman, Y., Homyonfer, M., Cohen, H., Sloan, J., Hutchison, J. L., & Tenne, R., "Inorganic fullerene-like material as additives to lubricants: structure–function relationship", ***Wear,*** 22(5): 975-982 (1999).

149. Z. S. Hu and J. X. Dong, "Study on antiwear and reducing friction additive of nanometer titanium oxide," ***Wear,*** 216(1): 92–96 (1998).

150. Berman, D., Erdemir, A., & Sumant, A. V., "Graphene: a new emerging lubricant", ***Materials Today,*** 17(1): 31-42 (2014).

151. Dou, X., Koltonow, A. R., He, X., Jang, H. D., Wang, Q., Chung, Y. W., & Huang, J., "Self-dispersed crumpled graphene balls in oil for friction and wear reduction", ***Proceedings of the National Academy of Sciences,*** 113(6): 1528-1533 (2016).

152. Zhu, C., Yan, Y., Wang, F., Cui, J., Zhao, S., Gao, A., & Zhang, G., "Facile fabrication of long-chain alkyl functionalized ultrafine reduced graphene oxide nanocomposites for enhanced tribological performance", ***RSC Advances,*** 9(13): 7324-7333 (2019).

153. Berman, D., Erdemir, A., & Sumant, A. V., "Reduced wear and friction enabled by graphene layers on sliding steel surfaces in dry nitrogen", ***Carbon,*** 5(9): 167-175 (2013).

154. Mutyala, K. C., Wu, Y. A., Erdemir, A., & Sumant, A. V., "Graphene-MoS2 ensembles to reduce friction and wear in DLC-Steel contacts", ***Carbon,*** 14(6): 524-527 (2019).

155. Xue, Q., Liu, W., & Zhang, Z., "Friction and wear properties of a surface-modified TiO2 nanoparticle as an additive in liquid paraffin", ***Wear,*** 213(2): 29-32 (1997).

156. Schiøtz, J., & Jacobsen, K. W., "A maximum in the strength of nanocrystalline copper", ***Science,*** 301(5638): 1357-1359 (2003).

157. Weertman, J. R., "Hall-Petch strengthening in nanocrystalline metals", ***Materials Science and Engineering: A,*** *166*(2): 161-167 (1993).

158. Yamakov, V., Wolf, D., Phillpot, S. R., Mukherjee, A. K., & Gleiter, H., "Deformation-mechanism map for nanocrystalline metals by molecular-dynamics simulation", ***Nature materials,*** *3*(1): 43-47 (2004).

159. Fan, G. J., Choo, H., Liaw, P. K., & Lavernia, E. J., "A model for the inverse Hall–Petch relation of nanocrystalline materials", ***Materials Science and Engineering: A,*** 409(1): 243-248 (2005).

160. Narayanunni, V., Kheireddin, B. A., & Akbulut, M., "Influence of surface topography on frictional properties of Cu surfaces under different lubrication conditions: Comparison of dry, base oil, and ZnS nanowire-based lubrication

system", ***Tribology International,*** 44(12): 1720-1725 (2011).

161. Liss, S. N., Milligan, T. G., Droppo, I. G., & Leppard, G. G., "Methods for analyzing floc properties", CRC Press, Florida, USA, 1-21 (2005).

162. Jhi, S. H., Louie, S. G., Cohen, M. L., & Ihm, J., "Vacancy hardening and softening in transition metal carbides and nitrides", ***Physical Review Letters,*** 86(15): 3348 (2001).

163. Morris, D. G., Joye, J. C. & Leboeuf, M., "Hardening and strain-ageing by vacancies and their aggregates in FeAl", ***Philosophical Magazine A,*** *69*(5): 961-980 (1994).

164. Pugno, N. M., "Young's modulus reduction of defective nanotubes", ***Applied Physics Letters,*** 90(4): 43-106 (2007).

165. Min, Y. "Role of inter nanoparticle forces in nanoparticle assembly," ***Polymer Engineering Faculty Research,*** China, 23-31 (2008).

166. Akbulut, M., Belman, N., Golan, Y., & Israelachvili, J., "Frictional properties of confined nanorods", ***Advanced Materials,*** 18(19): 2589-2592 (2006).

167. Tao, N. R., Wang, Z. B., Tong, W. P., Sui, M. L., Lu, J., & Lu, K., "An investigation of surface nanocrystallization mechanism in Fe induced by surface mechanical attrition treatment", ***Acta materialia,*** 50(18): 4603-4616 (2002).

168. Novoselov, K. S., Geim, A. K., Morozov, S. V., Jiang, D., Zhang, Y., Dubonos, S. V., ... & Firsov, A. A., "Electric field effect in atomically thin carbon films", ***Science,*** 306(96): 666-669 (2004).

169. Cesano, F., & Scarano, D., "Graphene and other 2D layered hybrid nanomaterial-based films: Synthesis, properties, and applications", ***Coatings,*** 3(5): 2-4(2018).

170. Tanjil, M. R. E., Jeong, Y., Yin, Z., Panaccione, W., & Wang, M. C., "Ångström-Scale, Atomically Thin 2D Materials for Corrosion Mitigation and Passivation", ***Coatings,*** 9(2): 133 (2019).

171. Xia, M., "2D materials-coated plasmonic structures for SERS applications", ***Coatings,*** *8*(4): 137 (2018).

172. Dai, W., Kheireddin, B., Gao, H., Kan, Y., Clearfield, A., & Liang, H., "Formation of anti-wear tribofilms via α-ZrP nanoplatelet as lubricant additives", ***Lubricants,*** 4(3): 28 (2016).

173. Liu, L., Zhou, M., Li, X., Jin, L., Su, G., Mo, Y., & Tian, Y., "Research progress in application of 2D materials in liquid-phase lubrication system", ***Materials,*** 11(8): 1314 (2018).

RESUME

I am Hamza Mohamed S ABUSHRENTA. I was born in Libya in 1988. I graduated elementary, preparatory and high school education in local schools located in my home city: TRIPOLI. I started my undergraduate studies at the Higher Institute of Industrial Technology - Al-Najila in TRIPOLI at the Mechanical Engineering Department in 2007/2008, from where I graduated in 2011. Currently, I work as a teaching assistant at the Higher Institute of Engineering Occupations – Tripoli, I am pursuing a master's degree in Mechanical Engineering, from Karabük University, Turkey.

CONTACT INFORMATION

Address: Karabük University
Graduate School of Natural and Applied Science
Demir-Çelik Campus/KARABUK
Mobile (Turkey): 05313162152
Mobile (Libya):+218919995556
E-mail: febxp17@gmail.com.